WIND TUNNEL SITE ANALYSIS OF DOW CHEMICAL FACILITY AT ROCKY FLATS, COLORADO

by

R. N. Meroney
F. H. Chaudhry

Prepared for

Research and Ecology
Rocky Flats Division
Dow Chemical Company
Golden, Colorado 80401

May , 1972

CER71-72RNM-FC-45

ABSTRACT

Tests were conducted on a model of the Dow Chemical Company plutonium recovery facility, Rocky Flats Division, and the surrounding topography to determine the dispersal and trajectories of potential effluents. Profiles of wind and turbulence over the facility were adjusted to forms expected for the given terrain. Dispersion and trajectory characteristics were determined by releasing a krypton-85 tracer gas from specific sources and sampling the plume downwind. Results suggest that the plumes depart only modestly from behavior suggested by the Pasquill-Gifford prediction methods. All results are tabulated and/or presented in a dimensionless manner suitable for prototype site evaluation.

TABLE OF CONTENTS

LIST OF TABLES

LIST OF FIGURES

LIST OF SYMBOLS

L	Length scale
Q	Source strength
R	Count rate
t	Measurement time
u'	Turbulent intensity
u_∞	Free stream tunnel velocity
$\bar{u}$	Mean velocity at same reference height
V	Stack exit velocity
x,y,z	Co-ordinates
z_o	Roughness length
χ	Concentration
σ	Standard deviation

1.0 INTRODUCTION

The purpose of this study was to investigate the problem of transport and dispersion of potential effluents released from within the boundaries of the Dow Chemical Company plutonium recovery facility, Rocky Flats Division, over the surrounding irregular terrain.

The Rocky Flats plutonium plant, operated by the Dow Chemical Company under U. S. Atomic Energy Commission contract is located only 8 miles northwest of densely populated areas of Denver. As a result of inadvertent releases of plutonium through fires (September 11, 1957 and May 11, 1969) and leakage of stored oil (Circa, 1964) the dispersion of plutonium as plutonium oxide from the site has attracted much public attention and concern (Gillies, 1972; Shepherd, 1970). A number of private (Martell, 1970) and public agency (Jacoe, 1970; Krey and Hardy, 1970) reports have been prepared discussing the existing levels of contamination and their implication in terms of public safety. Since it is the nature of accidents that they occur unexpectedly such that all details of their occurrence are rarely fully known, there has continued to exist questions concerning the initial dispersal and trajectory of gases and particulates during these and any future incident.

Specific questions which it is the purpose of this study to speak to are

1) Is it likely that hot gases in an escaping plume over a processing building will loft above the building cavity and

wake to deposite material beyond plant boundaries, without leaving evidence of passage within the complex at ground level?

2) Will the presence of the processing complex and/or terrain irregularities modify plume behavior to the extent that conventional estimates of plume extent and dilution are markedly inaccurate?

3) Is there any most undesirable accident configuration with respect to plume dispersal?

4) What array of monitoring devices will suffice to adequately measure the ground level signature of any gas or particle plume?

5) What are the expected dilution levels for a given source-release configuration for inner and outer plant boundaries?

This report will not attempt to make any interpretation with respect to physiological implications of a given dosage level since it is not within the authors' area of expertise. In addition the subsequent movement of contaminents, once deposited, by wind and erosion will not be described.

Three methods are available for studying this problem, field measurement programs, numerical and analytical simulation, and laboratory simulation. At this time, all three methods are necessary and must complement one another since no single method appears capable of providing complete solutions. This report deals with an effort to isolate peculiarities of dispersion associated with the Rocky Flats building complex and local terrain in order to modify and interpret diffusion formulae predictions.

The use of conventional diffusion formulae to calculate concentration fields produced by sources on or near buildings in irregular terrain often leads to misleading answers. Such formulae are developed under the assumption that all flow lines are straight and parallel. Over uniformly rough, flat ground this assumption is reasonably accurate. Flow near buildings and over irregular terrain contains curved streamlines, sudden changes in surface roughness, local regions of separation, wake turbulence, and even induced vortex-like motions associated with stagnation regions and wind shear. Currently the optimum procedure for estimating concentrations under such circumstances is to obtain experimental data for a few configurations. When a laboratory simulation is performed to accomplish these goals, the extrapolation of such data to the full scale natural atmosphere will indroduce some unavoidable error. However, an appreciation of the atmospheric motions involved suggests such deviations will not be by orders of magnitude. It should be understood that the study of diffusion over terrain and near buildings is still in its infancy and much work is necessary to validate and refine the results presented herein.

When similarity conditions can be satisfied between prototype and model several benefits of laboratory simulation may be realized:

1) The essential variables can be controlled at will,
2) The reduction in time and expense of extensive field studies,
3) The determination of the most effective sites for meteorological instruments and samples in the actual prototype, and
4) The inherent possibility of locating particular problem areas in advance.

Since the wind tunnel will probably continue to be the principle source of data for these problems, a discussion of scaling criteria and similitude follows. A separate section is devoted to the model, wind tunnel and instrumentation utilized. Finally, results are presented and discussed.

2.0 SIMULATION OF FLOW AND DISPERSION

2.1 Current State of Mathematical Model Theories

Calculation of peak and mean ground concentrations of diffusing gases or particulates are normally based on some semi-empirical model which relates the release rate from an elevated or ground-level point source to the concentration at some point downwind. Models have been suggested by Sutton (1967), Hay and Pasquill (1962), Roberts (1923), and Cramer (1957). These models require the assumptions of plane homogeneous atmospheric turbulence and constant mean lateral and mean vertical velocities. These assumptions are satisfied for a point release over a flat undisturbed terrain. Plume dispersion is sufficiently modified by the presence of the local building structure or ground topography that the only approach currently available is one of wind tunnel model tests (Moses, et al, 1969; Halitsky, et al, 1963).

Numerical programs to predict diffusion over irregular terrain or within a building complex have not been sufficiently improved to be effective for general usage. Hino (1968) published the results of a joint computer simulation to wind tunnel comparison of dispersion from an industrial stack over irregular terrain. His program did not permit separation over the sharper terrain features. Hotchkiss (1971) recently reported the movements of particulates within hypothetical building complexes by means of a marker and cell computational technique. Computer storage and time seems prohibitive for the current generation of computers.

In addition, considerable effort has been made to determine the effects of vertical stack velocity and gas buoyancy on the effective release height. Recently Carson and Moses (1967) and Briggs (1969) have reviewed over 30 plume rise formulas constructed to calculate effective stack heights for conditions where there are no effects from local terrain or buildings. They concluded that no available plume rise equation can be expected to accurately predict short term plume rise.

2.2 Brief Survey of Similarity Criteria

The use of a wind tunnel for model tests of atmospheric gas diffusion is dependent on the expression of concentration results in a non-dimensional coefficient whose value is independent of the variations in scale between model and prototype. The concentration coefficients will only be independent of scale if certain similarity criteria are met by the modeled flows. These criteria are generally understood as a result of analysis or experience, and they are discussed in detail by Halitsky (1963), Martin (1965), and Cermak (1966). Basically, model laws may be divided into those which govern the areas of geometric, dynamic and kinematic similarity. In addition, one must specify equivalent upstream and ground boundary conditions.

The basic tool of laboratory simulation is similitude or similarity, defined as a relation between two mechanical (or flow) systems (often referred to as model and prototype)* such that by proportional alterations of the units of length, mass, and time, measured quantities in

---

*Prototype - actual air flow involving full scale. Model - airflow involving smaller scale than prototype but usually with geometrically similar boundaries.

the one system go identically (or with a constant multiple of each other) into those in the other. In the case of flow around or over obstacles such as mountains, geometrical, kinematical, dynamical, and thermal similarity must be achieved.

Geometrical similitude exists between model and prototype if the ratios of all corresponding dimensions in model and prototype are equal. This is easily realized by using undistorted scale models of the prototype geometry. Kinematic similitude exists between model and prototype

1) if the paths of homologous (having the same relative position) moving particles are geometrically similar, and
2) if the ratio of the velocities of homologous particles are equal.

Dynamic similitude exists between geometrically and kinematically similar systems if the ratios of all homologous forces in model and prototype are the same. Thermal similarity exists for model and prototype if the density stratification is the same.

Numerous problems arise in constructing a model of flow over rough terrain and buildings. An important concern is friction, since, in general, it is difficult to obtain equality of Reynolds numbers in model and prototype. In the atmosphere a typical value is $Re \sim 10^{10}$; in the model $Re \sim 10^{4}$ (the difference depends primarily upon the scale one it attampting to model). Since the flow in the model and the atmosphere is turbulent, adopting the terminology of Reynolds (1894), we must compare the mean motions in the model which the mean-mean motions in the atmosphere at corresponding points. The equations of motion in the model and for the atmosphere are Reynold's equations of

mean-mean motion with forces produced by both molecular friction and turbulent transport of momentum (Reynold's stress terms). The forms of these two sets of equations will differ unless

1) Molecular friction and turbulent friction terms are neglected in both systems, or
2) Molecular friction is negligible compared to turbulent friction in the atmosphere and the turbulent friction is expressible in terms of mean-mean motion and has the same form as in the equations of Navier-Stokes, viz. proportional to the Laplacian of the respective velocity components.

Both view points have been utilized in previous modeling work. Viewpoint (1) has been applied for aerodynamically rough flow when the drag is predominantly due to pressure forces exerted normally on the projecting roughness of the surface, and is therefore virtually independent of viscosity. Thus, when the flow is over rough sharp-edged topographical features or building complexes, mean flow patterns are independent of the Reynold's number if that number exceeds a lower limit which is dependent upon the geometrical form. In such instances a value of 10^3 for the ratio $(Re)_p/(Re)_m$ may not introduce signigicant error in the modeled mean-flow patterns. This implies that surface or drag forces are directly proportional to the mean flow speed squared. In turn, this condition is the necessary condition for mean turbulence statistics such as root-mean square value and correlation coefficient of the turbulence velocity components to be equal for the model and the prototype flow. In such a case the viscous effects no longer dynamically govern the flow and the equation of motion reduces to Euler's equation for potential flow.

Buildings and building complexes produce nonuniform fields of flow which perturb the regular upstream atmospheric wind profiles. Around each building a boundary layer exists, where the velocity is zero at the surface but increases rapidly to a relatively constant value a short distance from the building wall. Outside of the boundary layer and downstream there exists a region of low velocities and pressures called the cavity. In this region circulations are such that flow may actually reverse with respect to the upstream winds. Surrounding the cavity but extending further downstream is a parabolic region called the wake in which the presence of the building is still evident in terms of deviations of velocity, turbulence, and pressure from conditions found in the upstream atmospheric boundary layer.

The formation of the wake and cavity regions are associated with a phenomena called boundary-layer separation. Under certain conditions the boundary layer actually detaches and enters the flow streaming about the building. This may occur at the corner of a sharp edged building or on a curved surface if the pressure increases due to a decelerating flow field. The separated boundary layer forms a sheet which completely surrounds the cavity region which contains relatively stagnant fluid. The extent of the cavity region for a fifty foot high building may be approximated by $5H \simeq 250$ feet. Based on the measurements of Evans (1957) the effect of alternate wind approach angles to an elongated rectangular complex may extend this to $6H \simeq 300$ feet.

Golden, as cited by Halitsky (1963), found that for flow about a cube for Reynolds numbers above 11,000, there was no change in concentration measurements.

Viewpoint (2) compares the gross mean characteristics of turbulent natural flows over topographical features by a laminar laboratory flow when the scale ratio $L_p/L_m = 10^3$. Thus, a tunnel flow speed is selected so as to equate the Reynold's number to that applicable on the full scale, i.e., the molecular viscosity in the model corresponds to the eddy viscosity on the full scale.

Another basic problem concerns thermal similarity. Scorer (1953) and Corby (1954) have indicated that thermal similitude requires large temperature gradients (1° C/cm^{-1}) at very low flow speeds (9 cm/sec^{-1}) in the model and considered such experimental control too difficult to achieve with the conventional wind tunnels. As the result of this problem, most model experiments have been achieved at neutral stability or when the static stability is very small. However, with the recent construction of larger wind tunnels capable of environmental control, the possibility of achieving the required temperature gradients and low flow speeds are an actuality; therefore, thermal restrictions are no longer an impossible barrier (see Cermak, et al, 1966).

Not only must the various dimensionless parameters be the same for both model and prototype, but in addition, the boundary conditions must be the same. This latter requirement not only demands geometric similarity of the lower boundary, but also similarity in upstream conditions and in conditions at the upper boundary.

The upstream conditions may be matched rather precisely by setting the model at varying distances from the leading edge of the boundary layer in the wind tunnel test section. The velocity and density distributions that may be obtained in the tunnel are, however, all similar to one another. The upper boundary conditions can only be matched if

the study of the prototype is restricted to the lower layers of the atmosphere, approximately one half the height of the troposphere, primarily because the increase in stability $d/dz(\ln\rho)$ cannot be reproduced in present wind tunnels without major modifications.

At the present time wind tunnels are capable of simulating certain aspects of atmospheric flow; several restrictions are necessary, however:

1) The prototype region is made comparatively small (~90 mi or less), so the effect of the Coriolis acceleration is negligible (i.e., convective accelerations predominate).
2) The effect of variation of hydrostatic pressure with height is negligible.
3) The effect of compressibility of the air is negligible (where prototype length $L \sim 1$ km or less).
4) The effect of condensation and evaporation processes are neglected (i.e., no clouds or precipitation).
5) The unsteady state of prototype winds are neglected (i.e., the model winds are steady state).

Yet, even with these restrictive assumptions worthwhile results have been obtained from laboratory simulation as briefly summarized in the next section. These restrictions are not critical for many, or even most, investigations of atmospheric diffusion and particle transport in the lower troposphere.

2.3 Past Work in Laboratory Simulation of Atmospheric Flow Over Terrains and Building Complexes

M. Abe (1941) simulated the air flow and cloud formation over Mt. Fuji using a laminar flow for a 1:50,000 model. Abe attempted to

achieve greater realism by arranging for wind shear, thermal similarity and change of wind direction with height. Unfortunately, Abe did not arrange these effects quantitatively to insure that strict dynamical similarity was achieved; yet, the photographed model flow was found to be in approximate agreement with some properties of the flow on site, insofar as he had deduced them from observations of the mountain clouds.

Field and Warden (1929-30) and later Briggs (1963) used the principles of flow over rough sharp-edged topographical features in modeling flow over the Rock of Gibraltar. In the model investigation no arrangements to simulate stability were made; hence, the flow obtained in the model corresponded to the full-scale case with zero static stability. The study of Field and Warden was performed at the National Physical Laboratory of Great Britain, on a 1:5,000-scale model in a low speed wind tunnel. This study was instigated in order to determine the types and distribution of possible disturbances before a full-scale field study was begun. It was found that wind directions and the distribution of vortices and vertical currents obtained with the model agreed closely with those occurring in nature at Gibraltar. However, the actual intensity of gustiness were not in good agreement with the prototype flow.

Nemoto (1961, Part I, II, and III) (1962, Part IV) has discussed the various aspects of similitude for several different model flows and has also derived similarity criteria for wind profiles near the ground and the intensity of turbulence. Nemoto used results from two different models to check his similarity criteria and found good agreement between model and prototype.

Halitsky, Tolciss, and Kaplin (Reports 1, 2, 3, and 4, 1962, 1963) studied the structure of the local wind field over a topographic model of Bear Mountain and surrounding terrain by means of wind tunnel measurements and evaluated the degree of correspondence between model and full-scale measurements of mean and turbulent wind properties. They were particularly interested in the region of very high turbulence in the lee of the mountain.

A number of wind tunnel studies have considered the effects of variations in a single building geometry on plume entrainment and dispersion (Halitsky (1963); Strom, et al (1957); Evans (1957); Jensen and Frank (1963)). These studies have permited the specification of pertinent scaling criteria for model studies of plume excursions near buildings.

Since each arrangement of a given plant and auxiliary buildings or terrain may have separate effects on the generation of mechanical turbulence and mean flow movement, any specific gas dispersion problem will require individual tests. Hence, there exist in the literature desciptions of a variety of different model studies on power stations and industrial plants. These studies are significant in that their results have been essentially confirmed by either direct prototype measurements or the absence of the gases or dusts the study was directed to remove. Kalinske (1945); Davies and Moore (1964); Hohenleiten and Wolf (1942); and Martin (1965) incorporate such comparisons within their text. Results of Halitsky et al (1963) have recently been compared with prototype measurements at the National Reactor Testing Station in Southeast Idaho (Dickson et al (1967)). Agreement of the diffusion concentration results were very satisfactory. Martin (1965) favorably

compared his wind tunnel study measurements about a model of the Ford Nuclear Reactor at the University of Michigan with prototype measurements. Finally, Munn and Cole (1967) have taken diffusion measurements on a power station complex at the National Research Council, Ottawa, Canada, to confirm the general entrainment criteria suggested by the model studies of Davies and Moore (1969).

A wind tunnel study of Point Arguello, California (Cermak and Peterka, 1966) was motivated by the desire to estimate the diffusion characteristics of toxic gases which might be released in the vicinity of missile launch sites on the U. S. Naval Missile Facility. Accordingly, the primary purpose of this study was to determine if wind patterns observed in a wind tunnel over a 1:12,000 scale model of the Point Arguello area are representative of the prototype wind patterns which are usually stably stratified. Since inversion flows were of primary interest, the laboratory study was confined primarily to low-speed flow (5 ft/sec) with a maximum attainable temperature difference (wind tunnel floor was 103°F cooler than the ambient air). Flow patterns for the stable stratification were well documented in the cases of flow approaching from an azimuth of 315° and from 340°. In order to minimize the apparent dissimilarity suggested by the large difference in Reynolds' numbers, the ideas of Abe were applied to the model. Two types of flow visualization techniques were used to obtain flow patterns. Photographs of an indicator paint (ammonia) on the model gave an indication of local flow directions at the surface, and photographs of smoke tracers over the model supplemented the indicator paint. In general, in comparing the results of the experimental work in the wind tunnel with comparable data from a field study, the authors

concluded that excellent similarity existed for wind-flow patterns and diffusion over the Point Arguello area and for the model inversion flow approaching from the northwest.

A 1:6,200 scale model of San Nicolas Island, California (Meroney and Cermak, 1965) was studied under conditions of inversion flow in the wind tunnel. Visualization procedures, including colored indicator paints and titanium tetrachloride smoke, were used to determine characteristic flow patterns over the island with wind orientation to the island of 315^{o}. Diffusion of toxic rocket exhaust products were simulated by the release of controlled amounts of helium. Concentration profiles of the helium plume were measured at various distances downwind of the island model. This study also looked at the effects of distorted vertical scaling. It was concluded one must approach problems with flat unrelieved terrain with caution.

A 1:400 scale model of the proposed Stock Island Fossil Fuel Power Plant at Key West, Florida (Meroney and Cermak, 1969) was studied under neutral and inversion conditions in the wind tunnel. The purpose of the study was to examine the effect of the power plant complex on effluent releases from a short stack, to determine the wind orientation for maximum entrainment, and to determine the feasibility of increasing stack velocity to lift the plume above building wake regions. Data included concentrations and visualization of plume trajectories.

A 1:200 scale model of the proposed Shoreham Nuclear Power Station, Long Island (Meroney, Cermak, and Chaudhry, 1968) and downwind terrain were studied in the wind tunnel for a variety of gas release conditions. Plume trajectories and concentrations were monitored utilizing a Kr-85

tracer technique. The effects of complex growth and curved building geometries on dispersion and entrainment were examined.

Systematic studies of the effects of building shape, orientation, stratification, and gas release position have been performed to determine the effect of entrainment on dispersion (Meroney and Yang, 1970; Meroney and Symes, 1971; and Meroney and Yang, 1971). Measurements of turbulence, concentration, and stratification revealed potential behavior for nuclear reactor hazards due to accidental entrainment-vessel breach. Gases released with low initial jet velocity were universally found to be entrained into the wake region and brought to ground level downwind.

In an extremely comprehensive study, Orgill, Cermak, and Grant (1971) considered the effects of atmospheric transport-dispersion over mountainous terrain. This joint field and laboratory study examined the dispersal of ground releases silver-iodide nuclei on weather modification. A comparison of model and field data showed satisfactory similitude was achieved by the laboratory on flow models. The results encourage the use of studies of transport diffusion over scaled topographic models for purposes of providing preoperational information on the movement of gaseous plumes.

2.4 Rocky Flats Climatology

In a memorandum to the ESSA files (NOAA) Dickson and Start commented on the Rocky Flats Climatology as follows:

1) The wind rose averaged over a 17 year interval at the Rocky Flats Plant is as given in Figure 1. West winds occur 25% of the time; over 50% of the winds have a westerly component. The strongest gusts and the directions of the most frequent strong gusts (speeds greater than 40 mph) are from the west. The resulting wind vector (derived from the wind rose frequencies and mean speeds) points almost exactly eastward.

2) The Denver airport wind rose shows that southerly to south-westerly winds are most frequent. Air flowing eastward from Rocky Flats should merge with the southerly air flow across Denver and be carried north - northeastward. The South Platte River Valley, about 20 miles east of Rocky Flats, is the terrain feature along which this transition from westerly flow should approach completion.

3) The wind direction on May 11, 1969, the day of the last serious fire, was mostly from the north - northeast at speeds from 2 to 8 mph. The wind direction following the September 11, 1957 fire was from the west - northwest at speeds from 2 to 15 mph.

4) Strong gusty winds frequently occur in the lee of the mountains at Rocky Flats; several days each year wind gusts exceed 70 to 80 mph. Consequently wind erosion has removed most of the fine soil and alluvium leaving mostly rock and sand particles at the ground surface. Two creeks, Walnut and Woman Creeks, pass to the north and south of the plant, respectively, in an easterly direction. These creeks begin to flow through significantly deep gullies (several hundred yards wide) as they flow by the eastern limits of the plant. The soil in the gullies which was wind eroded from the flats is finer and deeper, and is more likely to become a trap for windborne particles of plutonium.

Data from 1968 prepared by the Health Physics Branch of Rocky Flats indicates that recent observations are consistent with the averages. Mean wind velocity was 7.6 mph, peak gust velocity was 84 mph from the west, and the predominate wind direction was from the west (25% of observations).

Due to the close proximity of the mountain range to the west, the authors were anxious to obtain typical records of vertical turbulence and velocity profiles for the Rocky Flats plateau. A large number of balloon records for the Marshall test site near Rocky Flats were provided by the National Center for Atmospheric Research, Boulder. Unfortunately the lowest level observation began at 500 feet and the data were extremely coarse. From the records examined, no consistent vertical wind shear, low level jet, or other idiosyncracy caused by the upwind mountain range for westerly winds was apparent. Hence it was concluded that the atmospheric shear layer may be typified by the aerodynamic surface roughness for the site. Examination of the site's local terrain and

vegetation suggests a roughness length of about .03 ft is appropriate. Wind profiles generated over rural terrain may be expected to produce a logarithmic velocity profile in the lower surface layer characterized by this roughness length.

2.5 Scaling Requirements for Rocky Flats Study

The investigation was conducted in a low-speed wind tunnel having a test section cross-section of 8 x 12 ft and a length of 52 ft. Three basic requirements for flow similarity are that the boundary-layer thickness of the flow approaching the model be 2 - 3 times the model height, that the flow be turbulent and that the longitudinal pressure gradient of the ambient flow be zero. Since the boundary-layer thickness for the tunnel is approximately 2 ft a model height of less than 1 ft is suggested. Another consideration in the selection of model scale is the degree of blockage presented by the model. The ratio of projected model area to area of wind tunnel cross-section should not exceed 1 - 2%. Based upon the foregoing considerations a model scale of 1:1000 has been selected for the investigation. Using this scale the model $\sim$ 0.5 ft high. The blockage ratio will be $\approx$ 0.2.

The model Reynolds number will be approximately 1000 times smaller than the prototype Reynolds number. Since the plant structures are of prismatic shape, dependence of the flow pattern on Reynolds number is negligible; therefore, the lack of equality in Reynolds numbers is not indicative of non-similarity in the flow characteristics.

The model consists of the processing plant structures, stacks, and other buildings in the immediate vicinity of the plant. The model was constructed from styrofoam and was fitted with several locations for gas release. Model terrain was constructed from layers of styrofoam

shaped to represent local irregularities. Since the scaled roughness height for the area is less than .00003 ft, the model surface was painted and not additionally roughened. The mountains west of the Rocky Flats Plant were not simulated in this study.

To meet the upstream boundary conditions the upstream velocity profile was conditioned artificially. A grid of stacked cardboard tubes 2-1/2 inch diameter and 3 feet long were placed longitudinally at the entrance section across the width of the tunnel in layers. This technique has an analogous wind shear and turbulence shaping function to those presented by Counihan (1969, 1970). It was determined that for a field roughness height of ~ 1 cm that the dynamic ratio $\frac{u^*}{u(z = 10\ m)} \simeq 0.58$. Hence all upstream velocity profiles were adjusted by means of the stacked tube barrier to this ratio.

3.0 APPARATUS AND INSTRUMENTATION

3.1 Description of Wind Tunnel Facility

The experimental work was carried out in the Environmental Wind Tunnel of the Fluid Dynamics and Diffusion Laboratory at Colorado State University. Its 12 ft wide test section can accommodate large models like that of the Rocky Flats Plant site. The environmental wind tunnel is an open-circuit type as shown in Fig. 4. A 150 H.P. blower is used to generate air speeds up to 60 ft/sec in a 12 ft x 8 ft test section. The air speed is set by varying the fan-blade pitch. The wind-tunnel ceiling can be adjusted to achieve a zero pressure gradient in the longitudinal direction. The large entrance is provided with honeycomb straighteners and a pair of screens to calm the flow into the test section and eliminate large-scale disturbances.

A sizable portion of the 52 ft long test section has a uniform free-stream velocity. The pressure gradient along the tunnel was zero for this set of measurements. The effect of the constriction at the end of the wind tunnel extends upstream for about 12 ft only. The section of the wind tunnel between $x = 20$ ft and $x = 32$ ft, thus, seemed the most suitable one for location of the model. Transverse velocity distributions at three different heights are shown in Fig. 13 for a free stream velocity of 10 ft/sec. These distributions are uniform and thus facilitate modeling of the approaching atmospheric flow which is a turbulent two-dimensional shear flow. The side-wall boundary layers are each about 10 inches thick, thus leaving a working width for the wind tunnel of more than 10 ft.

3.2 Model Construction

This model simulates the prototype area of the Rocky Flats facility and the surrounding topography. The horizontal and vertical scale of the model is 1:1000 which was determined by the width of the wind tunnel. The construction material was styrofoam and expanded polystyrene beadboard of 1/4 inch and 1/2 inch thickness.

The topographic features of the model were obtained from U. S Geological Survey maps at a scale of 1:24,000. The profile features were digitized on cards with an Auto-Trol Model 3800/4D Digitizer and 1:1000 scale maps prepared by an Auto-Trol Model 6030 Series Digital Plotter. Only slight modifications of some terrain features were caused by the fitting together of the model sections. The dimensions of the overall model is approximately 15 ft long and 12 ft wide. The model is divided into 12 major subsections which can be fitted together when in the wind tunnel.

The final stages of model construction consisted of filling in terrain features with plasticene clay and applying several coats of latex paint for protecting and hardening the surface. Roads, asphalt areas, vegetation, and ponds were delineated by colored latex paint.

The principle features of the model are the Rocky Flats building complex, and Woman and Walnut Creeks to the south and north, respectively. Figure 5 shows the topographic model during construction and as installed during an experimental period in the wind tunnel.

3.3 Instrumentation

3.3.1 Velocity profiles.--The velocity distributions were measured with a pitot-static tube of standard design, 32 mm in diameter. The two pressure ports of the tube were connected to the two ports of an

electronic differential pressure transducer. The pitot-tube was mounted on a remote control vertical carriage and its vertical position was monitored through a potentiometer mounted on the carriage. The D.C. output of this differential-capacitor device was recorded on an x-y plotter versus the height of the pitot tube. Dynamic pressure profiles were converted to wind velocity by evaluating local density from local temperature and barometric-pressure measurements.

3.3.2 Turbulence intensity profiles.--Longitudinal turbulence intensity $\left(\frac{\sqrt{u'^2}}{u_\infty}\right)$ profiles were measured by the use of a hot-wire probe mounted normally to the flow. The hot-wire sensor used in these experiments was 0.00035 in. diameter tungsten wire mounted on a Disa probe. A constant temperature hot-wire anemometer (FDDL-IL WW-WC-769-3) designed at Colorado State University was used. The mean value of the anemometer output was measured by an integrator in conjunction with a Hewlett-Packard digital voltmeter. For the rms of the fluctuating signal a Disa Type 55 D 35 RMS voltmeter was used.

3.3.3 Visualization.--Smoke was used to visually observe the diffusion patterns over the model. Titanium tetrachloride was released to provide dense smoke required for photographic purposes. The model was illuminated by means of floodlights and photographs were taken with a Polaroid-Land camera.

3.3.4 Concentration measurements.--Concentration measurements over the topographic model were obtained by releasing radioactive krypton-85 from sources located in the model and using Geiger-Mueller tubes to determine the relative amount of krypton in samples of the gas-air mixture. The method was developed in detail by Chaudhry (1969) but only information relevant to this study will be discussed.

Krypton-85 is a radioactive noble gas with a half life of 10.6 years. The gas decays by emission of beta particles with small amounts of gamma rays. The gas has many advantages over the other tracers used in wind-tunnel dispersion studies. It is diluted with air about a million times before use, and as such, has properties very similar to those of air. Its detection procedure is fairly simple and direct.

Figure 6 shows the wind tunnel arrangement for obtaining radioactive concentration measurements. The radioactive method consists of (a) release, (b) sampling, and (c) detection system.

A. Release system

The tracer release system or source is shown schematically in Fig. 6. A cylinder of premixed krypton-85 at a concentration of 1.8μ - curie/cc was located outside of the tunnel and provided the tracer gas. The flow rate of krypton-85 mixture was controlled by a pressure regulator at the bottle outlet and monitored by one or two flow meters, depending on the number of sources.

Source probes shown in Fig. 6 were placed on the surface of the model by drilling holes through the model and tunnel floor. Mayon tubing connected the source probes to the cylinder containing krypton-85. The flow rate for the source was approximately 600 cc/min and was low enough so as not to excessively disturb the oncoming flow near the source.

B. Sampling and detection system

The samples of gas were drawn from the wind tunnel through a rake of eight sampling tubes 0.2 cm in diameter mounted on a carriage as shown in Fig. 7. The eight samples of gas were drawn from the wind tunnel through Mayon tubings at a rate of 250 cc/min which was low enough to prevent sucking in gas from the sides except in the lowest few

centimeters above the model. The samples were then passed through the eight TGC-308 tracerlab Geiger-Mueller sidewall cylindrical counters. A vacuum pump was used to draw the samples and exhaust them back into the wind tunnel. Each sampling line had an electric valve inserted into it in order to avoid intermixing of the samples in different lines. These valves could be opened or closed at the same time by a common switch.

Output from each G.M. tube could be connected to the same scaler and high voltage. Although the count for each G.M. tube had to be recorded one by one, this sampling scheme helped conserve krypton-85 because eight samples were taken for one release of the gas.

C. Experimental procedure

A typical experiment for determining concentration data was conducted according to the following procedure:

1) The sampling probe was located at a chosed position on the model by the traversing mechanism of the wind tunnel carriage.

2) The wind tunnel was started and the desired free stream velocity was established for the experiment.

3) The common valve was opened and the electric valves were switched on to open. The pump was then started and was left running for 1-1/2 minutes to flush the G.M. tubes. The sampling flow rate was set for all the G.M. tubes.

4) The necessary release rate through the source probe was then established by source flowmeters.

5) Samples were drawn for 1-1/2 minutes and then the electric valves were closed and the common valve was also closed. This enclosed krypton-85 gas samples in the jackets. The flow of gas was then stopped.

6) The samples enclosed around the G.M. tube were then counted, one by one, by the scaler from 2 to 4 minutes, depending on the sampling probe distance from the source. The increased counting time improved the accuracy for very dilute samples.

7) The above procedure was then repeated for a new position of the sampling probe.

D. Analysis of data

The procedure for analyzing the concentration data was as follows:

1) Counts of the pulses generated in the G.M. tubes and displayed by the ultrascaler counter were recorded for all eight probes at the various locations.

2) These counts were transformed into concentration values by the following steps:

$$\text{Cpm} - \text{Background (Cpm)} = \text{Cpm}^*$$

$$\text{Cpm}^* \times \text{Counting Yield } (\mu\mu \text{ Curie/cc/Cpm}) = \chi(\mu\mu \text{ Curie/cc})$$

The counting yield varied according to the G.M. tube.

3) For counts over 1,000 a dead time correction[Δ] had to be applied to the readings, and in this case the correction is,

$$\text{Cpm} - \text{Background} = \text{Cpm}^*$$

$$\frac{\text{Cpm}^*}{1 - 1.77 \times 10^{-6} \times \text{Cpm}^*} = \text{Cpm}^*$$

$$\text{Cpm}^* \times \text{Counting Yield} = \chi(\mu\mu \text{ Curie/cc}) \ .$$

4) Average concentration values were determined for the known probe heights and then plotted with respect to height. Concentration curves were drawn for each location and then values of the average concentration were interpolated for every 100 meters of prototype scale.

[Δ]The time taken for the positive space charge to move sufficiently far from the anode for further pulses to occur.

5) The concentration parameter $\chi \bar{U}/Q$ was then computed by desk computer at all locations. A sample computation is shown below:

$$q = 600 \text{ cc/min} = 10 \text{ cc/sec}$$

$$Q_{total} = 1.8 \ \mu \text{ Curie/cc} \times 10 \text{ cc/sec}$$

$$= 18.0 \ \mu \text{ Curie/sec} \ .$$

Let $\bar{U} = 10$ ft/sec $= 300.5$ cm/sec and $\chi = 80 \ \mu\mu$ Curie/cm^3 then

$$\frac{\chi \bar{U}}{Q} = \frac{300.5 \times 80}{1.8} \times 10^{-2} = 133.3/m^2$$

6) So far the values of the concentration parameter apply to the model and it is desirable to express these values in terms of the field. At the present time there is no set procedure for accomplishing this transformation. The simplest and most straightforward procedure is to make this transformation using the scaling factor of the model. Since

$$1m]_{model} \equiv 1000 \ m]_{field}$$

one could write

$$\frac{\chi \bar{U}}{Q}\Big]_{model} \frac{1}{(1000)^2} \equiv \frac{\chi \bar{U}}{Q}\Big]_{field}$$

or in terms of the above example,

$$\frac{133.3}{m^2}\Big]_{model} \equiv \frac{\chi \bar{U}}{Q} \equiv \frac{1.33 \times 10^{-2}}{m^2}\Big]_{field}$$

This simple scaling of the concentration parameter from model to field appears to give reasonable results.

E. Errors in concentration measurements

Where data is obtained with a scaler counter, the apparent activity of a radioactive source is found by subtracting the background rate from the observed sample-plus-background rate. The background rate is measured separately and has an uncertainty of its own due to random radioactive sources.

If the background is present, the standard deviation in the net counting rate σ_{R_s} for a sample is

$$\sigma_{R_s} = \left(\frac{R_{s+b}}{t_s} + \frac{R_b}{t_b}\right)^{1/2}$$

where R_{s+b} is the observed sample-plus-background rate, R_b is the background rate, t_s and t_b are the measurement time for the sample and background, respectively. The standard deviation in the sample rate depends, then, upon both the time for sample measurement and that for background-rate measurement. When R_{s+b} is large in comparison with R_b, a long background measurement is not needed to make the error contribution from the background rate negligible. On the other hand, when R_{s+b} is comparable to R_b, both t_s and t_b must be very long for small values of σ_{R_s}. In the present experiments, an effort was made to keep the probable errors in concentration measurements within 10%. For this reason the sample counting time and background counting time were manipulated with this end in view. More detailed information on errors in radioactivity measurements can be found in Chaudhry (1969) and Overman and Clark (1960).

3.4 Data Collection Program

The data to be obtained was as follows:

1) Mean wind speed and temperature in the air stream approaching the model

2) Turbulence intensities in the approaching air stream

3) Flow patterns over and immediately downstream from the structures -- visualized by smoke with releases from the stack. Photographs of the smoke were made to record the gross flow patterns

4) Concentration downstream of the stack. Radioactive Krypton was used as the tracer for concentration determinations.

The testing program studied dispersion for neutral flow conditions only. Exit velocity and temperature of the effluent were varied in an effort to determine how the vertical momentum of the effluent effects the downwind concentration. Wind speed and aximuth were varied to cover the anticipated range of concern.

For neutral flows the combinations of test variables studied were as follows:

Wind Speed	Wind Direction	Smoke Visualization	Kr-85 Concentration
10 ft/sec	45^{o}	Yes	Yes
	90^{o}	"	"
	270^{o}	"	"
	315^{o}	"	"

Release locations were ~ 5 positions each wind orientation.

4.0 RESULTS

The results of the experiments performed on the model of Rocky Flats plant are presented in this chapter. The characteristics of model flow and the plan of data are explained.

4.1 Characteristics of Flow

All the experiments were carried at a wind tunnel free stream velocity of 8.5 ft/sec under neutral conditions. The atmospheric boundary layer was modeled to produce a roughness length equivalent to thin grass ($z_o \simeq 1$ cm, field) on flat surface. The ratio $\frac{u_*}{\overline{U}(10m)}$ in the flow profile approaching the model was maintained at 0.58. Figures 8 and 9 show the development of the velocity profile over the model for west and east winds. The east winds travelling up along the inclined planes add momentum in the lower layers such that the velocity profile bulges out at East Guard Station. The profile is conditioned by the building complex as the winds pass over the plant. Figures 10 and 11 present the distribution of turbulence intensity with height. Intensity of turbulence at 10 m level increases from about 9% in the approach flow to 13% over the factory complex. No comparison of model velocity data with that in the prototype is possible because the latter is not available. However, as the model velocity profiles were carefully produced to reflect the characteristics of the site, it was hoped that prototype flow is adequately represented in the model.

4.2 Diffusion Data

Turbulent diffusion of gaseous effluent released at five different positions over the model was studied. These sources are located as follows.

1) Manufacturing Building (BLDG. NO. 881)
2) Fabrication - Assembly Building (BLDG. NO. 707)
3) Manufacturing - Assembly Building (BLDG. NO. 776-777)
4) Cutting oil barrels storage area (located on Central Avenue east of factory complex)
5) 250 foot stack

The sources located on top of building were mounted flush with the roof and were capped to model the actual exhausts. Krypton-85 gas was released continuously through each of these sources and diffusion data were obtained for four wind directions viz, west, east, north-west, and north-east. Krypton-85 concentrations at ground level and in the vertical at plume center were measured at distances equivalent to 1000', 2500', 4000', 6000', and 9000'; the last depended on model extent.

All concentration data are converted into non-dimensional form as $\frac{\chi \bar{U} L^2}{Q}$ where χ is the average concentration ($\mu ci/ft^3$), Q is the source strength ($\mu ci/sec$) and $\bar{U}$ is the mean wind speed (ft/sec) at a reference height L(ft). The reference height was chosen as 20 ft being about the average height of buildings and the height at which meteorological instrumentation at the Rocky Flats plant are placed. Thus $\bar{U}$ would also be adequate for comparison of diffusion data to standard diffusion curves of Gifford and Pasquill because the average height of the

potential pollution sources other than the stack is also about 20 ft.

The non-dimensionalized diffusion data for various sources and wind directions is presented in Tables I to IV. At each distance from the source, the tracer concentration was observed at, at least, eight cross wind positions at the ground and in the vertical. The coordinates x, y, z, shown in the tables, are explained in the definition sketch in Figure 12.

4.3 Analysis of Diffusion Data

The diffusion data presented in tabular form has been analyzed in order to mark some of the features of the turbulent diffusion process at the Rocky Flats plant and beyond. In Figures 13 to 17 are plotted the traces of the positions of maximum ground level concentration and the concentrations equivalent to 50% and 10% of the maximum value for various source locations and wind directions. The effect of the topography in controlling the path of the plume is especially noticeable for the wind from the north-west direction. The plumes have a tendency to bend northward as they cross Woman Creek due to the protruded Rocky Flats ridge formations. The closer the source is to Woman Creek (for example, the source atop BLDG. NO. 881), the more profound is this shift. A similar effect is observed during the wind from the north-east. As the valleys are nearly aligned with east and west, there is only slight modulation of plume path. The concentration distributions are observed to be very asymmetrical wherever plume experiences a push from the ridges running across its path. The ground level concentration distributions due to the plume originating from 250-foot stack do not show any effect of the topography on diffusion process.

The diffusion data is also presented in the form of isopleths of non-dimensional concentration defined earlier. The veritcal plume cross-sections at the center-plane are shown in Figures 18 - 37. These graphs demonstrate the effect of topography (buildings and terrain) on vertical diffusion. Such effect is at its extreme in Figure 19 for the release atop manufacturing building (BLDG. NO. 881) during north-west winds. A sudden drop in ground surface causes the effluent to be enveloped in the valley and the diffusion pattern is similar to that from an elevated source. Of special importance are the isopleths in the vertical plane due to the releases from the 250-foot stack which are graphed in Figures 34 to 37. They depict the magnitude and position of the most concentrated effluent aloft over the Rocky Flats plant. Such information can be useful in calculations of average gamma doses during continuous releases.

The distribution of concentration at ground level are shown in the isopleths (Figures 38 to 57) superimposed on the contour plan of the plant site. The characteristics noted earlier from the plume width plots are visible more profoundly from these figures.

4.4 Visualization of Diffusion Patterns

Smoke plumes were released from each source site for each and direction to monitor the behavior of the instantaneous plume trajectories. Since the smoke was formed by an exothermic reactions of titanium tetrachloride with the water vapor in the air the plume itself was warmer than the ambient air by approximately $\sim 5^{o}C$ at the release point. This temperature rise is representative of the condition of release which might exist upon release during a fire.

Examination of the trajectories displayed in Figures 58 and 59 for the lateral motions of a plume emitted from Source #1 in a west wind displays meandering of scales associated with the Rocky Flats building complex. These larger scale plume movements are integrated into the concentration measurements, since the averaging times were large compared with the plume excursions.

Figures 60 to 65 display vertical plume outlines for the various release sites. In all cases the plumes were entrained into the building complex wake -- no lofting is apparent. Fig. 61 for Source #2 shows very graphically the initial intense mixing over the height of the building complex wake. Figure 64 for the release at the oil site displays a somewhat slower vertical mixing which is commensurate with the downward distance of this site from the nearest sharp-edged building. Releases from the Rocky Flats stack are initially carried above the plant grounds. However as the plume intercepts the growing building wake it also is brought to ground level. Releases from the stack at neutral buoyancy are hence effective at removing effluents from the immediate building complex; however further downwind ground level concentrations are identical with releases at ground level.

5.0 ANALYSIS AND DISCUSSION

5.1 Comparison with Pasquill-Gifford Estimation Technique

The results of the experimental study presented in the last chapter are quite useful in providing a total picture of the diffusion phenomenon. However, in view of the fact that despite its volume the information is limited to few discrete wind directions and at the most extends to 2 miles downwind from the source, it is essential to analyze the data in a more general frame. It should then be possible to generalize and to extrapolate the information to situations which have not been experimentally tested. Such a frame of reference is provided by the Pasquill-Gifford scheme of estimating atmospheric diffusion. The concentration distributions are considered Gaussian and they **are** describable by their second moments i.e., by σ^2. The diffusion from a continuous point source is assumed to be given by

$$\frac{\chi(x,y,z)}{Q} = \frac{1}{2\pi\sigma_y\sigma_z\bar{u}} \exp\left[-\left(\frac{y^2}{2\sigma_u^2} + \frac{z^2}{2\sigma_z^2}\right)\right]$$

where σ_y and σ_z are standard deviations of the lateral and vertical concentration distributions and are different functions of x, the distance from the source, for different stability categories. The present study is limited to diffusion in neutral conditions in the atmosphere which corresponds to "D" category in Pasquill's method.

The observed lateral ground level and axial vertical concentration distributions have been analyzed to obtain the standard deviations

σ_y and σ_z according to the Gaussian assumption.* A comparison of the observed σ_z with that in Pasquill model is made in Figures 66 to 69 for various wind directions. The effect of the building complex on diffusion is apparent from the high variability in concentrations for different sources at the first sampling position 1000 ft from the source. Away from the source, the data on σ_z tend to fall together but the observed σ_z is nearly always greater than that predicted by Pasquill's "D" category. The effect of the topography is synonymous to thermal instability and depends upon the wind direction. For most of the wind directions studied, σ_z predicted from Pasquill's curve is on the average 20% short of the observed value. The northwest winds blow across the valleys and cause relatively greater vertical spreads which lie midway between Pasquill's "C" and "D" categories (Fig. 67).

The comparison of data on σ_y with Pasquill is shown in Figures 70 to 73. Whereas the two compare well for winds from northwest and northeast, east and west winds cause lesser lateral spreading than Pasquill's "D" category. For east and west winds Pasquill's "E" category may represent the horizontal spread more adequately.

One of the most important characteristics of diffusion is variation of maximum ground level concentration with distance. Figures 74 to 77 compare the observed concentrations to the Pasquill's prediction curve. The rate of decrease of concentration matches well for all the wind directions. Pasquill's curve predicts concentrations for northwest and northeast winds fairly well. For east and west winds,

---

*For asymmetrical observed distributions, σ_y was taken to be average of the standard deviations of the two limbs.

the concentrations are under-predicted. A comparison of ground level concentration measured due to 250-doot stack is made in Figure 78. The plume descends much sooner than predicted by Gaussian model. This is not unexpected since the stack velocity/wind velocity ratio V_S/U_∞ was less than one. The maximum ground level concentration observed experimentally is about six times the predicted and occurs at about half the predicted distance from the source. A final comparison of observation with Gaussian plume model is made of the area under ground concentration isopleths for the source atop BLDG. NO. 707 in Figure 79. The agreement is rather complete. There is some scatter for large concentrations due to the vicinity of buildings.

These comparisons show that standard method of calculating diffusion can be used with some confidence at the Rocky Flats Plant. The effect of the topography is rather gentle and is no greater than the confidence that can be placed in the Gaussian diffusion model.

5.2 Conclusions and Recommendations

On the basis of the results from this study the following conclusions and recommendations are presented:

1) It is unlikely that hot gases released in the immediate vicinity of any processing building roof will loft above the building cavity and wake to deposit material beyond plant boundaries without leaving evidence of passage within the complex at ground level.

2) The plutonium processing complex, auxiliary buildings, and local terrain at the Rocky Flats Plant site do not markedly distort plume behavior from that suggested by classical plume model theories.

3) For those wind orientations examined there did not appear to be any most meteorologically undesirable wind direction with respect to plume trajectory or dispersion distortion.

4) An array of monitoring devices arranged along the north-south road which exists to the east of the plant site should intercept plumes if they are placed at 500 ft intervals or closer if one desires to detect plumes with 90% of maximum. If samplers are placed at 1000 ft one should detect within 60% of any maximum.

5) Release configurations studied suggested a maximum concentration of .022 by the time a plume crosses the inner security fence and a maximum concentration of .014 as a plume crosses the outer security fence (see Figure 9).

6) The effect of any future processing buildings on plume dispersion on the Rocky Flats Plant site must be examined independently of this study, since wind vector shifts and sheltered areas associated with new construction may modify plume behavior.

7) A computer model including topography, surface shear, deposition, entrainment, and soil movement should be developed for the Rocky Flats site. This program would provide real time estimation of effluent movement beyond the initial dispersion calculated by the Pasquill-Gifford type technique.

REFERENCES

Abe, Masanao, "Mountain Clouds, Their Forms and Connected Air Currents, Part II," Bull. Centr. Met. Obs., Japan 7 (3), 1941.

Briggs, G. A., Plume Rise, Atomic Energy Commission Critical Review Series, Division of Technical Information, TID-25075, 1969.

Briggs, J., "Airflow Around a Model of the Rock of Gilbraltar," Meteorological Office Scientific Paper No. 18, pp. 20, 1963.

Carson, J. E. and H. Moses, "Validity of Currently Popular Plume Rise Formulas," USAEC Meteorological Information Meeting, (September 11-14, 1967), Chalk River, Canada, AECL-2787, pp. 1-15.

Cermak, J. E., et al., "Simulation of Atmospheric Motion by Wind-Tunnel Flows," Colorado State University, Report Number CER66-67JEC-VAS-EJP-GJB-HC-RNM-SI-17, (1966).

Cermak, J. E. and J. Peterka, "Simulation of Wind Fields Over Point Arguello, California, by Wind-Tunnel Flow over a Topographic Model," Fluid Dynamics and Diffusion Laboratory, Report No. CER65JEC-LAP64, Colorado State University.

Chaudhry, F. H. and R. N. Meroney, "Turbulent Diffusion in a Stably Stratified Shear Layer," FDDC Report CER69-70FHC-RNM12, (U. S. Army Electronics Command Technical Report C-0423-5), 1969.

Corby, G. A., "The Airflow Over Mountains--A Review of the State of Current Knowledge," Quart. Jour. of the Royal Meteorological Society, Vol. 80, No. 346, pp. 491-521, 1954.

Counihan, J., "Further Measurements in a Simulated Atmospheric Boundary Layer," Atmos. Environ., Vol. 4, pp. 259-275, 1970.

Counihan, J., "An Improved Method of Simulating an Atmospheric Boundary Layer in a Wind Tunnel," Atmos. Environ., Vol. 3, pp. 197-214, 1969.

Cramer, H. E., "A Practical Method for Estimating the Dispersal of Atmospheric Contaminants," Proceedings, First Nat'l. Conf. on Appl. Meteor., Amer. Meteor. Soc., C. pp. 33-35, Hartford, Conn., (Oct. 1957).

Davies, P.O.A.L., and P. L. More, "Experiments on the Behavior of Effluent Emitted from Stacks at or Near the Roof Level of Tall Reactor Buildings," Int. Jour. Air Water Pollution, Vol. 8, pp. 515-533, (1964).

Dickson, C. R. and G. E. Start, "Plutonium Releases to the Environment at Rocky Flats," Memorandum to the Files, ESSA Research Laboratories, February 4, 1970.

Dickson, C. R., G. E. Start, and E. H. Markee, Jr., "Aerodynamic Effects of the EBR-II Containment Vessel Complex of Effluent Concentrations," USAEC Meteorological Information Meeting, Chalk River, Canada, AECL-2787, pp. 87-104, (September 11-14, 1967).

Evans, B. H., "Natural Air Flow Around Buildings," Research Report 59, Texas, Engineering Experiment Station, (1957).

Field, L. H. and R. Warden, "A Survey of Air Currents in the Bay of Gibraltar," Geophysical Memoirs, No. 59, 1929-30.

Gillies, F., (1972), "Rocky Flats It's Always There," Denver Post Bonus Section, Denver Post, March 21, 8 pp.

Halitsky, J., "Gas Diffusion Near Buildings," Geophysical Science Laboratory Report No. 63-3, New York University, (February 1963).

Halitsky, J., J. Golden, P. Halpern, and P. Wu, "Wind Tunnel Tests of Gas Diffusion from a Leak in the Shell of a Nuclear Power Reactor and from a Nearby Stack," Geophysical Sciences Laboratory Report No. 63-2, New York University, (April 1963).

Halitsky, J., J. Tolciss, and E. L. Kaplin, "Wind Tunnel Study of Turbulence in the Bear Mountain Wake," Quarterly Progress Reports No. 1, 2, 3, and 4, Contract No. DA 36-039 SC-89081, Department of Meteorology and Oceanography, New York University, 1962.

Hino, M., "Computer Experiment on Smoke Diffusion on a Complicated Topography," Atmos. Environ., Vol. 2, pp. 541-558, (1968).

Hohenleiten, H. L. von and E. Wolf, "Wind Tunnel Tests to Establish Stack Heights for the Riverside Generating Station," Trans. ASME, Vol. 64, pp. 671-683, (Oct. 1942).

Hotchkiss, R. S., "The Numerical Calculation of Three-Dimensional Flows of Air and Particulates about Structures," Los Alamos Scientific Laboratory LA-CD-13071, 8 pp., 1971, (Presented at Atmospheric Diffusion and Turbulence Meeting, New Mexico, Dec. 1971).

Jacoe, P. W., (1970), "Surveillence Information on the Rocky Flats Plant," (Letter dated June 9, 1970), Colorado Department of Health, Denver, Colorado, 6 pp.

Jensen, M., and N. Frank, "Model-Scale Test in Turbulent Wind, Part I," The Danish Technical Press, Copenhagen, (1963).

Kalinske, A. A., "Wind Tunnel Studies of Gas Diffusion in a Typical Japanese Urban District," National Defence Res. Council OSCRD Informal Report No. 10.3A-48 and 48a, (1945).

Krey, P. W. and E. P. Hardy, (1970), "Plutonium in Soil Around the Rocky Flats Plant," U. S. Atomic Energy Commission, Health and Safety Laboratory Report 235, New York, N. Y., 44 pp.

Martell, E. A. (chairman), (1970), "Report on the Dow Rocky Flats Fire: Implications of Plutonium Releases to the Public Health and Safety," Colorado Committee for Environmental Information, Boulder, Colorado, January 13, 13 pp.

Martin, J. E., "The Correlation of Wind Tunnel and Field Measurements of Gas Diffusion Using Kr-85 as a Tracer," Ph. D. Thesis, MMPP 272, University of Michigan, (June 1965).

Meroney, R. N., Cermak, J. E., and Chaudhry, F. H., "Wind Tunnel Model Study of Shoreham Nuclear Power Station Unit 1, Long Island Lighting Company," Progress Report No. 1, FDDL Report CER68-69RNM-JEC-FHC1, CSU, July 1968.

Meroney, R. N., Cermak, J. E., and Chaudhry, F. H., "Wind Tunnel Model Study of Shoreham Nuclear Power Station Unit 1, Long Island Lighting Company," Progress Report 2, CER68-69RNM-JEC-FHC14, October 1968.

Meroney, R. N. and J. E. Cermak, "Wind Tunnel Modeling of Flow and Diffusion Over San Nicolas Island," Progress Reports for 4th and 5th Quarters, Contract No. 123 (61756) 50192A (PMR), Fluid Dynamics and Diffusion Laboratory, Colorado State University, 1965.

Meroney, R. N., et.al., "Wind Tunnel Model Study of Diffusion from a Steam Electric Generating Plant at Stock Island, Key West, Florida," FDDL Report CER69-70RNM-JEC-BTY-SU-CRS14.

Meroney, R. N., and C. R. Symes, "Cone Frustrums in a Shear Layer," FDDL Report CER70-71CRS-RNM11, (AEC Report No. C00-2053-5), 1970.

Meroney, R. N. and B. T. Yang, "Gaseous Dispersion into Stratified Building Wakes," FDDL Report CER70-71BTY-RNM8 (AEC Rept. No. C00-2053-3), 1970.

Meroney, R. N. and B. T. Yang, "Wind Tunnel Study on Gaseous Mixing Due to Various Stack Heights and Injection Rates Above an Isolated Structure," FDDL Report CER71-72RNM-BTY16 (AEC Control Report No. C00-2053-6), 1971.

Munn, R. E. and A. F. W. Cole, "Turbulence and Diffusion in the Wake of the Building," Atmospheric Environment, Vol. 1, pp. 34-43, (1967).

Nemoto, S., "Similarity Between Natural Wind in the Atmosphere and Model Wind in a Wind Tunnel," Papers in Meteorology and Geophysics, Tokyo, Vol. 12, No. 1, pp. 30-52, 1961; Vol. 12, No. 2, pp. 117-128, 1961; Vol. 12, No. 2, pp. 129-154, 1961; and Vol. 13, No. 2, pp. 171-195, 1962.

Orgill, M. M., J. E. Cermak, and L. O. Grant, "Laboratory Simulation and Field Estimates of Atmospheric Transport-Dispersion over Mountainous Terrian," Fluid Dynamics and Diffusion Laboratory Technical Report CER70-71MMO-JEC-LOG40, May 1971.

Overman, R. T. and H. M. Clark, Radioisotope Techniques, McGraw-Hill Book Co., Inc., New York, 1960.

Pasquill, F., Atmospheric Diffusion, D. Van Nostrand Co., London, (1962).

Reynolds, O., "On the Dynamical Theory of Incompressible Viscous Fluids and the Determination of the Criterion," Phil. Trans. A., 186, 1894.

Roberts, O. F. T., "The Theoretical Scaling of Smoke in a Turbulent Atmosphere," Proc. Roy. Soc., A. 104, p. 640, (1923).

Shepherd, J., "The Nuclear Threat Inside America," Look, Vol. 34, #25, pp. 21-27, December 15, 1971.

Shepherd, J., (1968), Rocky Flast Climatology, (Prepared by Rocky Flats Division, Dow Chemical Company, Health Physics), 10 pp.

Sherlock, R. H. and E. A. Stalker, "The Control of Gases in the Wake of Smokestacks," Mechanical Engineering, Vol. 62, No. 6, pp. 455-458, (June 1940).

Slade, D., ed., (1968), Meteorology and Atomic Energy - 1968, U. S. Atomic Energy Commission, Division of Technical Information, TID-24190, 445 pp.

Strom, G. H., M. Hackman, and E. J. Kaplin, "Atmospheric Dispersal of Industrial Stack Gases Determined by Concentration Measurements in Scale Model Wind Tunnel Experiments," J. of APCA, Vol. 7, No. 3, pp. 198-204, (November 1957).

Sutton, O. G., "The Theoretical Distribution of Airborne Pollution from Factory Chimneys," Quar. J. R. Meteor. Soc. 73, p. 426, (1947).

TABLE I WEST WIND VERTICAL VARIATION OF CONCENTRATION AT PLUME AXIS

Source	x=1000'		x=2500'		x=4000'		x=6000'		x=9000'	
	z	Conc	z	Conc	z	Conc	z	Conc	z	Conc
#1	0	43787	0	10521	0	5123	21	3104	42	1331
	42	25857	42	9023	42	4597	63	2928	125	1290
	83	11305	83	6576	83	3662	105	2667	208	1076
	125	3498	167	3066	167	2531	188	1733	333	665
	167	929	250	1114	250	1380	313	958	458	321
	208	208	333	275	333	590	438	448	583	150
	250	29	417	55	417	240	563	113	708	55
	333	26	500	14	500	61	688	55	833	0
#3	0	43616	0	10530	21	5334	21	2783	42	1872
	42	35623	42	9477	63	4658	63	2557	125	1611
	83	14979	83	7446	105	4154	105	2161	208	1400
	125	2546	167	3254	188	2575	188	1568	333	984
	167	362	250	732	271	1203	313	622	458	622
	208	92	333	142	355	408	438	116	583	208
	250	0	417	0	438	148	563	20	708	98
	333	20	500	0	521	35	688	14	833	91

Source	x=1000'		x=2500'		x=4000'		x=6000'		x=9000'	
	z	Conc	z	Conc	z	Conc	z	Conc	z	Conc
#2	0	31124	0	9501	0	5115	0	2496	42	1449
	42	27725	42	8034	42	4704	42	2491	125	1383
	83	17557	83	6110	83	3790	83	2317	208	1100
	125	8615	167	2635	167	2170	167	1678	333	840
	167	3120	250	787	250	998	292	813	458	492
	208	1117	333	107	333	500	417	191	583	284
	250	119	417	14	417	98	542	64	708	64
	333	0	500	26	500	35	667	6	833	46
#5	0	1282	0	3460	0	3460	0	2167	0	1374
	83	8389	83	4287	83	3049	83	1895	167	1140
	167	16591	167	4339	167	2971	167	1822	333	683
	250	4420	250	2873	250	2774	250	1261	500	428
	333	286	333	1114	333	2086	333	1004	667	171
	417	0	417	226	417	1125	417	581	833	0
	500	0	500	20	500	506	542	197	1000	20
	583	14	583	6	583	176	667	41	1167	6

Source	x=1000'		x=2500'		x=4500'		x=7500'	
	z	Conc	z	Conc	z	Conc	z	Conc
#4	0	41516	0	7872	0	5444	0	1493
	42	21879	42	6468	42	4658	42	1753
	83	8300	83	4247	83	4001	83	1626
	125	2254	167	1533	167	2635	167	1380
	167	451	250	390	250	1169	292	778
	208	84	333	92	333	674	417	399
	250	29	417	29	417	260	542	162
	333	0	500	6	500	101	667	81

TABLE II NORTHWEST WIND VERTICAL VARIATION OF CONCENTRATION AT PLUME AXIS

Source	x=1000'		x=2500'		x=4000'		x=6000'			
	z	Conc	z	Conc	z	Conc	z	Conc	z	Conc
#1	0	20592	0	4634	0	3228				
	42	31061	42	4478	83	3168				
	83	28281	83	4192	167	2473				
	125	14010	125	3159	250	1490				
	167	4579	167	2297	333	798				
	208	775	208	1345	417	301				
	250	52	292	417	500	40				
	292	87	375	104						
#3	0	27796	0	8476	21	3908	0	2129		
	42	26571	42	7631	63	3836	83	1857		
	83	17181	83	6714	146	3315	167	1565		
	125	5878	125	4270	229	2132	250	1148		
	167	1802	167	3107	312	1484	333	700		
	208	472	208	1768	395	703	458	324		
	250	75	292	538	478	269	583	35		
	292	69	375	35	562	179	708	9		
#5	0	1044	63	3743	0	2346	0	1253		
	83	4675	146	3781	83	2387	83	1232		
	125	9445	188	3625	167	1941	167	1250		
	167	12130	230	3049	250	1915	250	1148		
	208	10582	272	2580	333	1420	333	775		
	250	5991	314	1704	417	900	417	561		
	333	833	397	610	500	477	500	362		
	417	17	480	52	583	197	583	205		

Source	x=1000'		x=2500'		x=4000'		x=6000'			
	z	Conc	z	Conc	z	Conc	z	Conc	z	Conc
#2	0	27436	0	7420	63	3214	0	1912		
	42	24416	42	8112	105	3197	42	2068		
	83	16400	83	6963	188	2566	125	2008		
	125	7012	125	5352	271	1715	208	1634		
	167	2566	167	3934	354	992	292	1470		
	208	584	208	2809	437	407	375	992		
	250	107	292	1067	520	162	458	656		
	292	43	375	281	603	69	541	356		
#4	0	48768	42	6756	0	3223				
	42	33424	83	5444	83	3266				
	83	11948	125	4041	167	2190				
	125	3981	167	2271	250	1163				
	167	1339	208	1290	333	498				
	208	310	250	590	417	191				
	250	61	333	101	500	41				
	292	35								

TABLE III NORTHEAST WIND VERTICAL VARIATION OF CONCENTRATION AT PLUME AXIS

Source	x=1000'		x=2500'		x=4000'		x=6000'			
	z	Conc	z	Conc	z	Conc	z	Conc	z	Conc
#1	10	30106	21	6798	10	3966				
	52	24187	63	5129	52	3425				
	93	9058	105	3191	135	1817				
	135	2719	147	1539	218	958				
	177	738	188	1175	302	281				
	218	133	230	257	385	9				
	260	6	313	6						
#3	0	15714	21	5387	0	4652	0	2465		
	21	18789	63	5977	42	4154	42	2638		
	63	11768	105	4663	125	3020	125	1964		
	105	4851	147	3344	208	1915	208	1339		
	147	1374	188	2051	292	778	292	712		
	188	168	230	984	375	226	375	284		
	230	29	313	162	458	78	458	153		
			396	14			542	46		
#5	21	1721	21	3234	21	2861	21	1967		
	104	8141	63	3992	104	3226	104	1825		
	187	11872	105	4551	187	2485	187	1744		
	229	6694	147	4860	271	1553	271	1227		
	271	2152	230	3570	354	683	354	683		
	313	324	313	1140	437	142	479	284		
	355	49	396	260	521	49	604	49		
			480	67	604	14	729	41		

Source	x=1000'		x=2500'		x=4000'		x=6000'			
	z	Conc	z	Conc	z	Conc	z	Conc	z	Conc
#2	21	20817	0	6324	21	3874	0	2245		
	63	20921	42	5742	63	3359	42	2343		
	105	10683	83	4848	146	1886	125	1831		
	147	3443	125	3226	239	894	208	1470		
	188	888	167	1976	322	532	292	1059		
	230	124	208	1223	405	234	375	474		
	272	14	292	217	489	49	458	217		
			375	14	572	20	541	122		
#4	21	39604	21	10903	10	5016	10	2491		
	63	21963	63	7750	52	4308	52	2271		
	105	6217	105	3477	135	2083	135	1739		
	147	1261	147	1206	218	596	218	1033		
	188	220	188	445	302	145	302	608		
	230	9	230	93	285	17	385	249		
			313	14			468	29		
							552	14		

TABLE IV EAST WIND VERTICAL VARIATION OF CONCENTRATION AT PLUME AXIS

Source	x=1000'		x=2500'		x=4000'		x=6000'		x=9000'		Source	x=1000'		x=2500'		x=4000'		x=6000'		x=9000'	
	z	Conc	z	Conc	z	Conc	z	Conc	z	Conc		z	Conc	z	Conc	z	Conc	z	Conc	z	Conc
#1	0	62131	10	15859	10	7652	5	3688	5	2042	#2	5	27167	10	9168	10	4458	0	2971	0	1409
	42	35397	52	12468	52	6845	47	3405	47	1921		47	25339	52	8167	52	6872	42	2598	42	1423
	83	10874	93	9304	135	3986	130	2534	130	1351		89	14609	93	6110	135	3295	125	2274	125	1224
	125	1733	135	5901	218	2074	255	1406	255	984		131	4935	135	4608	218	1970	250	1415	250	972
	167	165	177	3564	302	958	380	477	380	477		172	1018	177	2899	302	978	375	677	375	581
	208	78	218	1791	385	217	505	133	505	182		214	107	218	1906	385	257	500	234	500	240
			260	709	468	55	630	93	630	35				260	830	468	29	625	78	625	93
			302	81	552	14	755	14	755	14				343	162	552	14	750	41	750	26
#3	42	26716	10	9370	0	5413	0	2905	0	1620	#5	21	787	21	2482	10	2161	21	1588	21	972
	83	25255	52	8661	42	5230	42	2855	42	1539		104	4273	104	3385	93	2372	104	1565	104	992
	125	10825	93	6090	125	3255	125	2210	125	1267		187	12194	187	4148	176	2303	187	1296	187	712
	167	2621	135	4093	208	2025	250	1296	250	694		229	9905	270	3234	260	1906	312	694	312	451
	208	532	177	2522	292	807	375	547	375	281		271	5606	354	1464	343	993	437	362	437	205
	250	67	218	1224	375	200	500	182	500	124		313	2300	437	341	426	466	562	84	604	67
			260	541	458	69	625	49	625	49		355	584	520	78	510	162	687	28	771	--
			343	46	541	14	750	20	750	41		438	20			593	46			938	20

	x=1000'		x=2500'		x=4000'		x=5500'		x=7500'			x=10500'	
#4	0	29467	0	11337	21	5395	0	4212	10	2878	#4	0	1148
	42	28084	42	10692	63	5332	42	4131	52	2592		42	1189
	83	9127	83	7579	146	3006	125	3104	135	2170		125	1140
	125	2045	125	4698	229	1449	208	2546	218	1684		208	833
	167	466	167	2687	313	445	292	1175	302	1004		292	457
	208	35	208	1400	396	41	375	474	385	567		375	249
			250	550	479	20	458	142	468	324		458	41
			333	81	563	35	542	35	552	122		542	20

TABLE V WEST WIND GROUND LEVEL CONCENTRATIONS

Source	x=1000'		x=2500'		x=4000'		x=6000'		x=9000'	
	Y	Conc	Y	Conc	Y	Conc	Y	Conc	Y	Conc
#1	292	75	417	58	541	110	750	49	625	495
	208	1666	250	1606	334	1530	563	208	417	940
	125	10507	125	6972	167	5115	375	703	208	1220
	42	40937	0	12876	0	5832	187	2094	0	1652
	-42	48132	-83	12749	-83	3194	0	3023	-187	1614
	-125	25862	-208	4368	-250	717	-187	3032	-375	1125
	-208	636	-323	732	-417	14	-375	1701	-584	550
	-292	90	-500	61	-625	20	-563	576	-791	182
#2	292	168	417	168	541	211	667	84	790	0
	208	955	250	2329	334	1499	417	992	458	182
	125	5977	125	4874	167	3642	208	2317	208	836
	42	24248	0	7793	0	5450	0	3315	0	1339
	-42	36526	-83	9818	-83	5641	-125	2661	767	1661
	-125	27043	-208	9413	-250	4493	-333	1684	-375	1467
	-208	11890	-323	6460	-417	2583	-541	639	-625	845
	-292	2962	-500	2170	-625	1044	-790	197	-958	257

Source	x=1000'		x=2500'		x=4500'		x=7500'	
	Y	Conc	Y	Conc	Y	Conc	Y	Conc
#3	292	1678	540	0	625	73	667	243
	208	9032	375	448	417	1041	417	1134
	125	30581	250	1872	250	2965	308	2494
	42	51192	125	5664	83	5358	0	3532
	-42	41067	42	14424	0	6173	-125	3113
	-125	14810	-42	7322	-167	6304	-333	2066
	-208	1901	-167	1886	-333	5071	-540	1096
	-292	304	333	116	-541	955	-791	379
#4	417	84	458	1264	625	228	750	127
	292	4322	333	6590	458	758	540	538
	208	33401	208	14843	333	1886	333	1345
	125	66267	125	14994	208	3830	167	1837
	42	55086	42	11939	83	5010	0	2682
	-42	27665	-42	7857	-42	5782	-167	2433
	-125	4394	-167	2702	-167	4174	-375	1082
	-250	101	-292	500	-333	1253	-583	373
#5	333	17	354	538	520	211	833	174
	208	41	250	1626	458	278	707	402
	125	315	146	3289	437	457	583	570
	42	567	42	3816	292	746	375	1545
	-42	391	-42	3173	167	1406	167	2106
	-125	49	-146	1556	83	1857	0	2135
	-208	20	-250	521	0	2216	-167	1634
	-333	0	-354	168	-83	3040	-333	1166
					-208	2175	-500	541
					-333	819	-667	292
					-437	136	-750	191

TABLE VI NORTHWEST WIND GROUND LEVEL CONCENTRATIONS

Source	x=1000'		x=2500'		x=2500'		x=4000'		x=4000'	
	Y	Conc	Y	Conc	Y	Conc	Y	Conc	Y	Conc
#1	292	43	375	35	-625	3223	417	104	-667	1360
	208	469	250	362	-750	2256	250	709	-750	1305
	125	5589	125	1371	-875	1351	83	1880	-915	634
	42	14910	0	3052	-1000	812	-83	3090	-1165	104
	-42	27413	-125	4892	-1125	512	-167	3246	-1500	35
	-125	28249	-250	6570	-1250	275	-250	3315		
	-208	7400	-375	5974	-1375	55	-417	2754		
	-292	252	-500	4594	-1500	26	-500	2366		

Source	x=1000'		x=2500'		x=2500'		x=4000'		x=6000'	
	Y	Conc	Y	Conc	Y	Conc	Y	Conc	Y	Conc
#2	500	104	500	69	-167	2722	625	110	750	43
	375	350	417	648	-250	1470	417	503	500	417
	292	4507	333	1753	-333	341	208	1548	250	1542
	208	21017	250	3107	-417	87	0	3171	0	2233
	125	31266	167	8216			-208	3194	-250	1429
	42	26337	83	9338			-417	2398	-500	758
	-42	16134	0	7802			-625	1180	-792	246
	-125	4577	-83	6087			-833	428	-1083	87
	-208	2673								
	-292	237								

	x=1000'		x=2500'		x=4000'		x=6000'	
#3	333	145	500	304	500	145	688	237
	208	4510	333	3078	292	804	458	752
	125	20956	167	8627	83	2430	229	1872
	42	36974	0	7125	-125	3836	0	2164
	-42	27268	-167	2421	-333	3214	-229	1776
	-125	10975	-333	515	-541	865	-458	741
	-208	5141	-500	84	-750	20	-688	388
	-333	1003	-750	14			-916	156

	x=1000'		x=2500'		x=4000'	
#4	375	9	500	110	875	26
	250	726	250	1062	541	388
	125	35108	83	3315	208	1513
	0	68752	-83	6645	0	3072
	-125	23910	-250	8919	-208	4131
	-250	341	-417	8577	-541	3850
			-667	3541	-875	1877
			-916	272	-1205	237

#5	208	179	625	69	541	46	730	119
	125	529	375	665	333	492	520	336
	63	576	250	1921	167	2019	312	958
	0	532	125	3133	0	2673	104	1574
	-63	341	0	2647	-208	1750	-104	1756
	-125	84	-125	1591	-416	298	-312	1414
	-208	--	-250	359	-625	20	-520	697
	-292	6	-457	26			-730	278

TABLE VII NORTHEAST WIND GROUND LEVEL CONCENTRATIONS

Source	x=1000'		x=2500'		x=4000'		x=6000'			
	Y	Conc	Y	Conc	Y	Conc	Y	Conc	Y	Conc
#1	250	10929	583	4594	1020	440				
	167	27873	458	6503	833	1128				
	83	46700	333	7550	645	2033				
	0	39092	208	8658	458	3081				
	-83	11841	83	5763	270	4255				
	-167	1241	-42	2623	83	4634				
	-250	20	-167	619	-104	1817				
			-292	101	-292	324				
#3	333	211	478	9	500	118	833	162		
	208	2363	333	188	333	564	583	717		
	125	8010	208	1238	167	2465	333	2091		
	42	19553	83	4267	0	3748	83	2427		
	-42	24425	-42	8369	-167	3816	-83	1950		
	-125	16894	-167	8418	-333	891	-333	998		
	-208	7414	-292	5508	-500	527	-583	211		
	-333	4085	-437	2265	-667	35	-833	20		
#5	188	9	417	17	541	35	1083	9		
	125	194	250	1073	333	356	833	168		
	63	301	125	2190	167	1562	667	558		
	0	804	0	3385	0	3052	417	1363		
	-63	888	-125	2737	-167	2763	208	2118		
	-125	665	-250	1631	-333	1250	0	1649		
	-250	168	-375	500	-500	190	-208	622		
	-333	81	-542	46			-417	301		
							-625	78		
							-1125	12		

Source	x=1000'		x=2500'		x=4000'		x=6000'			
	Y	Conc	Y	Conc	Y	Conc	Y	Conc	Y	Conc
#2	208	382	167	605	625	153	853	136		
	125	2705	0	5366	417	1389	625	859		
	42	13429	167	10391	208	3795	395	1449		
	-42	25998	333	4284	0	3489	167	2352		
	-125	35145	500	388	-208	1695	63	2476		
	-208	18318	667	14	-417	249	292	1192		
	-333	2861					521	324		
#4	125	191	500	660	573	4198	667	373		
	42	7585	417	2034	458	5268	500	1108		
	-42	61943	333	5002	333	5540	333	2092		
	-125	37315	250	10007	208	6159	167	2948		
	-208	4443	167	12833	83	5595	0	3159		
	-292	20	83	10628	-42	3188	-167	2925		
			0	7348	-167	1050	-333	1661		
			-83	1831	-292	289	-500	738		
			-167	567						
			-250	78						
			-333	35						

TABLE VIII EAST WIND GROUND LEVEL CONCENTRATIONS

Source	x=1000'		x=2500'		x=4000'		x=6000'		x=9000'	
	Y	Conc	Y	Conc	Y	Conc	Y	Conc	Y	Conc
#1	250	69	333	229	375	457	500	211	584	171
	167	2789	208	2424	250	2673	333	1270	375	706
	83	35403	83	15800	125	6393	167	3417	208	1582
	0	98309	0	17241	0	8378	42	4718	42	2323
	-83	43940	-83	13052	-125	6243	-83	4065	-83	2236
	-167	2225	-167	6188	250	2482	-208	2323	-250	1499
	-250	29	-292	599	375	359	-375	576	-417	683
			-417	20	500	87	-542	95	-625	127
#3	333	819	437	78	542	78	375	625	625	26
	208	2398	313	1073	375	524	188	1655	417	315
	125	8534	188	4360	208	2204	0	2656	208	683
	42	21852	63	7759	42	3726	-188	3385	0	1351
	-42	41117	-63	12734	-83	4432	-375	2225	-208	1886
	-125	24995	-188	10299	-250	5387	-563	723	-417	1883
	-208	4148	-313	5141	-417	2815	-750	162	-625	1041
	-333	182	-437	1036	-584	500			-813	353

Source	x=1000'		x=2500'		x=4000'		x=6000'		x=9000'	
	Y	Conc	Y	Conc	Y	Conc	Y	Conc	Y	Conc
#2	292	793	437	171	542	43	604	69	625	52
	208	4785	313	1013	375	610	417	422	417	168
	125	16967	188	4114	208	3477	371	1365	208	900
	42	36265	63	8861	42	5812	42	2774	0	1559
	-42	35536	-63	10328	-83	4681	-125	2963	-208	1661
	-125	13145	-188	5702	-250	2473	-312	1857	-417	1215
	-208	2447	-313	1455	-417	697	-500	781	-625	717
	-292	176	-437	561	-584	87	-688	150	-833	136
#5	125	35	167	64	438	9	417	69	417	43
	63	162	42	437	292	67	250	174	208	203
	0	246	-83	1334	146	379	83	555	0	515
	-63	304	-208	1499	0	963	-83	1296	-208	938
	-125	321	-375	801	-146	2011	-250	1750	-417	1229
	-188	174	-542	168	-292	1973	-417	1733	-625	1015
	-250	119			-438	1146	-584	929	-833	550
	-313	14			-584	284	-751	338	-1041	217

	x=1000'		x=2500'		x=4000'		x=5500'		x=7500'	
#4	292	61	375	69	417	492	541	9	625	17
	208	321	250	972	240	2450	333	402	417	182
	125	13134	125	5129	83	6463	167	1661	208	900
	42	54499	0	12604	-42	7452	0	4400	0	2497
	-42	64341	-83	13411	-167	6538	-167	4825	-208	3038
	-125	44351	-208	11337	-292	4241	-333	2942	-417	1932
	-208	22000	-333	5768	-459	1892	-500	1120	-625	576
	-292	9969	-458	1438	-625	197	-708	176	-833	41

Source	x=10500'	
	Y	Conc
#4	625	61
	375	208
	167	703
	-42	1449
	-250	1976
	-458	1516
	-666	660
	-916	101

TABLE IX NONDIMENSIONAL CONCENTRATIONS AT INNER AND OUTER PLANT BOUNDARIES

Source Number / Wind Direction	#1		#2		#3		#4		STACK	
	INNER	OUTER	INNER	OUTER	INNER	OUTER	INNER	OUTER	INNER	OUTER
West	21150	4750	9580	4460	14900	5450	90200	49000	4000	2850
Northwest	4690	1315	10940	1700	17600	1715	5620	1450	1250	1535
Northeast	--	3610	10950	2200	6500	--	21100	2950	3860	1460
East	12000	4980	7660	3190	13500	3450	5620	3300	1370	1800

Numbers in table are $\frac{\chi \bar{u} L^2}{Q} \times 10^{-6}$

INNER - Inner security fence

OUTER - Outer security fence

Note: Dosage is

$$D = \left(\frac{\chi \bar{u} L^2}{Q}\right) \times \left(\frac{V_s}{\bar{u}}\right)\left(\frac{A_s}{L^2}\right)$$

where V_s = source exit velocity

A_s = source area

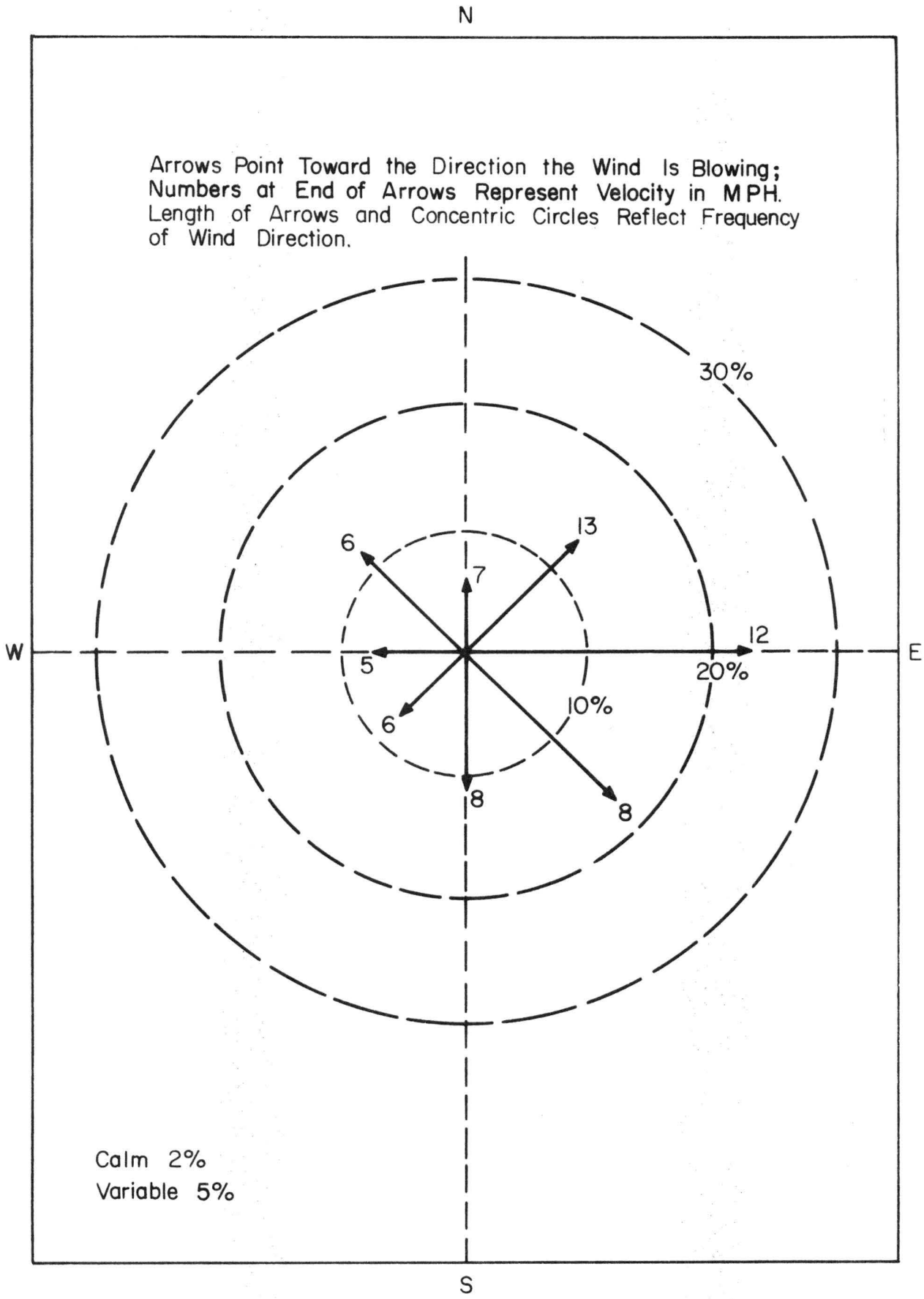

Fig. 1. Average wind rose at Rocky Flats Plant 1953-1970

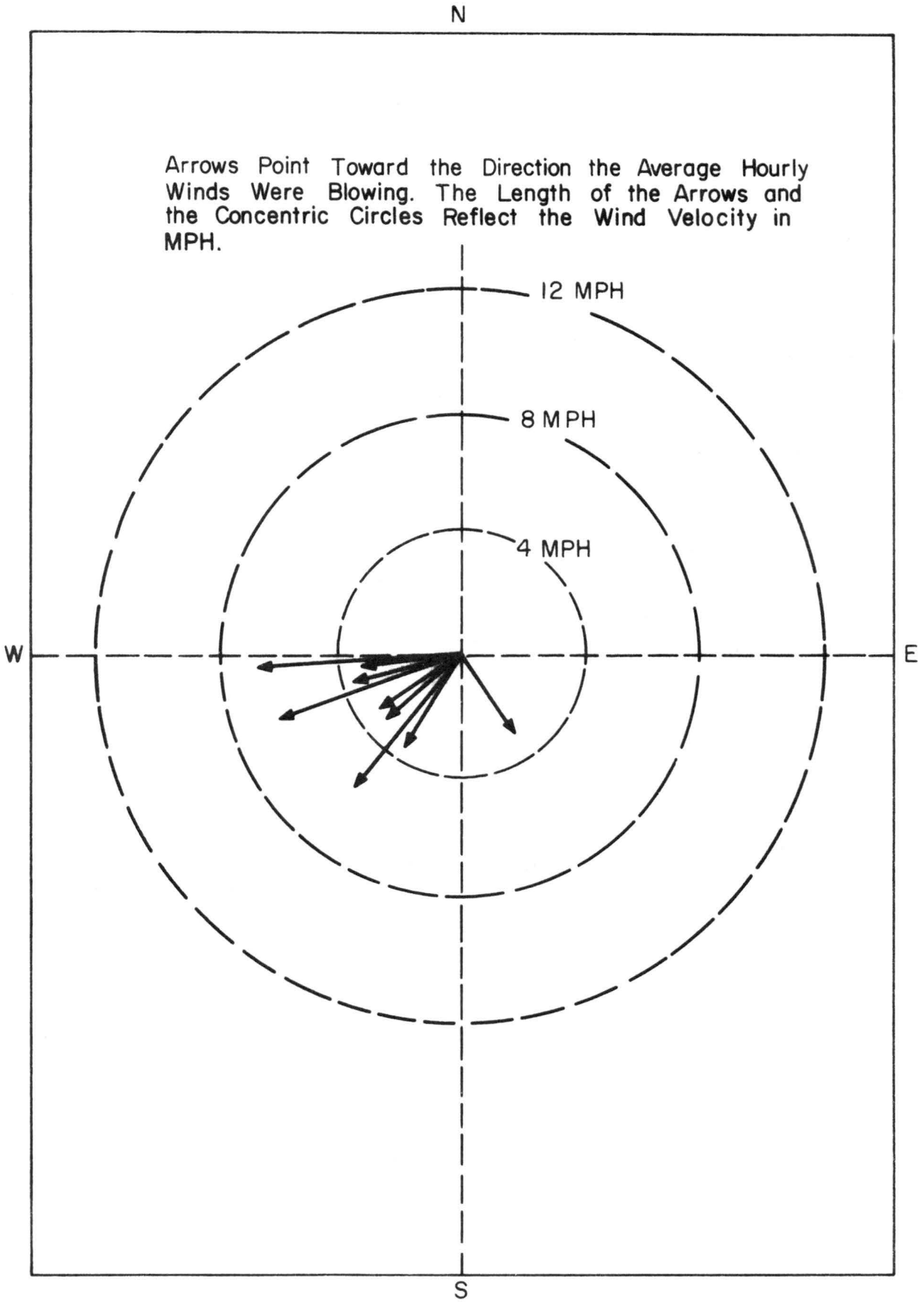

Fig. 2. Average hourly winds during fire of May 11, 1969

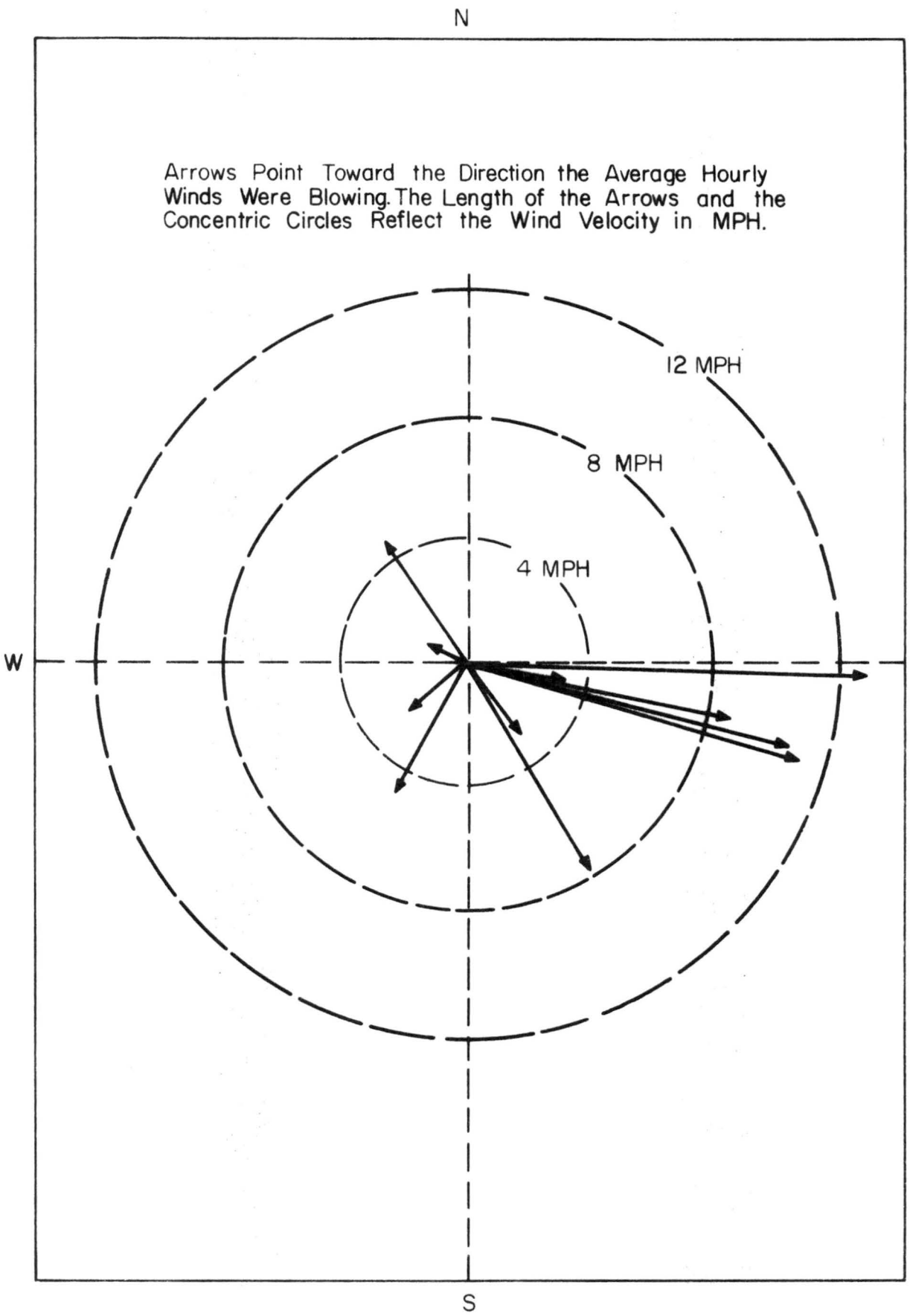

Fig. 3. Average hourly winds during fire of September 11, 1957

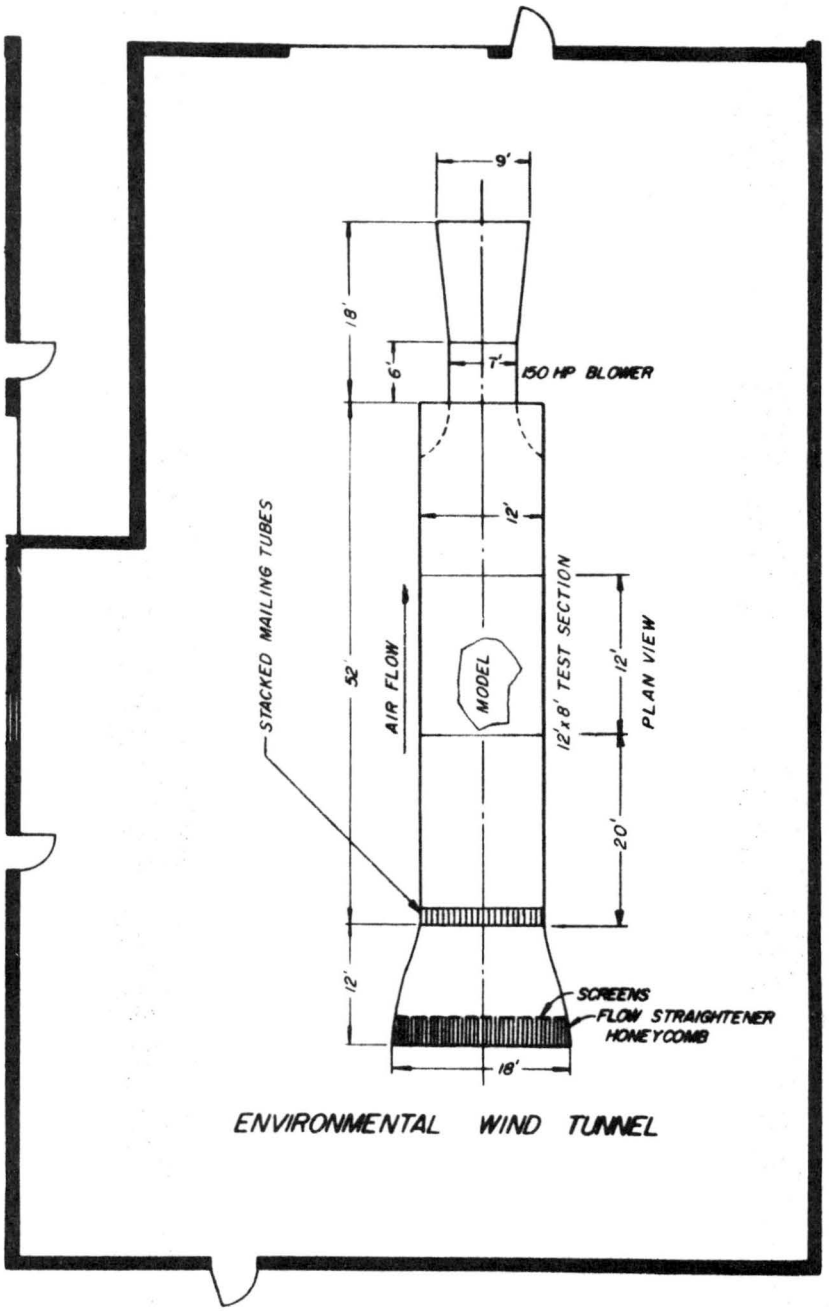

Fig. 4. Environmental wind tunnel

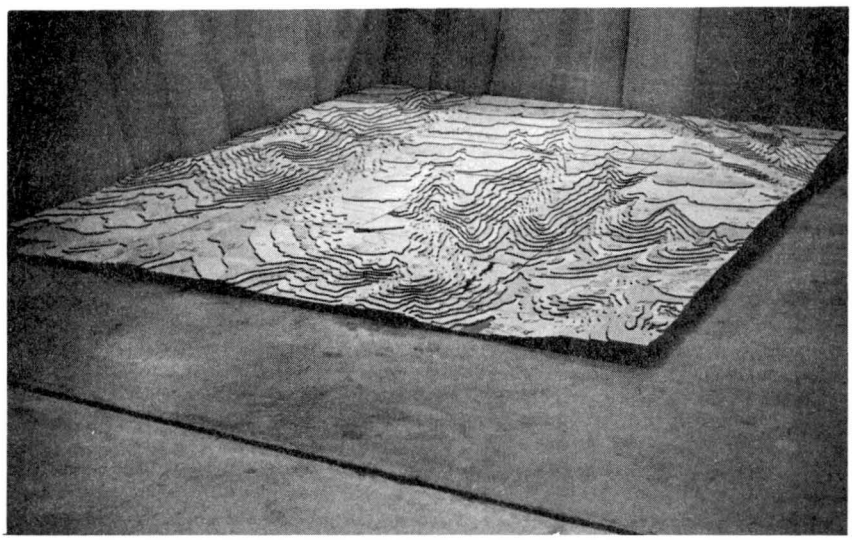

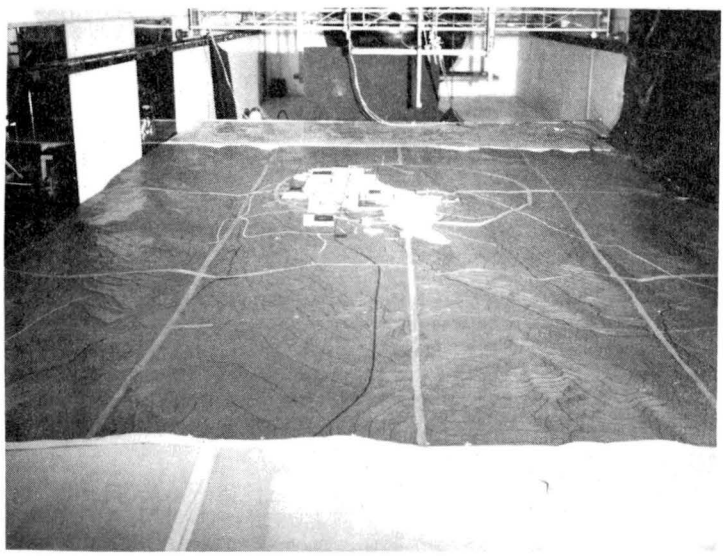

Fig. 5. Rocky Flats topographical model during construction and in wind tunnel

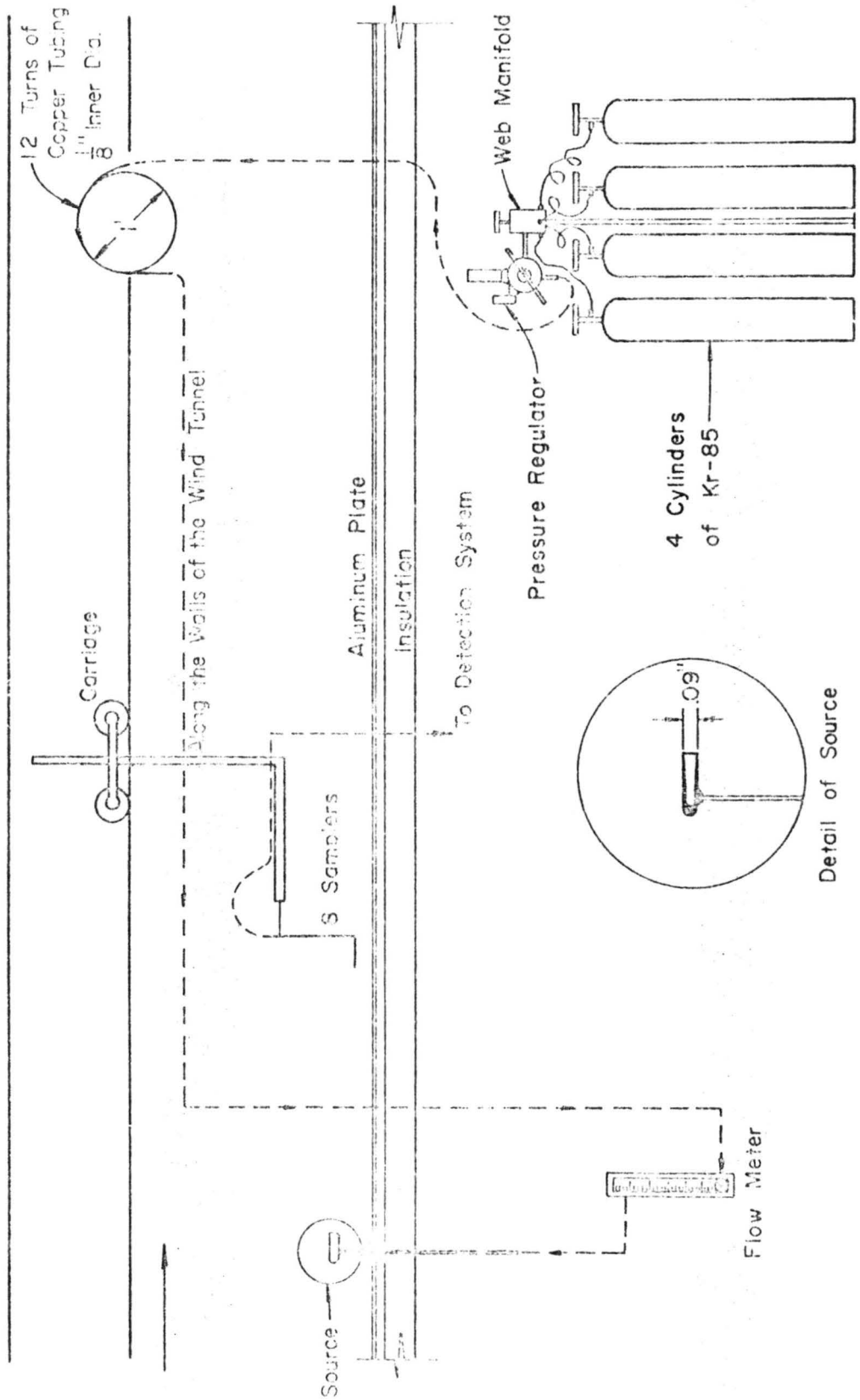

Fig. 6. Gas tracer apparatus - source

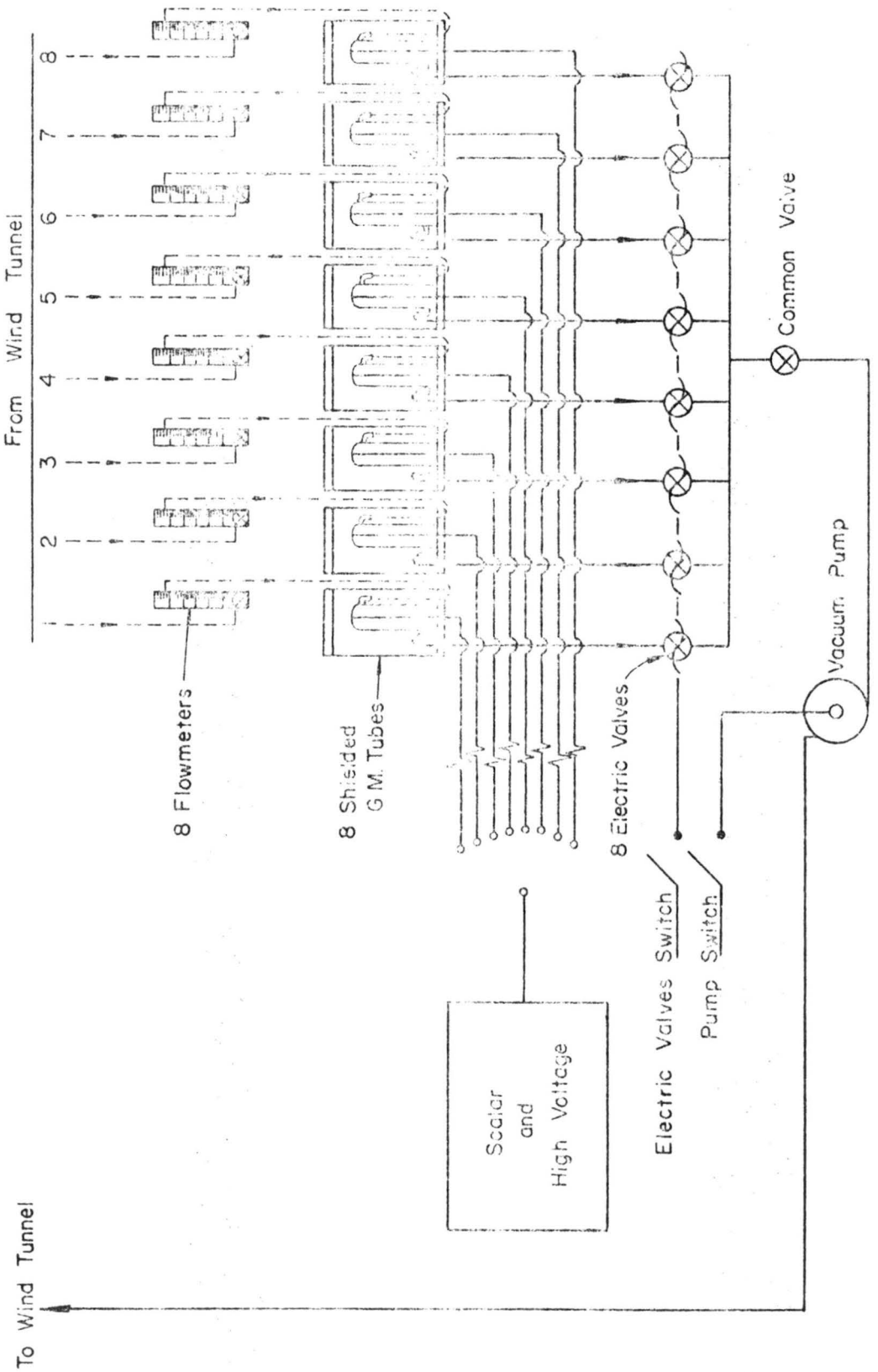

Fig. 7. Gas tracer apparatus - sampler

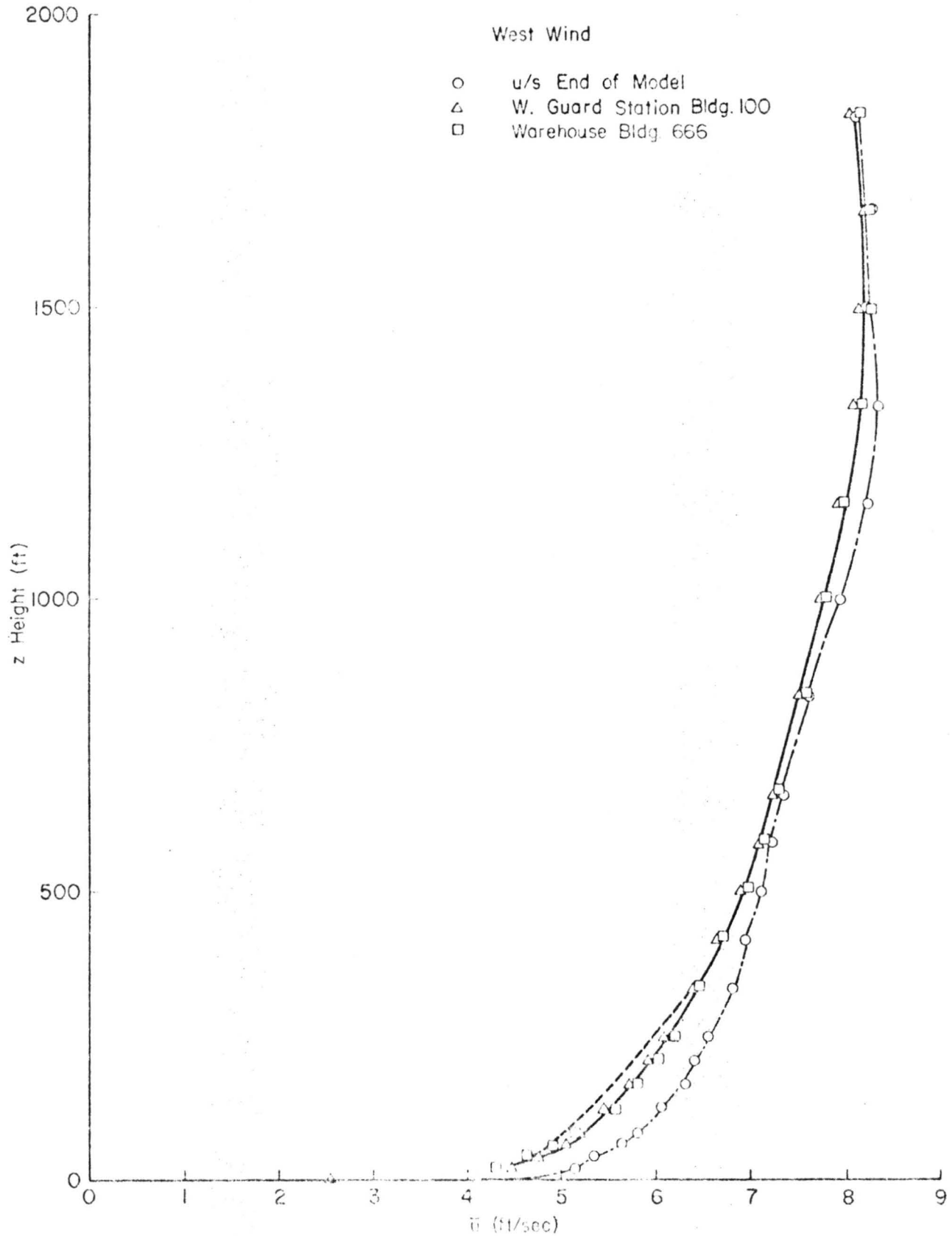

Fig. 8. Vertical wind profiles - west wind

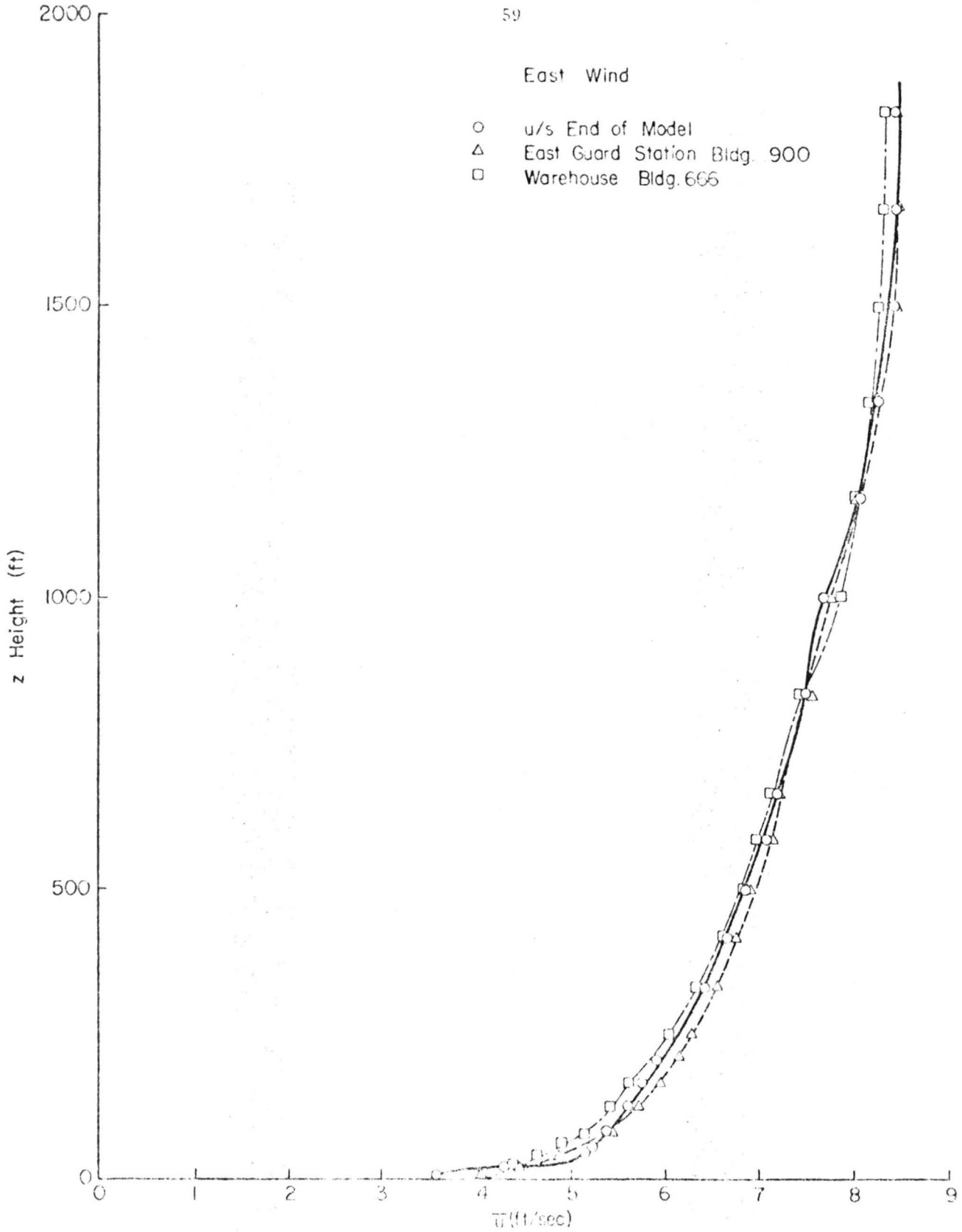

Fig. 9. Vertical wind profiles - east wind

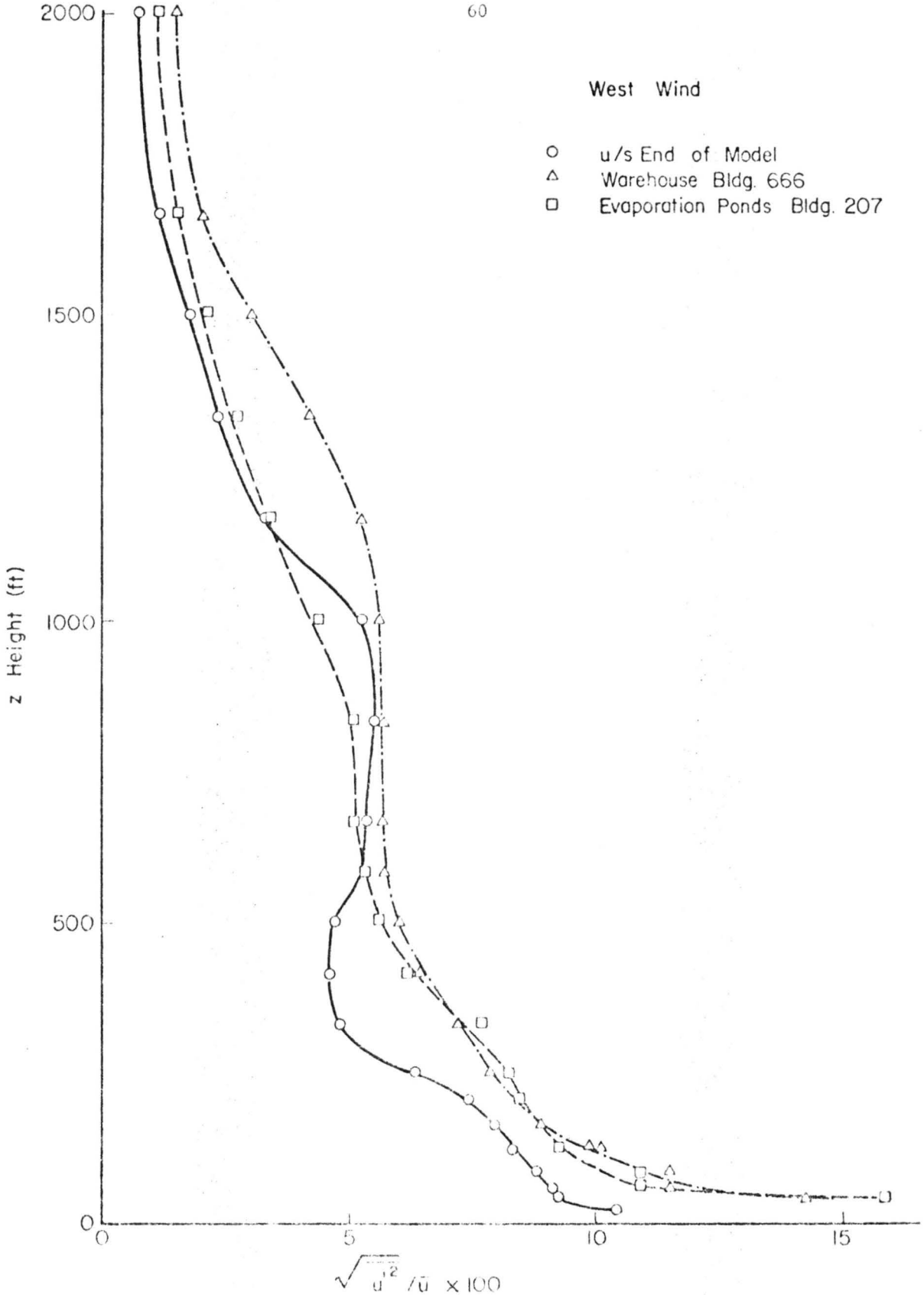

Fig. 10. Vertical turbulent intensity profiles - west wind

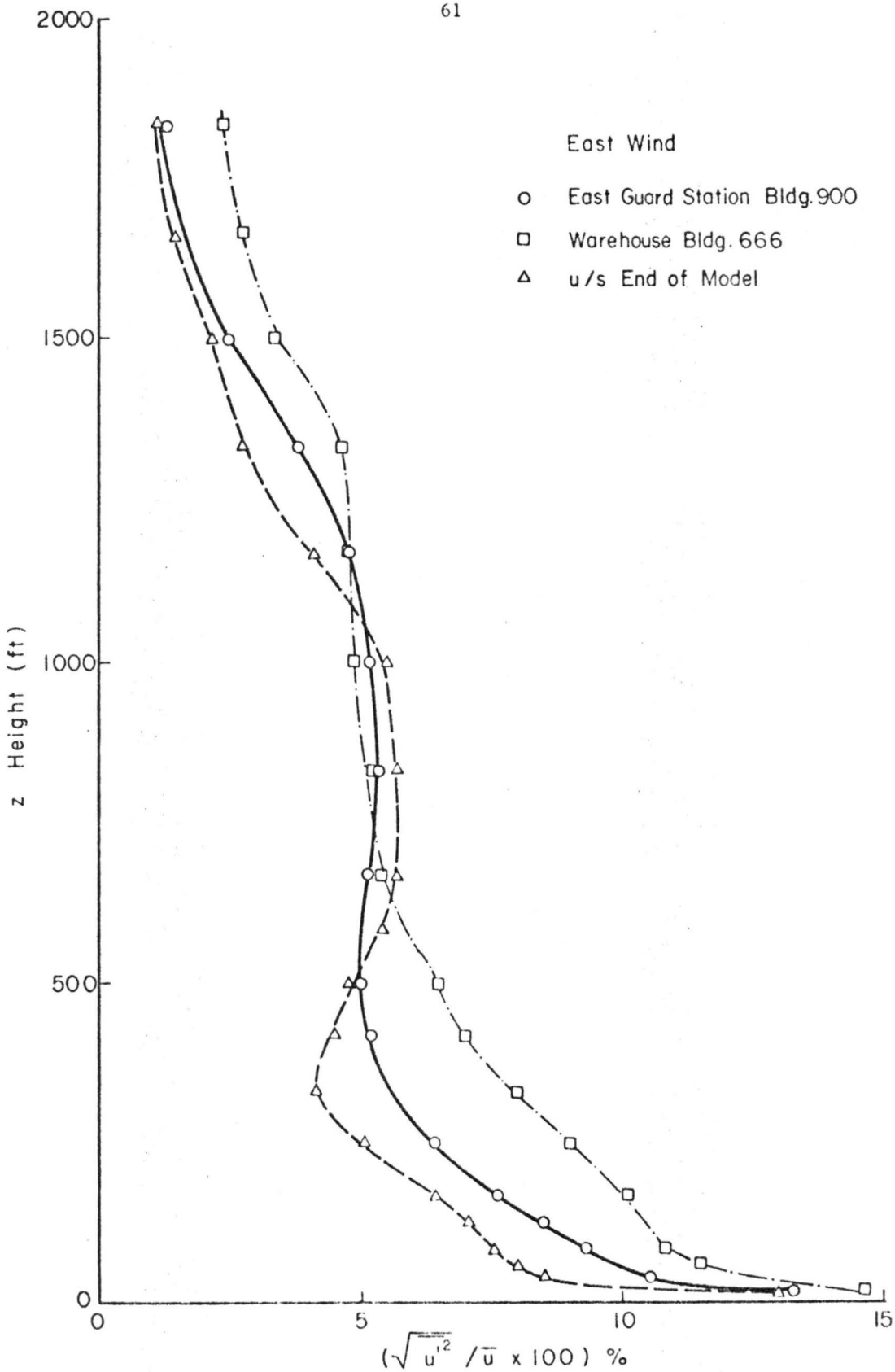

Fig. 11. Vertical turbulent intensity profiles - east wind

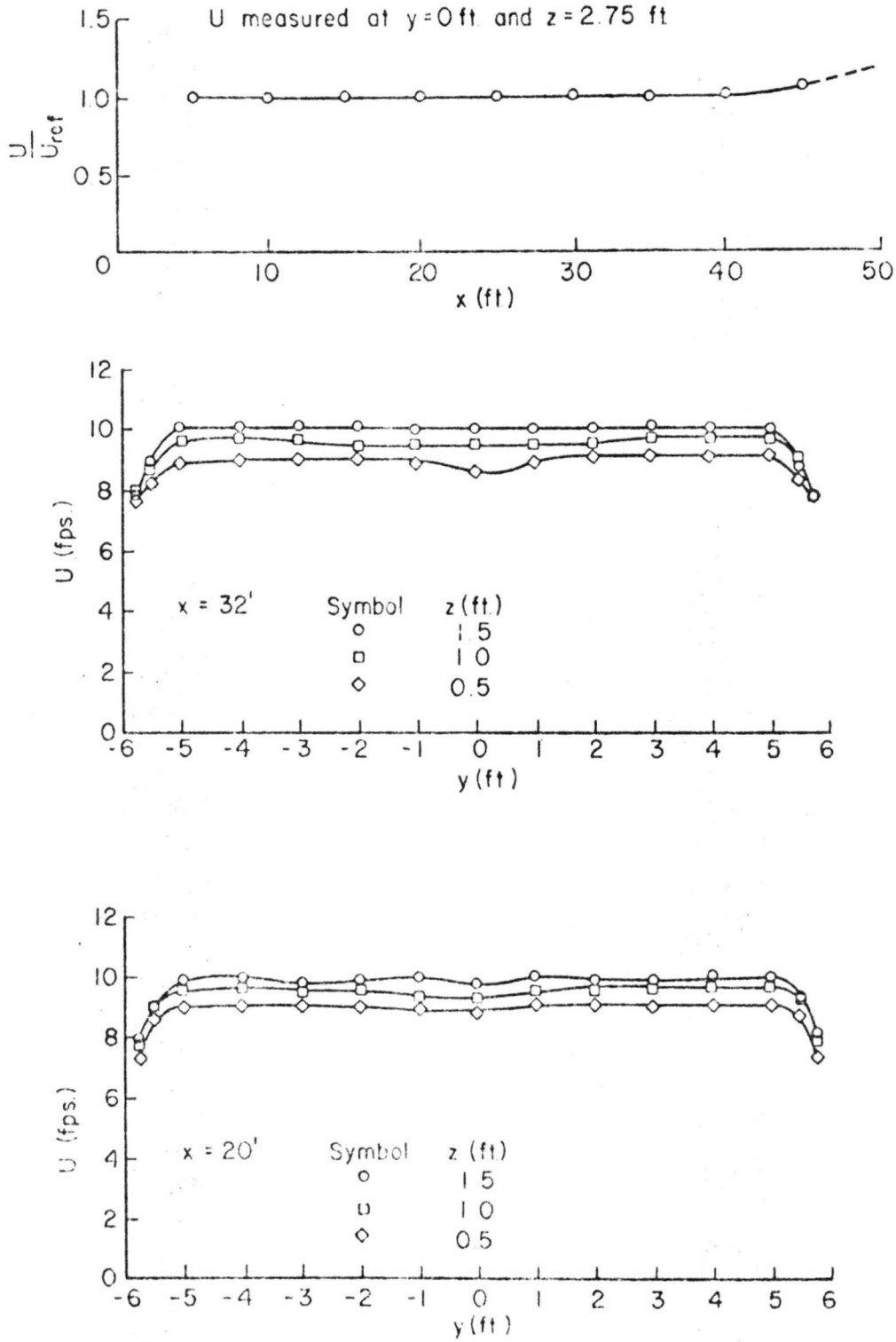

Fig. 12. Longitudinal and transverse velocity distributions

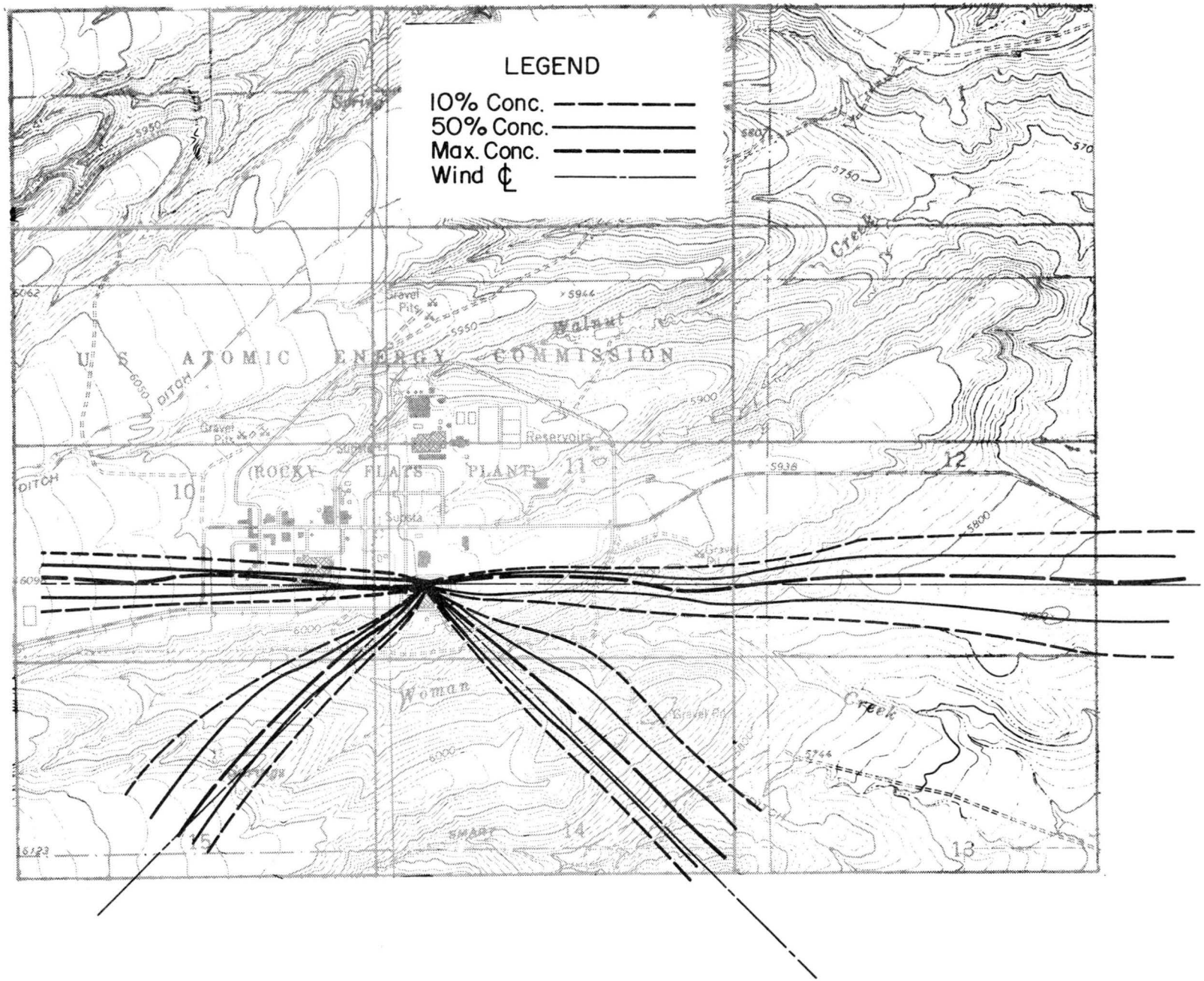

Fig. 13. Ground level plume trajectories and spread - source 1

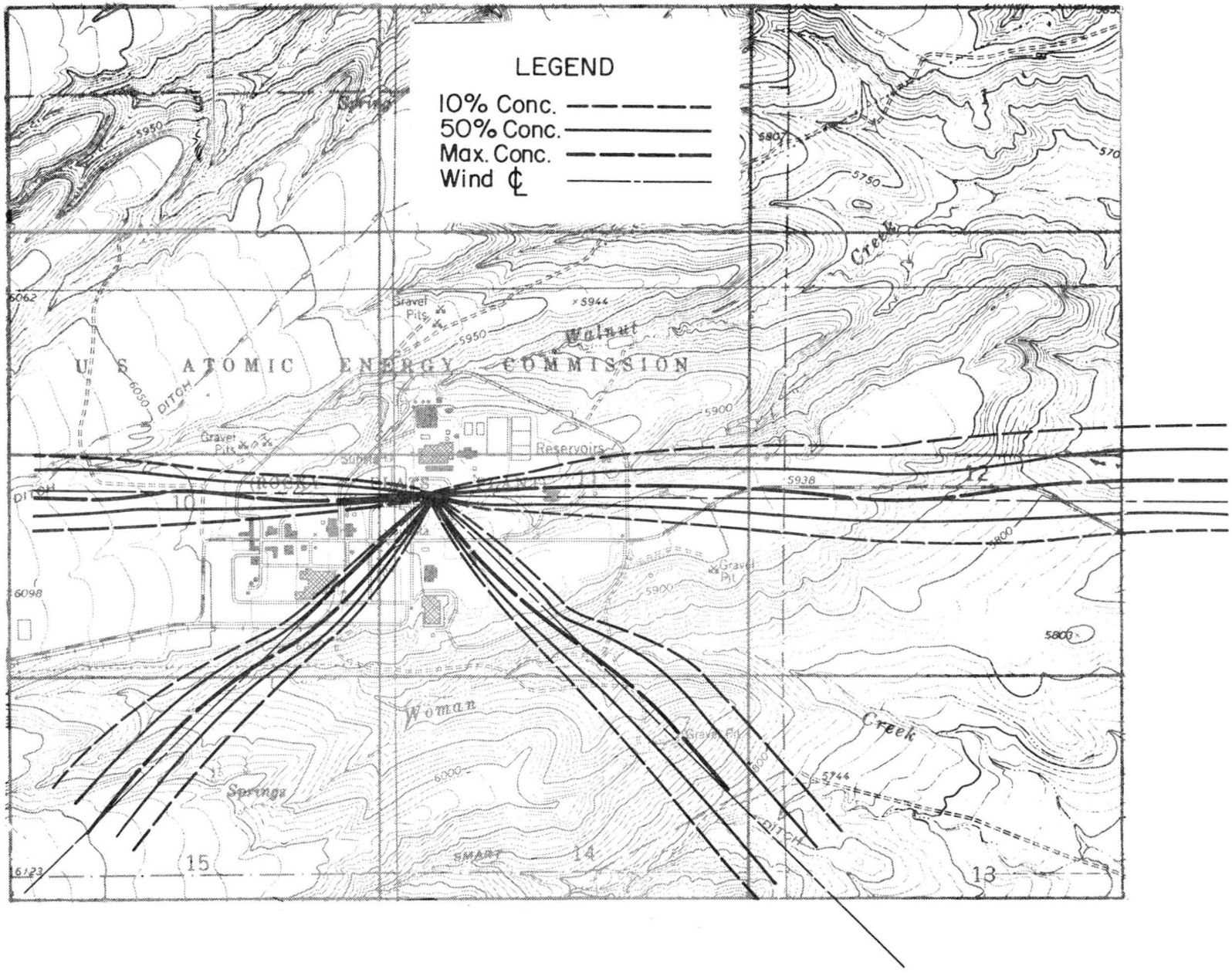

Fig. 14. Ground level plume trajectories and spread - source 2

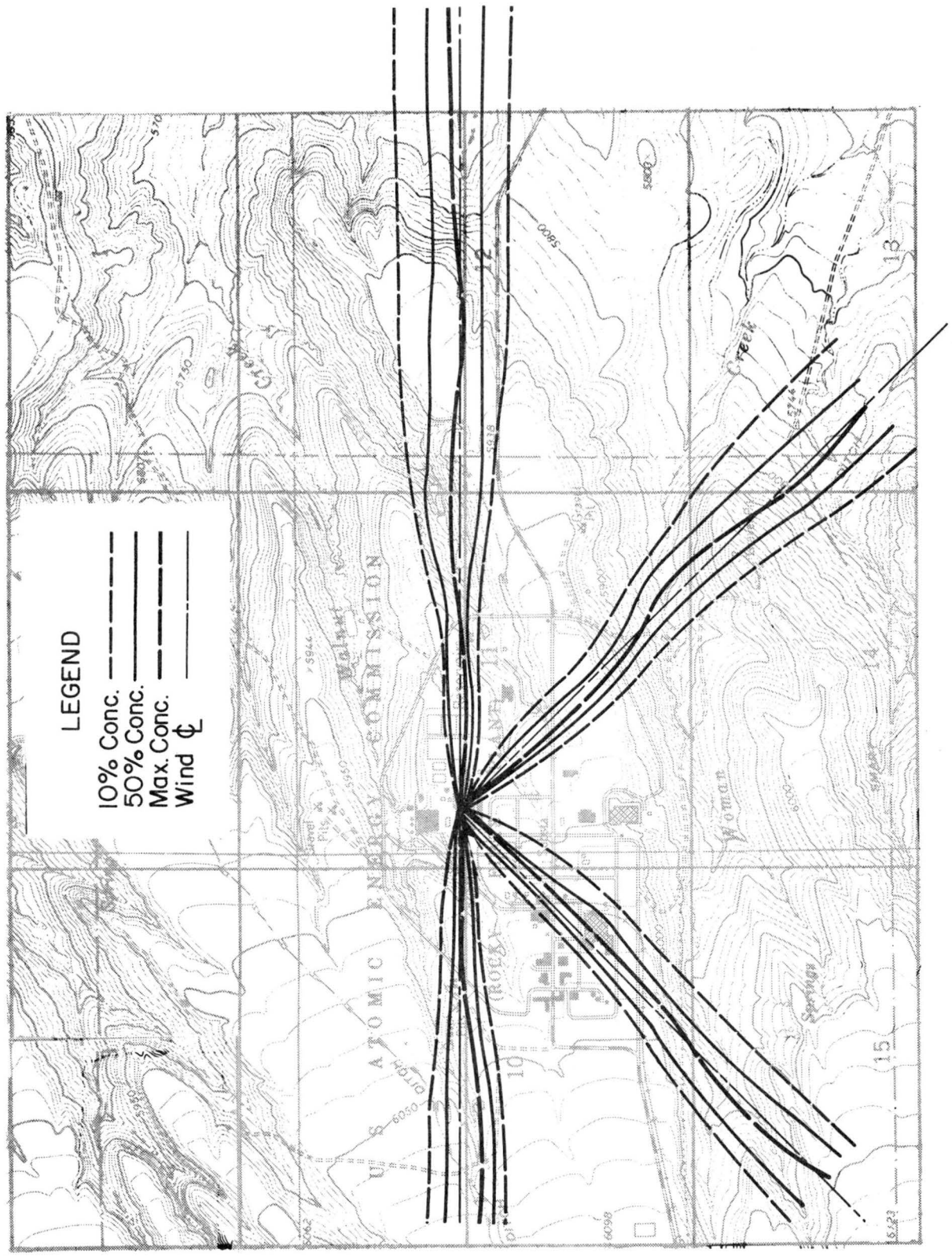

Fig. 15. Ground level plume trajectories and spread - source 3

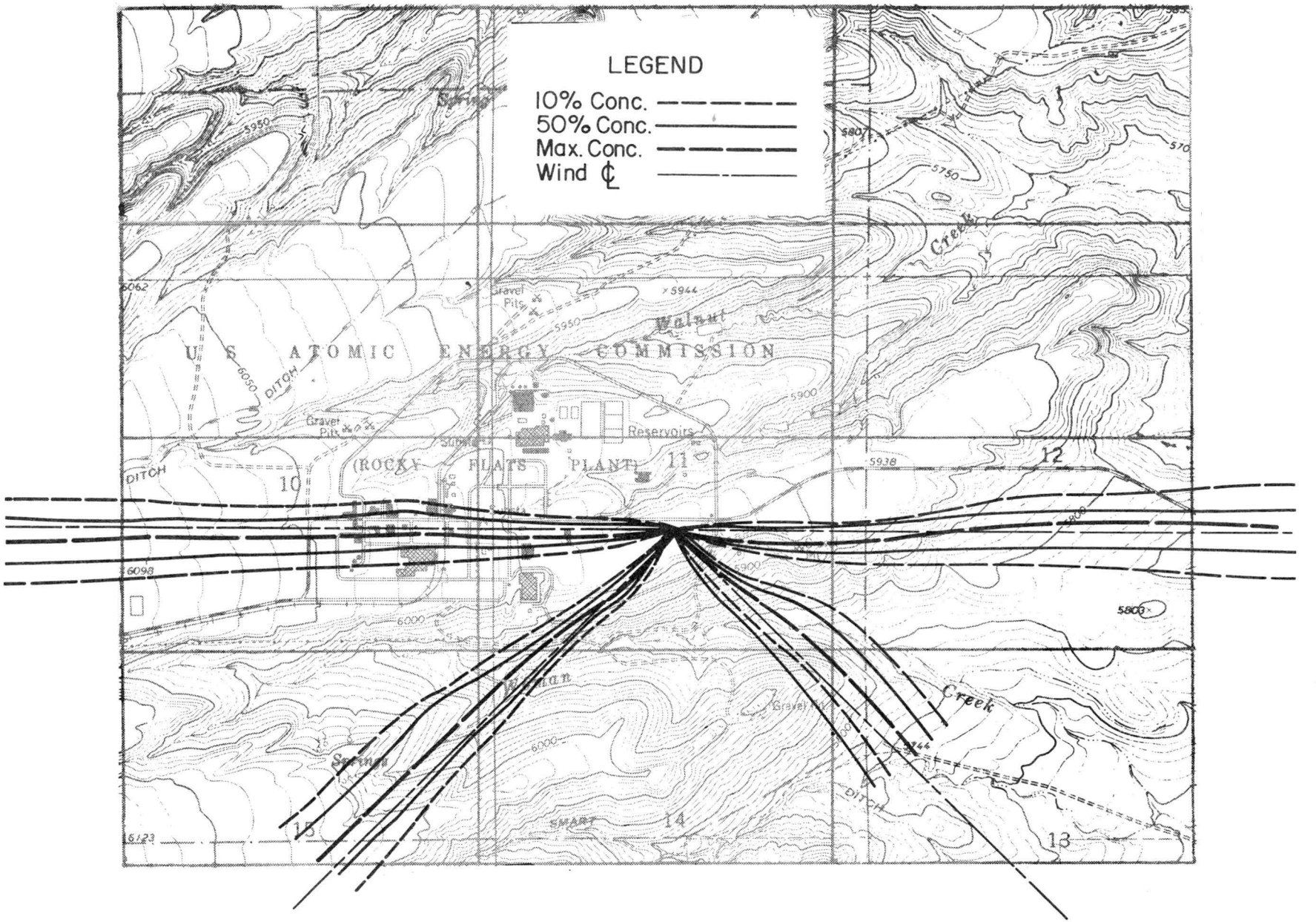

Fig. 16. Ground level plume trajectories and spread - source 4

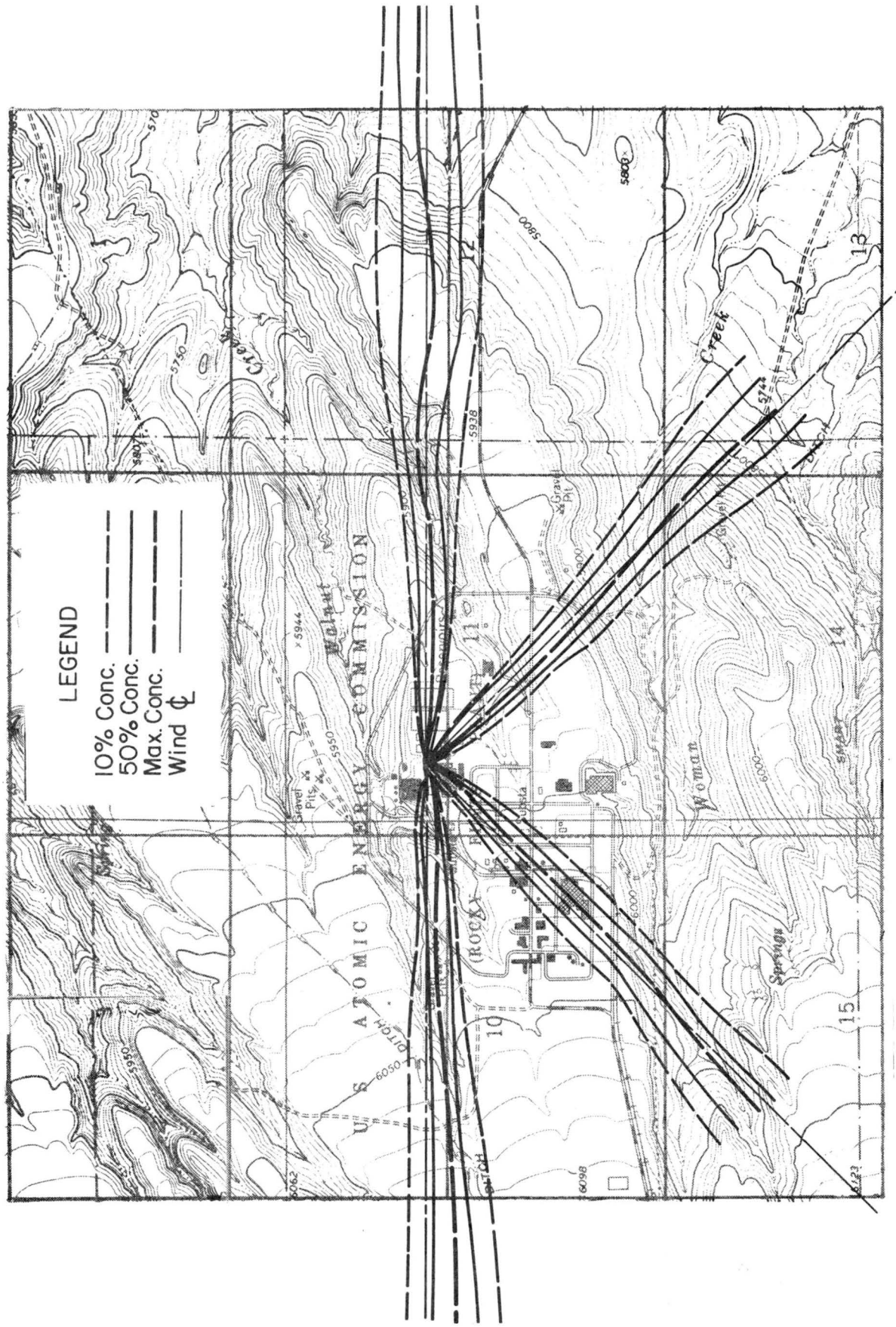

Fig. 17. Ground level plume trajectories and spread - stack

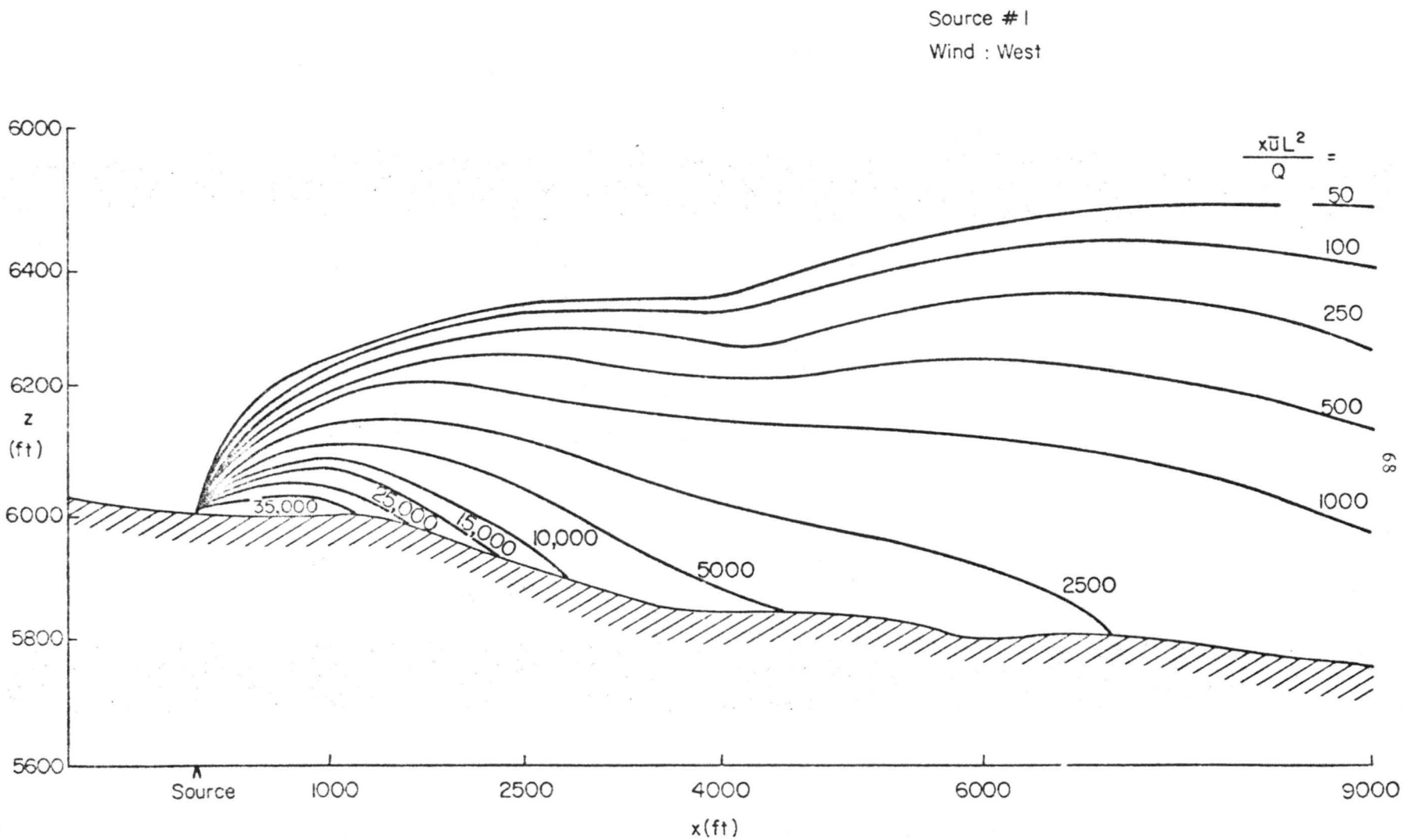

Fig. 18. Vertical concentration isopleth - source 1, wind orientation W

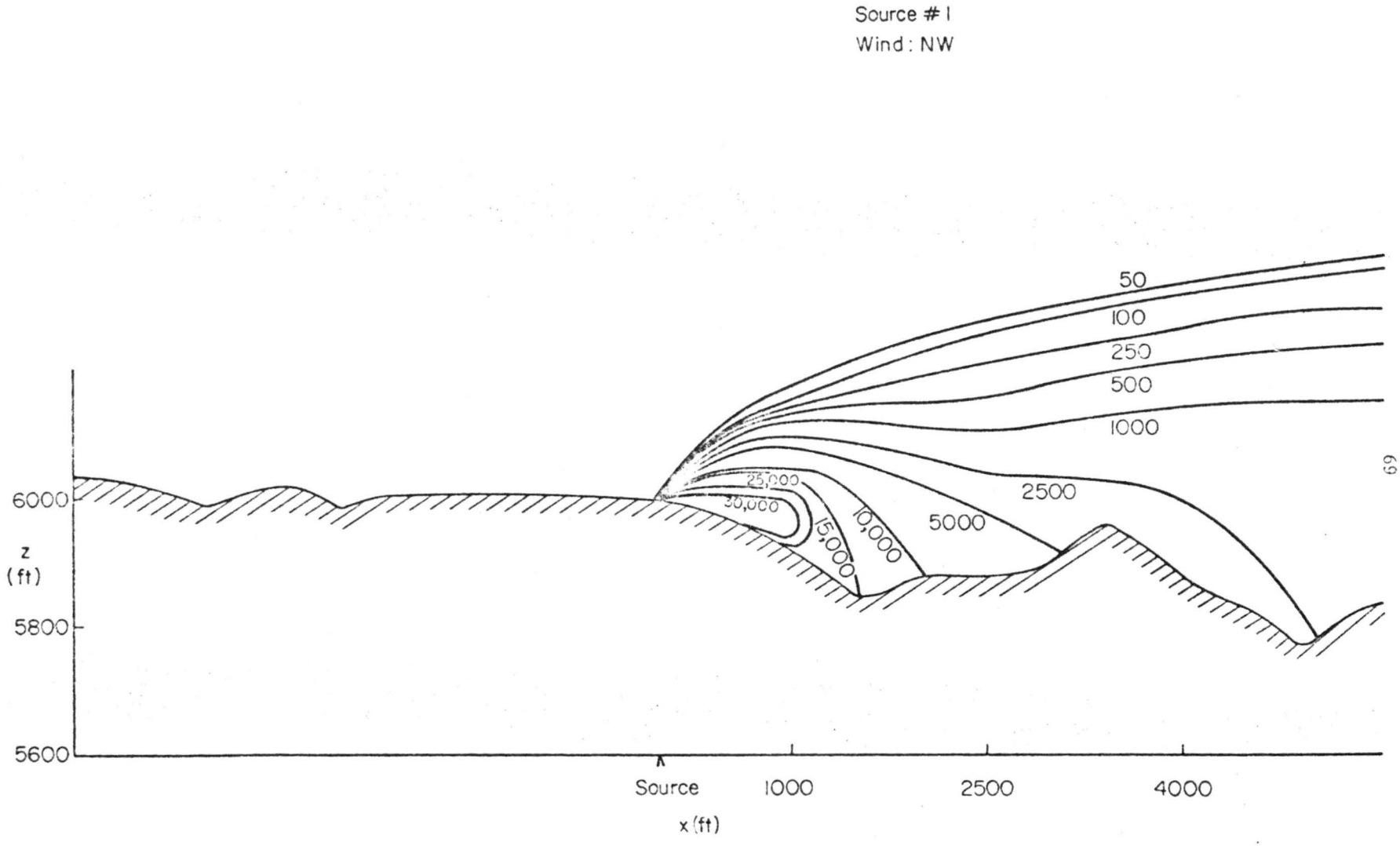

Fig. 19. Vertical concentration isopleth - source 1, wind orientation NW

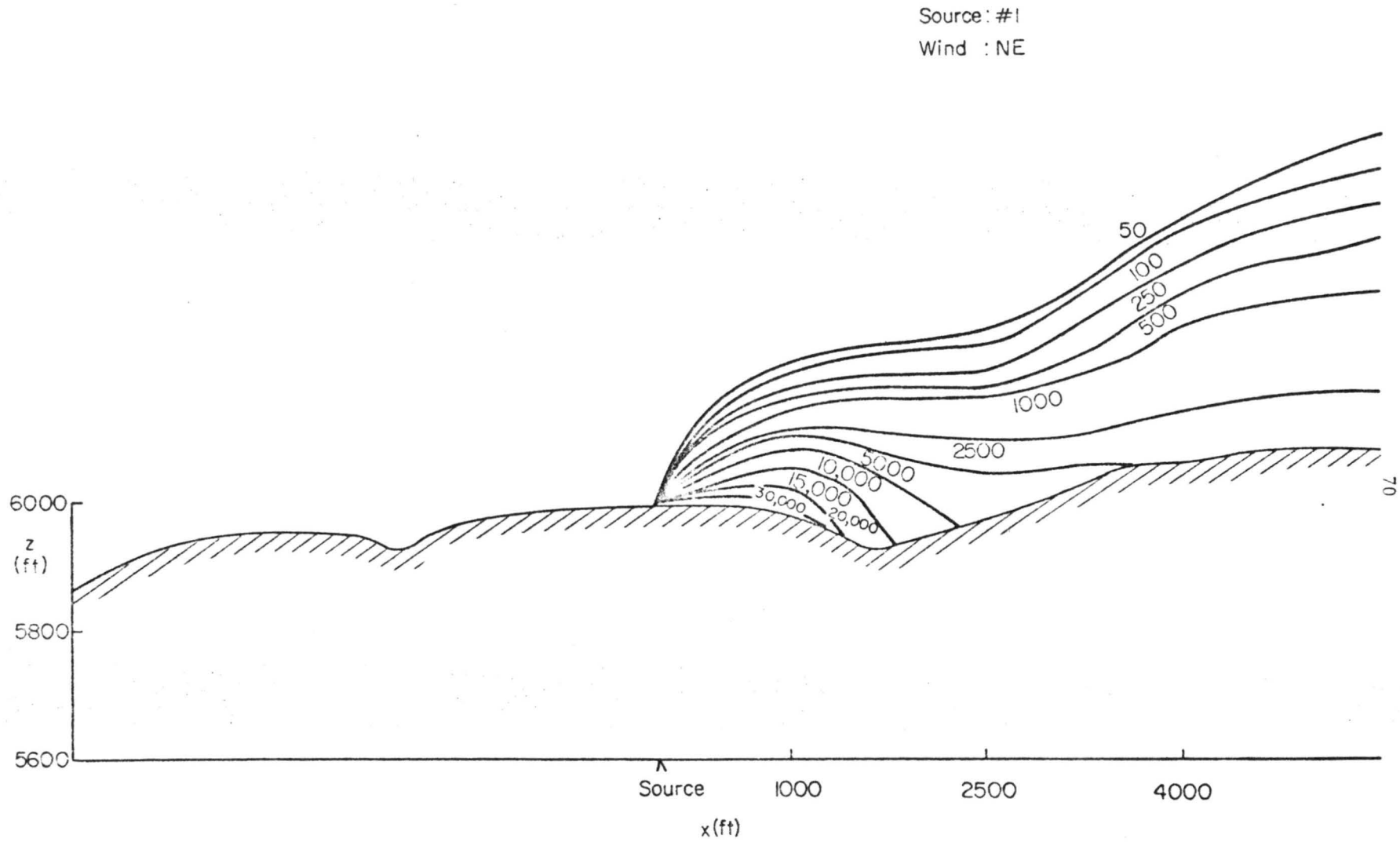

Fig. 20. Vertical concentration isopleth - source 1, wind orientation NE

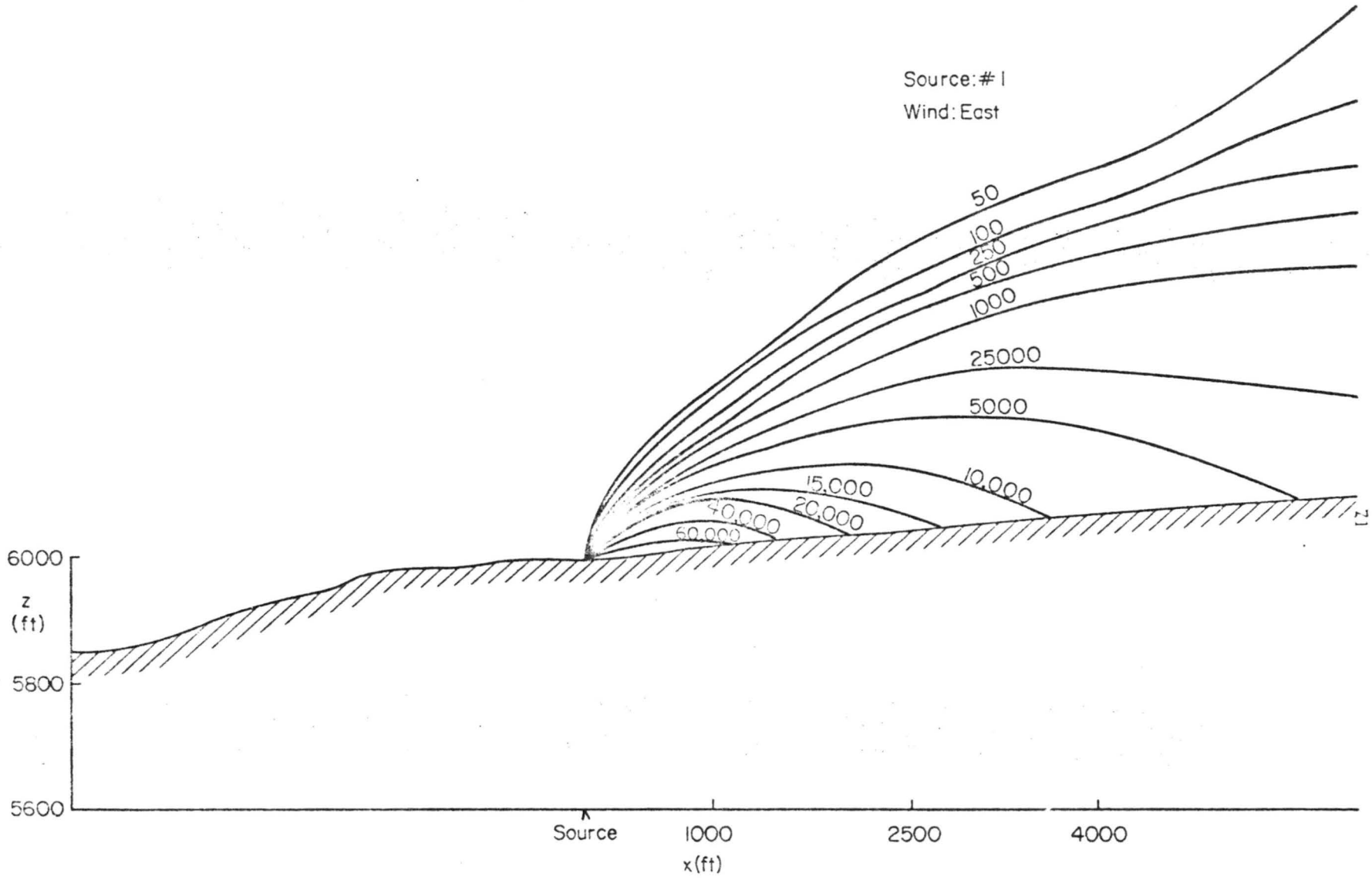

Fig. 21. Vertical concentration isopleth - source 1, wind orientation E

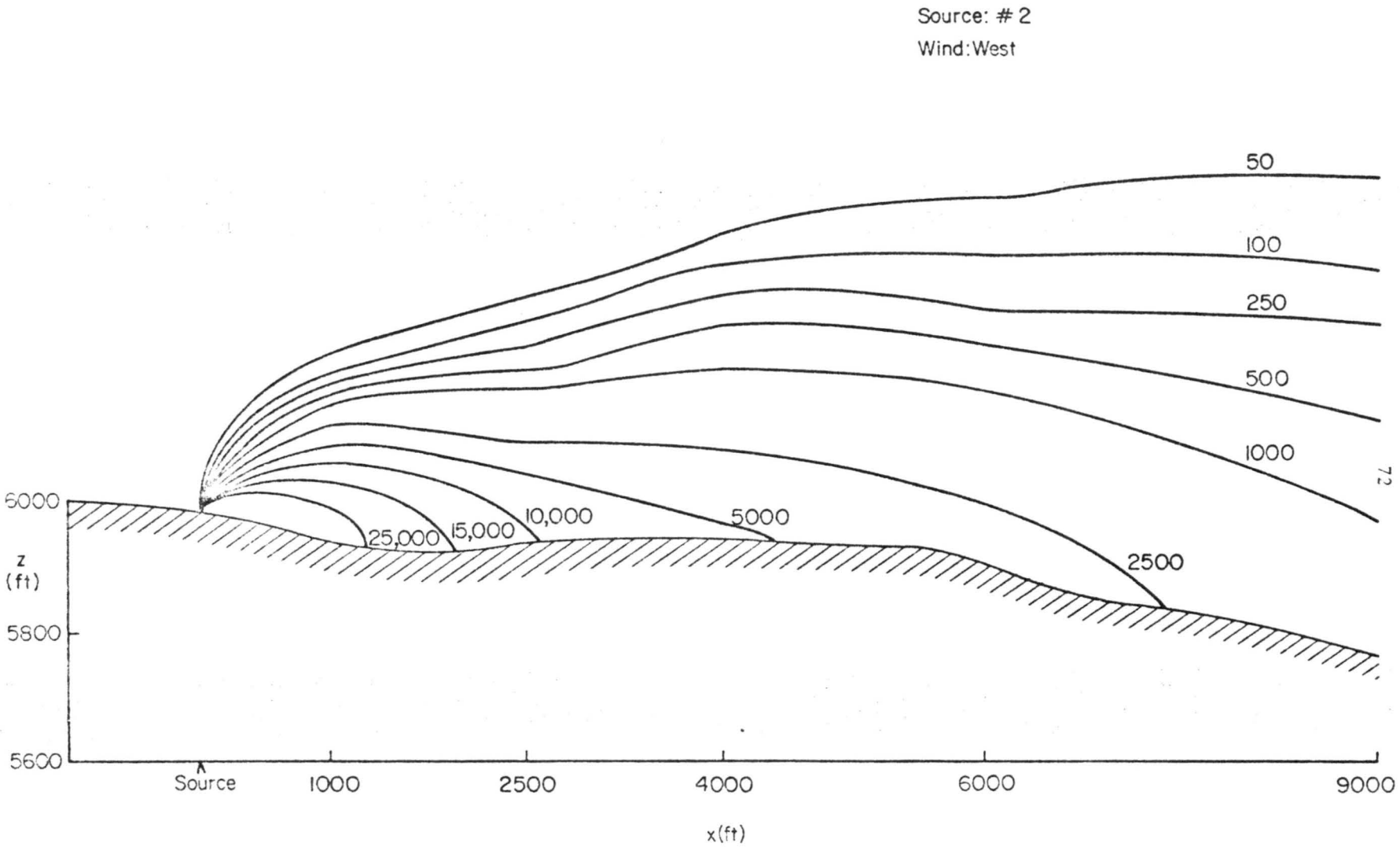

Fig. 22. Vertical concentration isopleth - source 2, wind orientation W

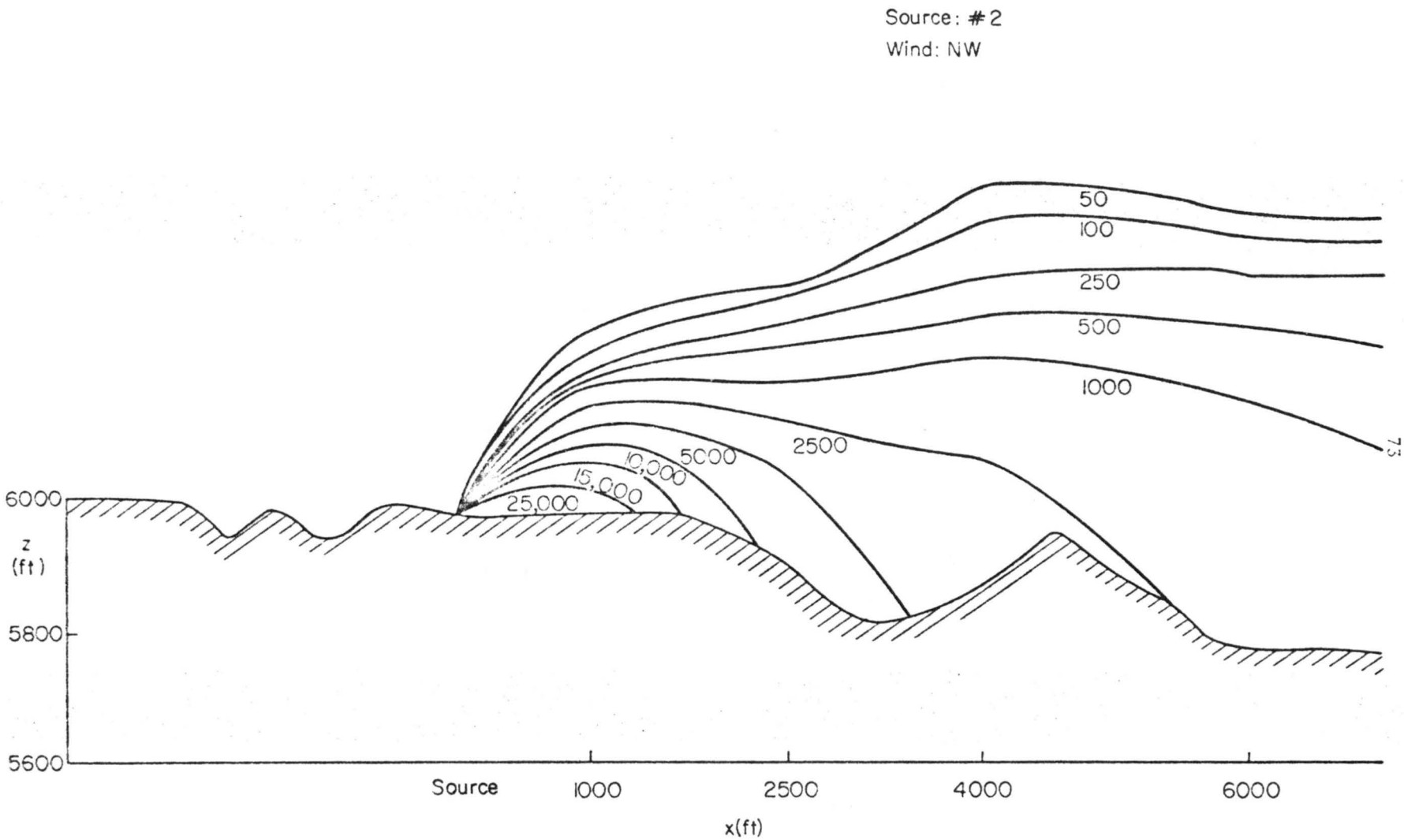

Fig. 23. Vertical concentration isopleth - source 2, wind orientation NW

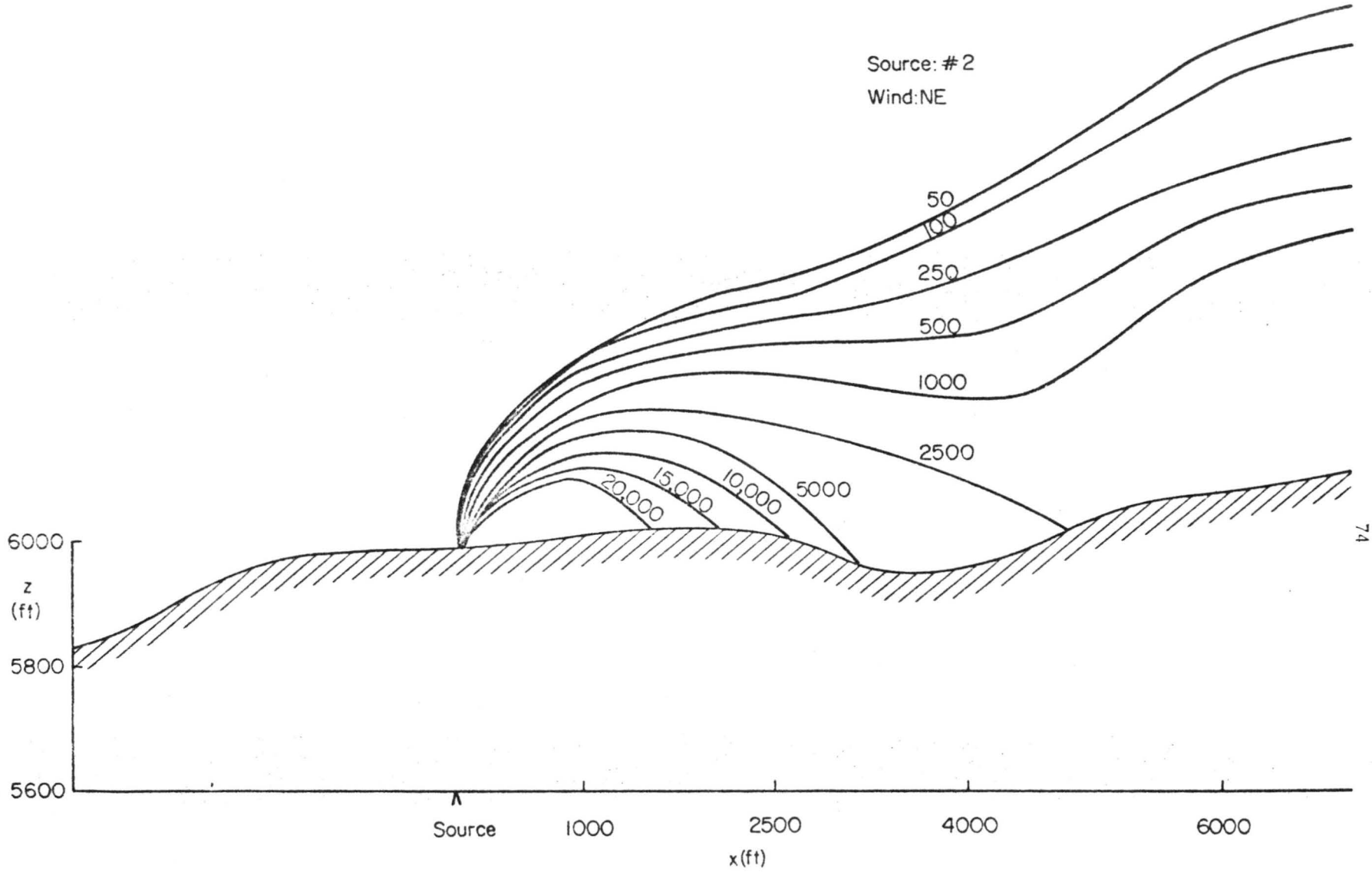

Fig. 24. Vertical concentration isopleth - source 2, wind orientation NE

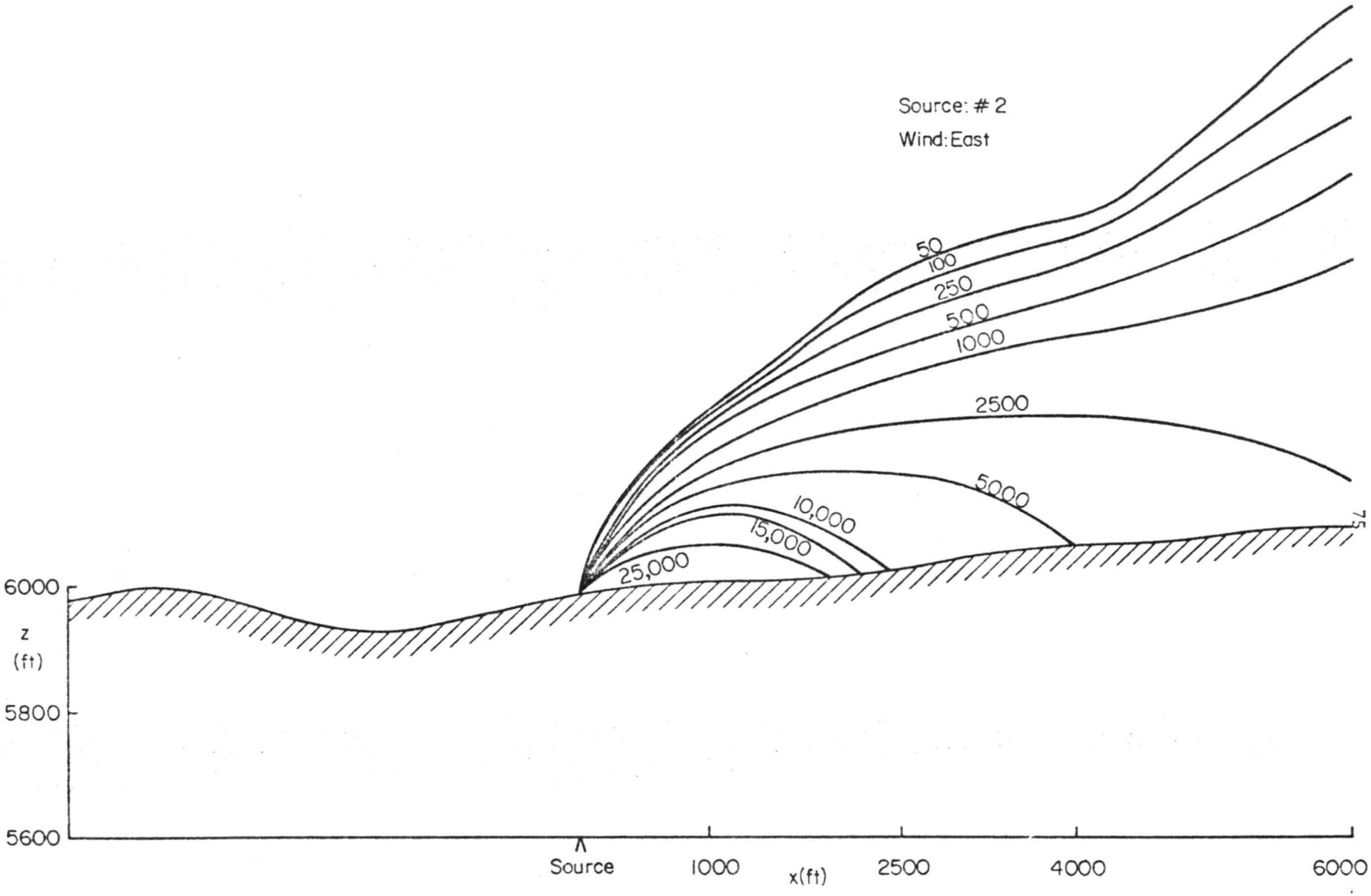

Fig. 25. Vertical concentration isopleth - source 2, wind orientation E

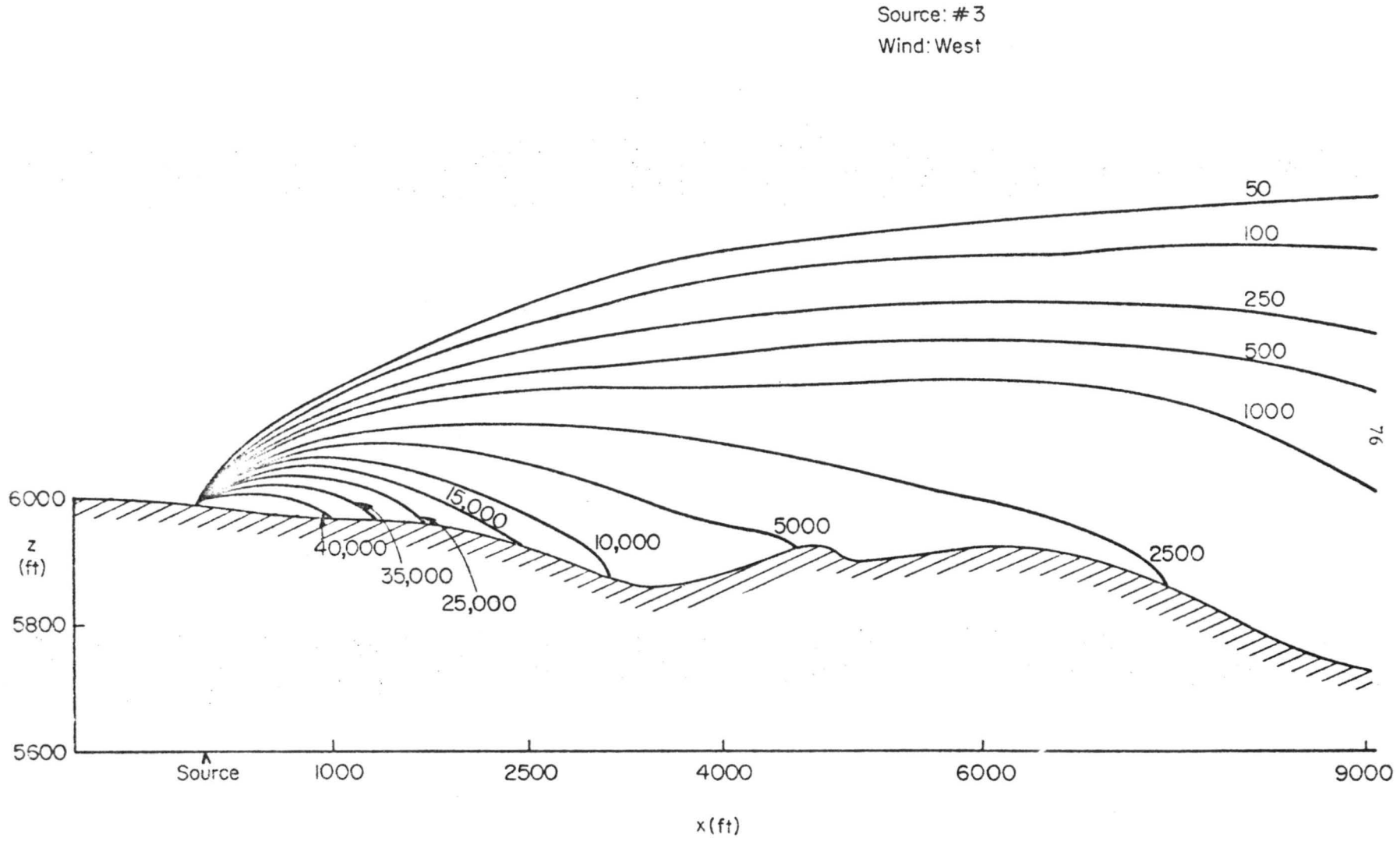

Fig. 26. Vertical concentration isopleth - source 3, wind orientation W

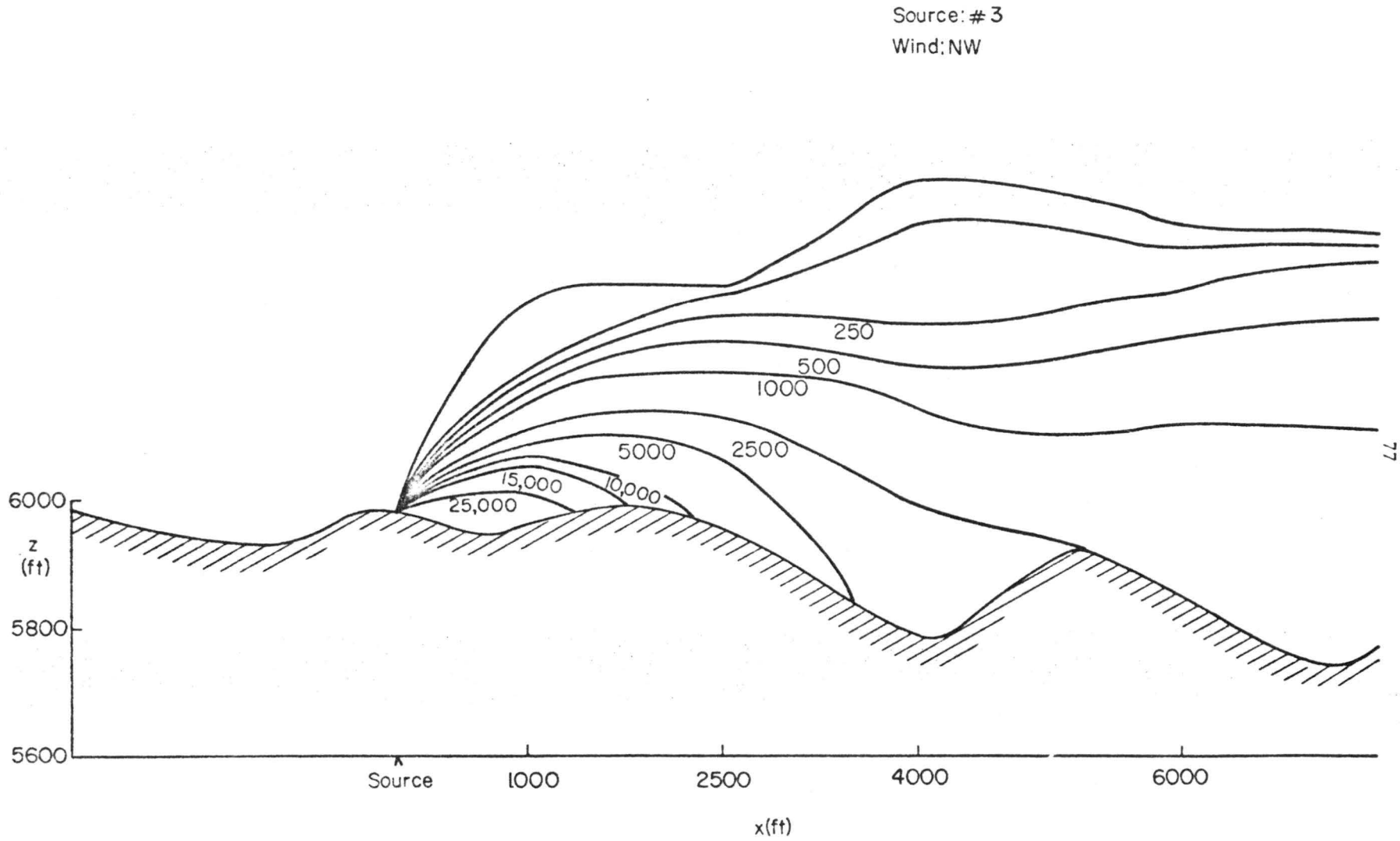

Fig. 27. Vertical concentration isopleth - source 3, wind orientation NW

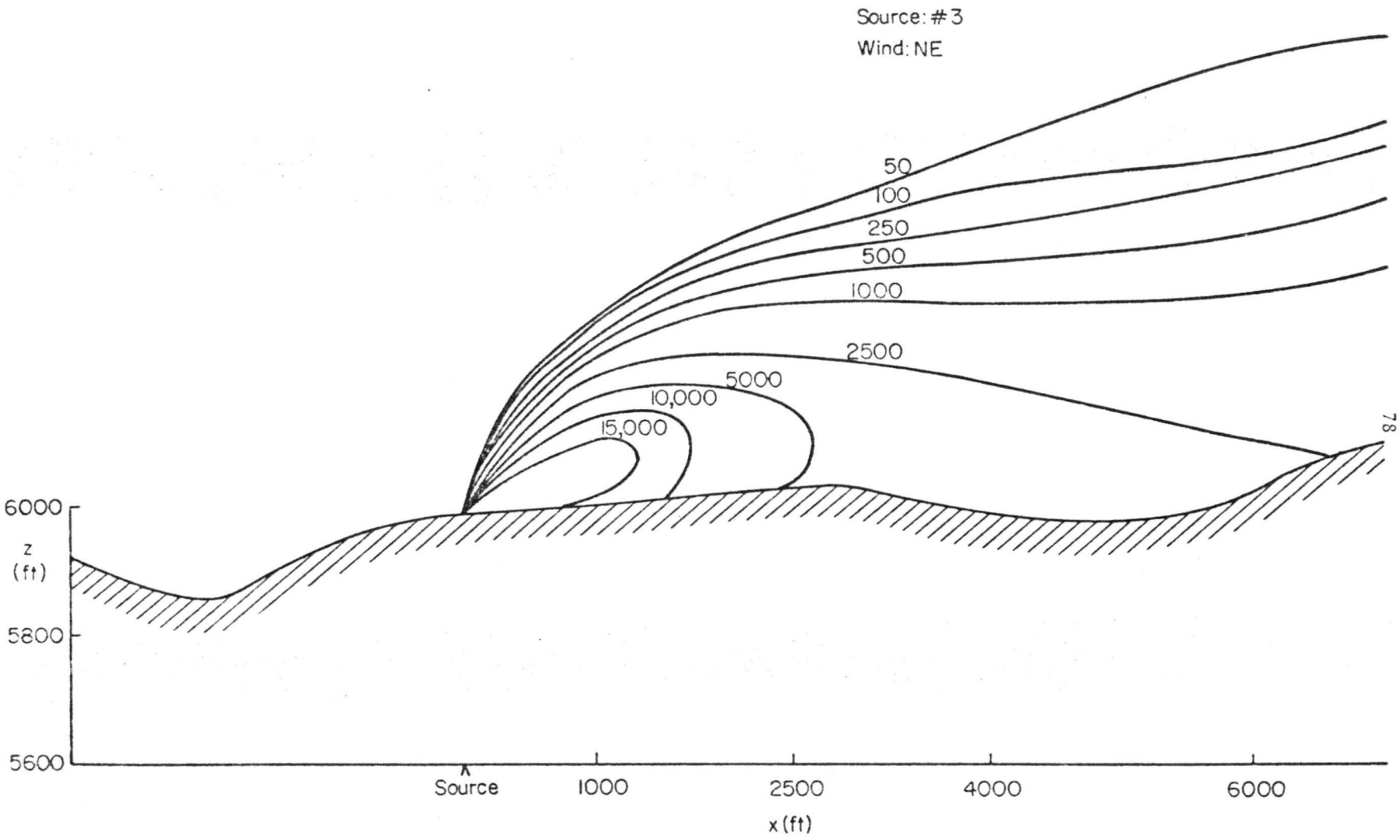

Fig. 28. Vertical concentration isopleth - source 3, wind orientation NE

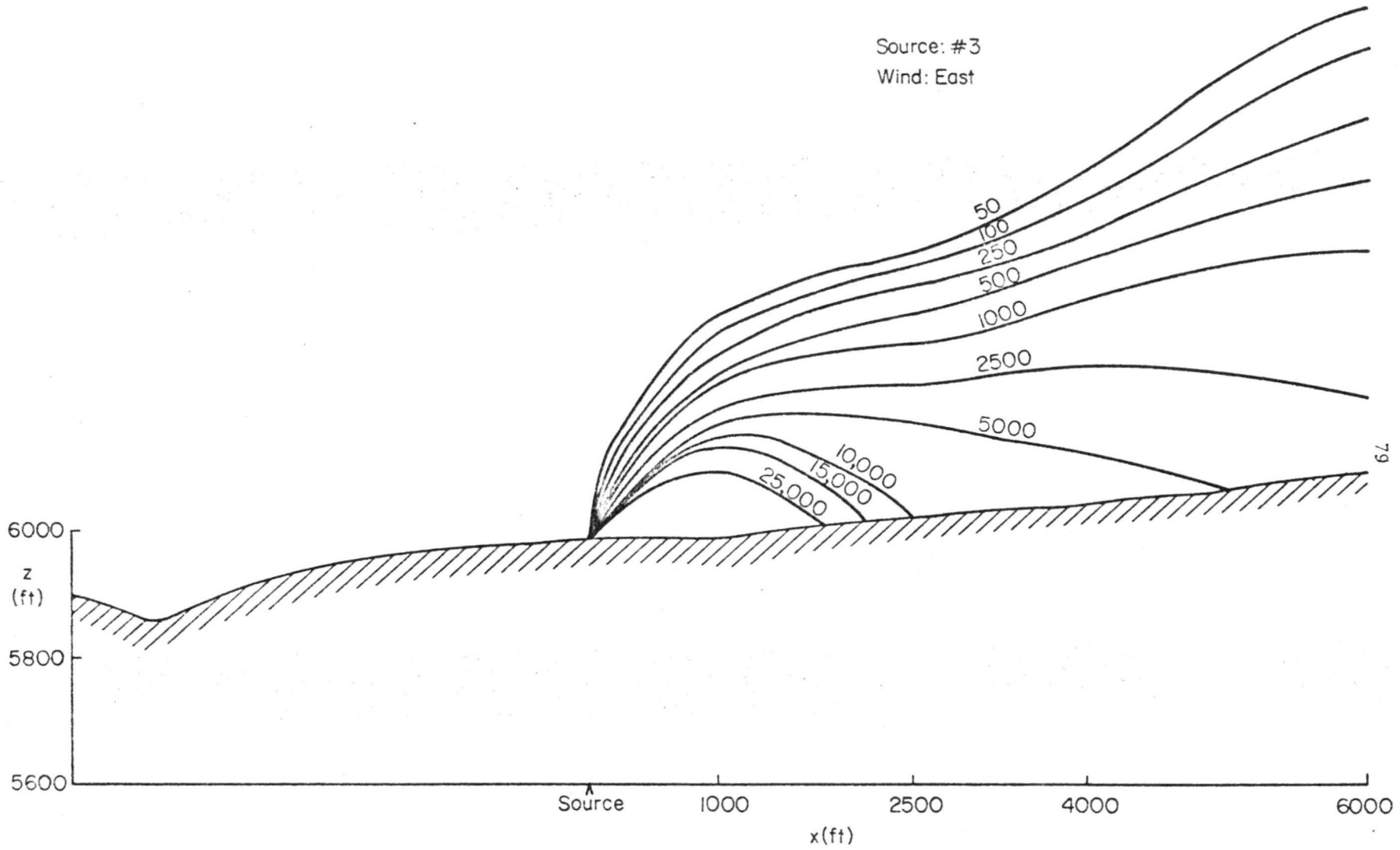

Fig. 29. Vertical concentration isopleth - source 3, wind orientation E

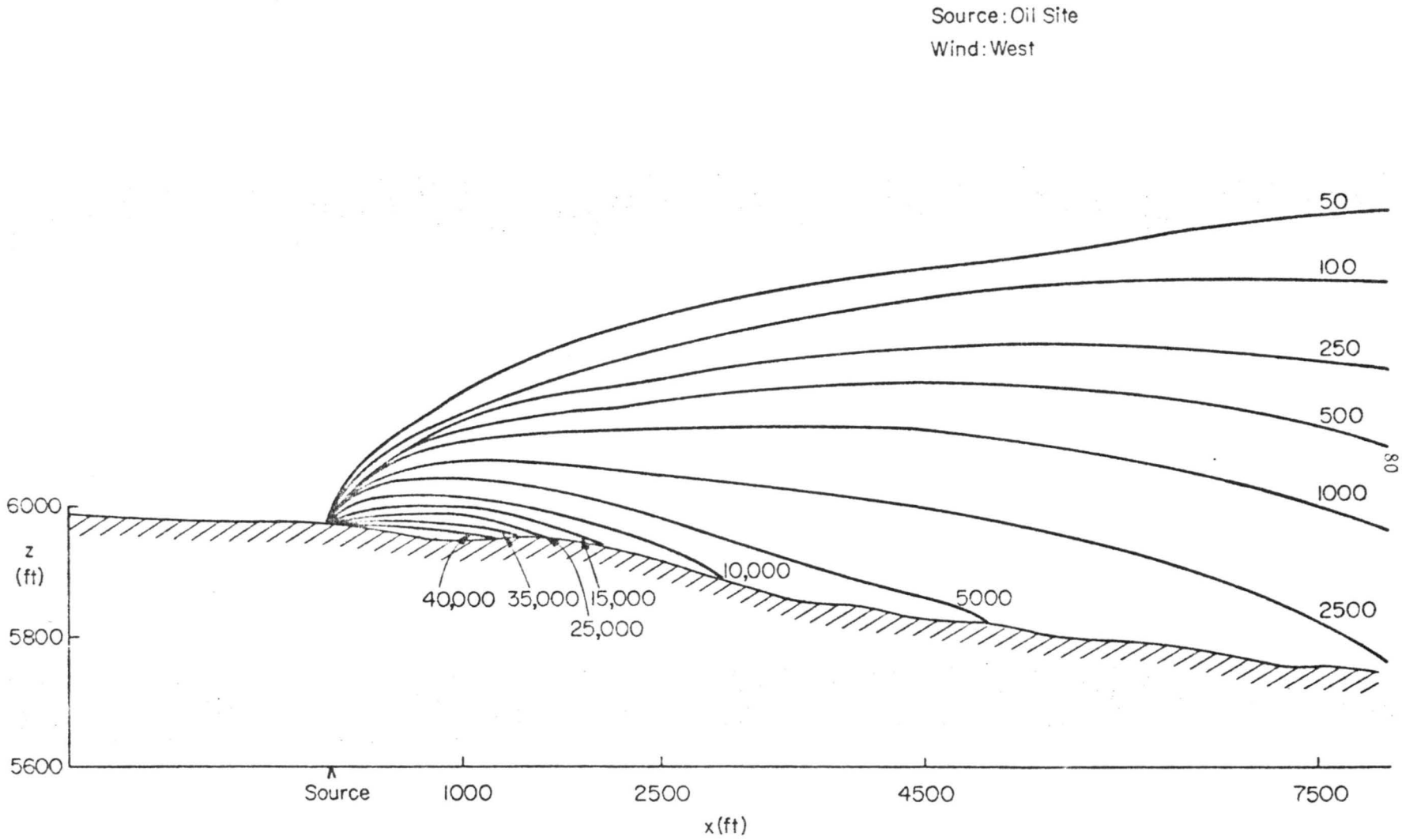

Fig. 30. Vertical concentration isopleth - source 4, wind orientation W

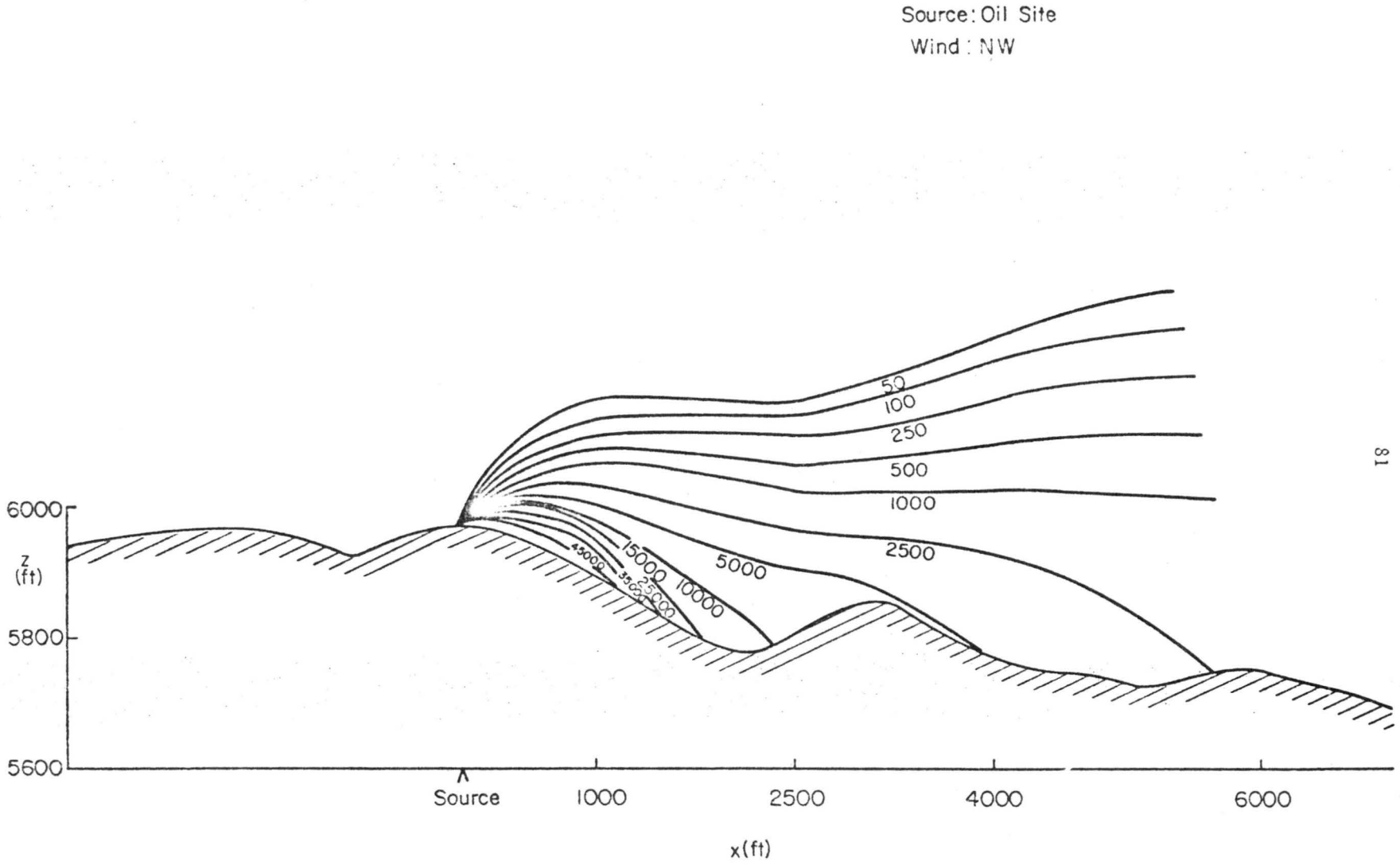

Fig. 31. Vertical concentration isopleth - source 4, wind orientation NW

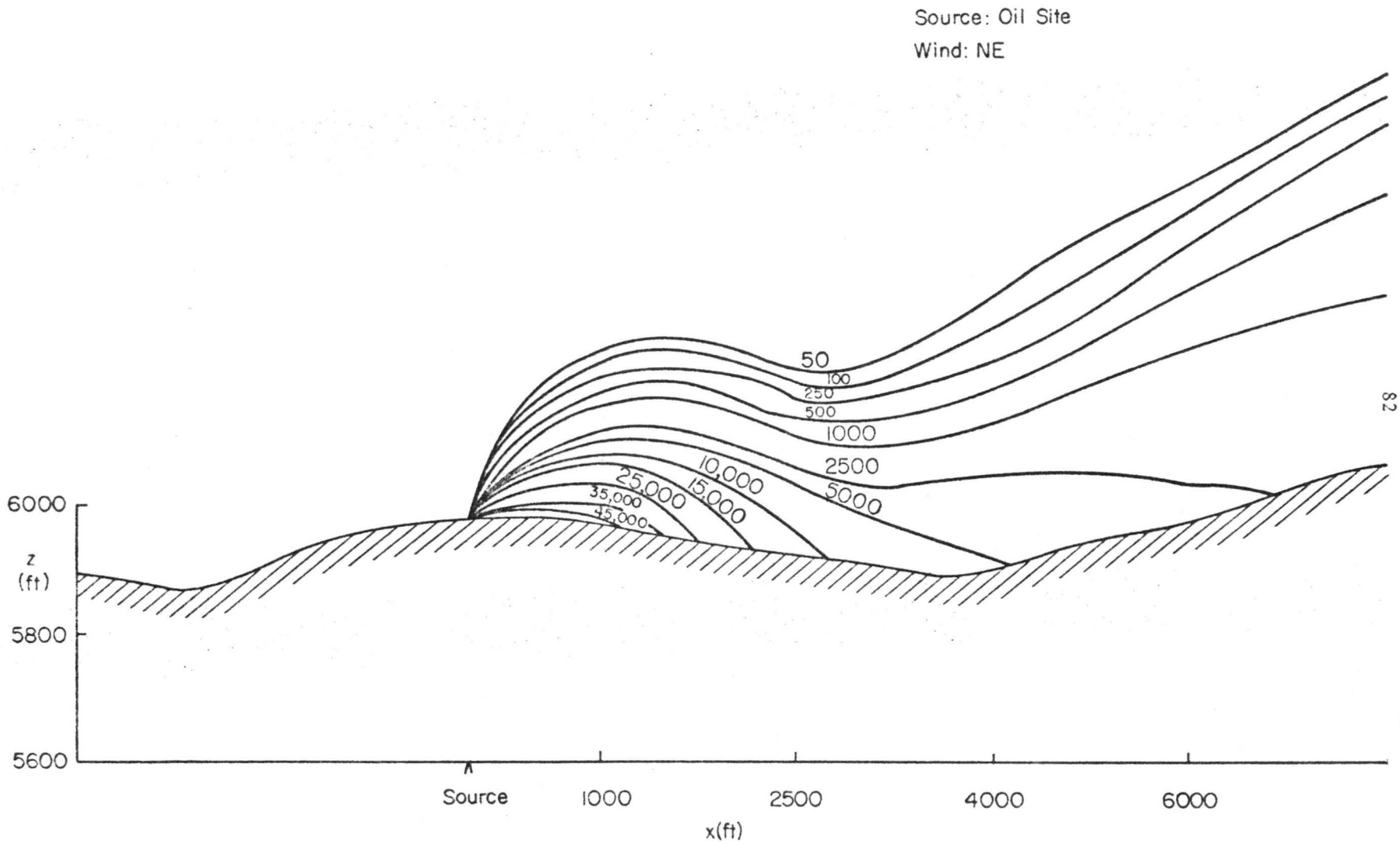

Fig. 32. Vertical concentration isopleth - source 4, wind orientation NE

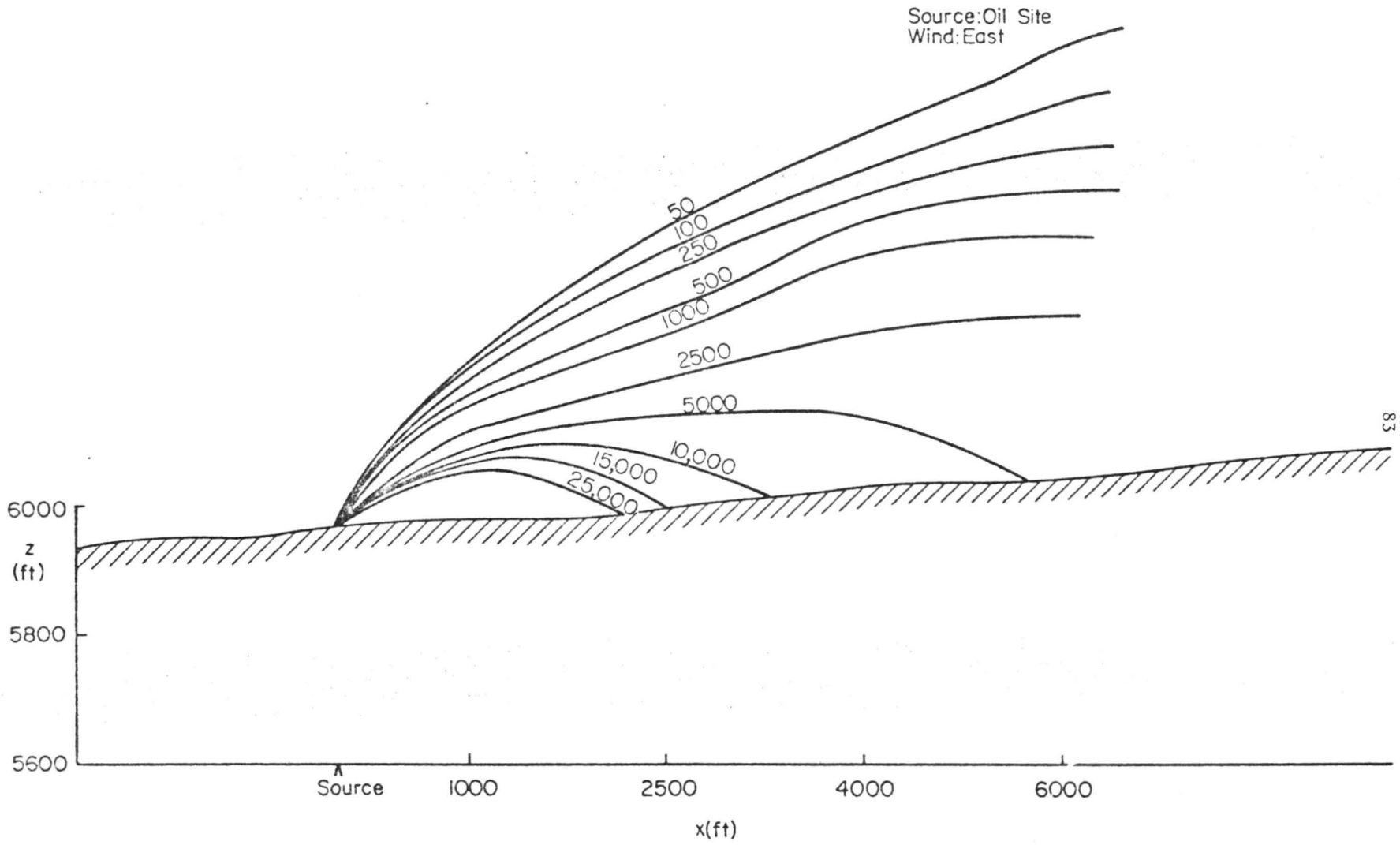

Fig. 33. Vertical concentration isopleth - source 4, wind orientation E

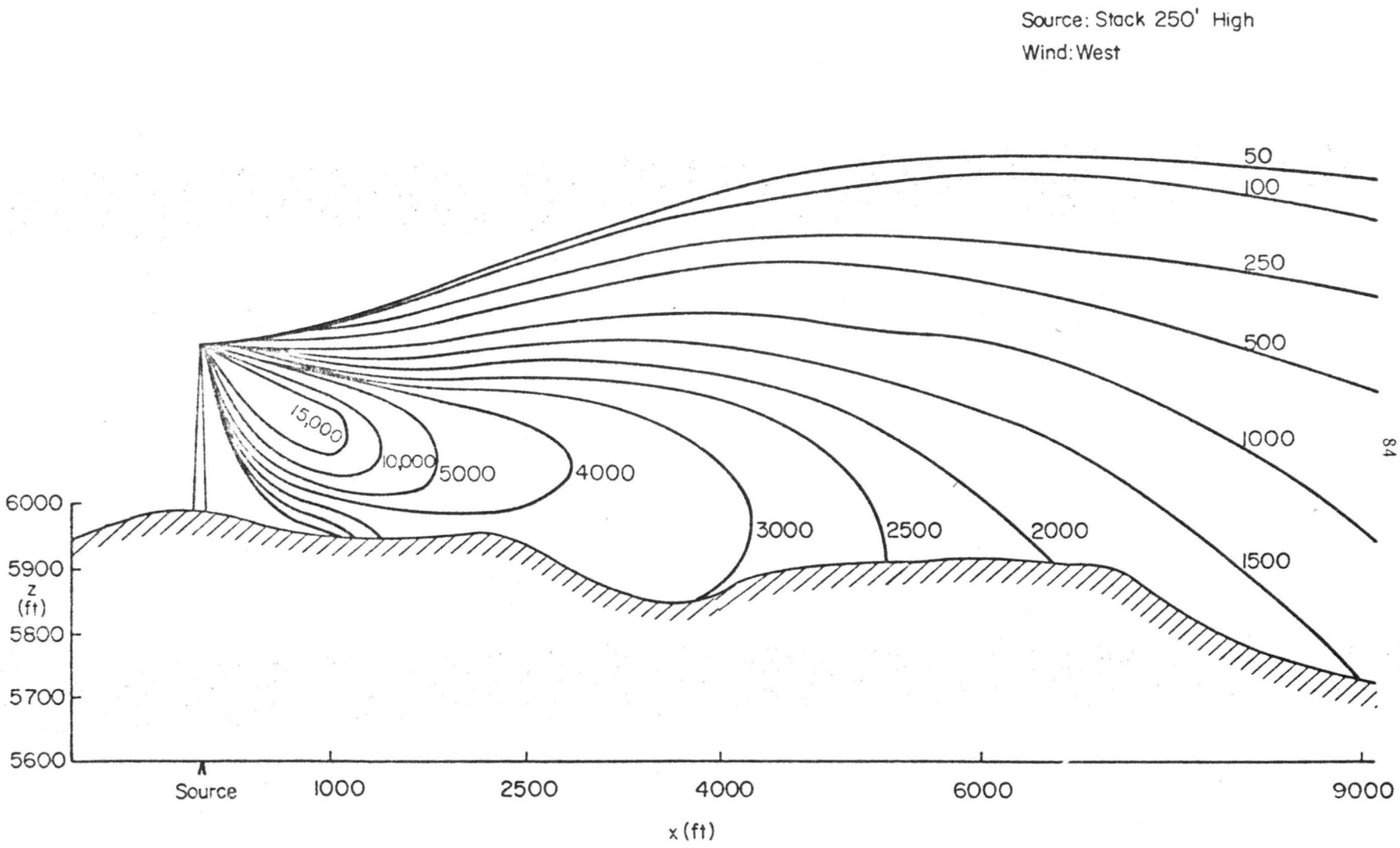

Fig. 34. Vertical concentration isopleth - source stack, wind orientation W

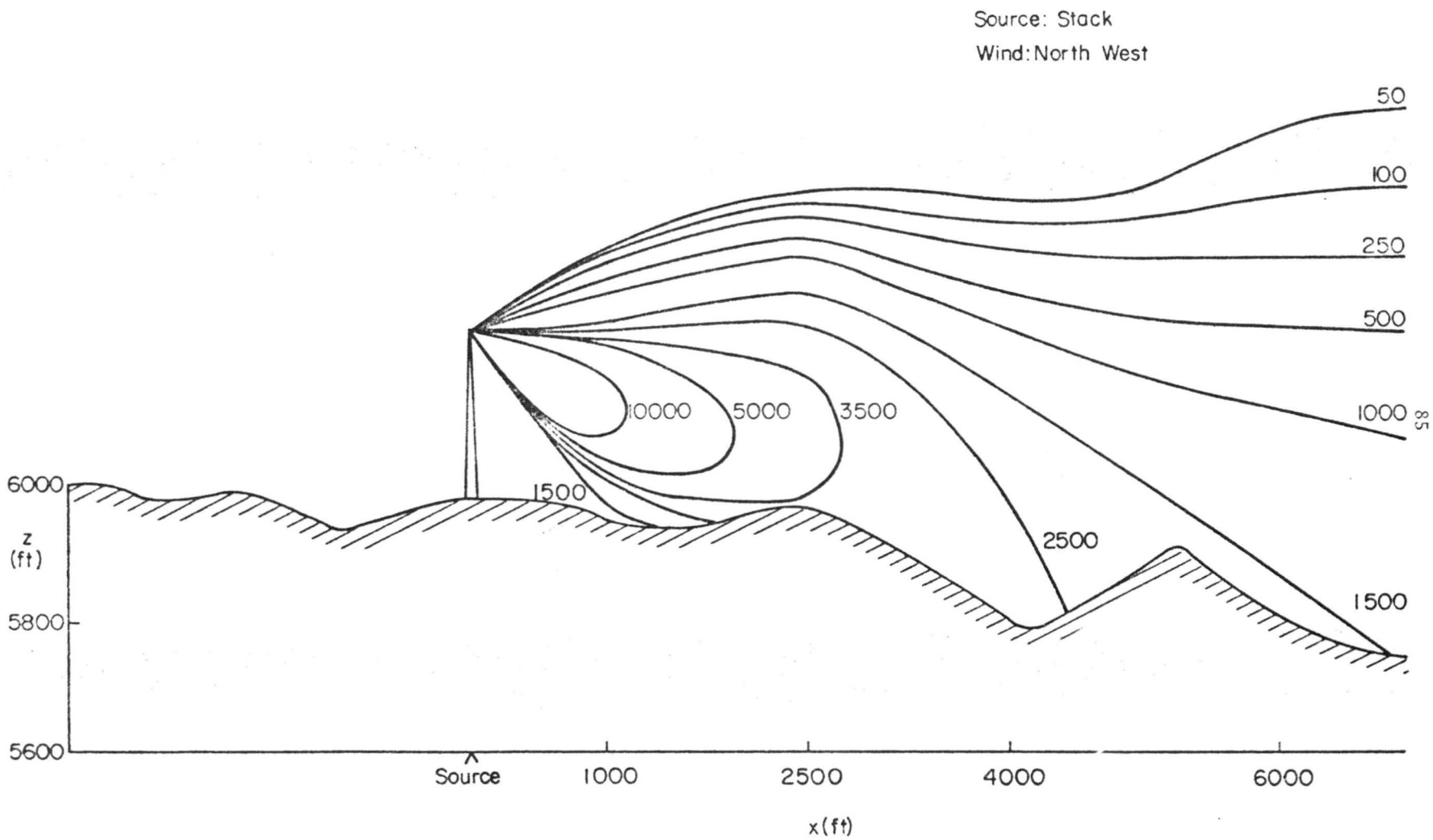

Fig. 35. Vertical concentration isopleth - source stack, wind orientation NW

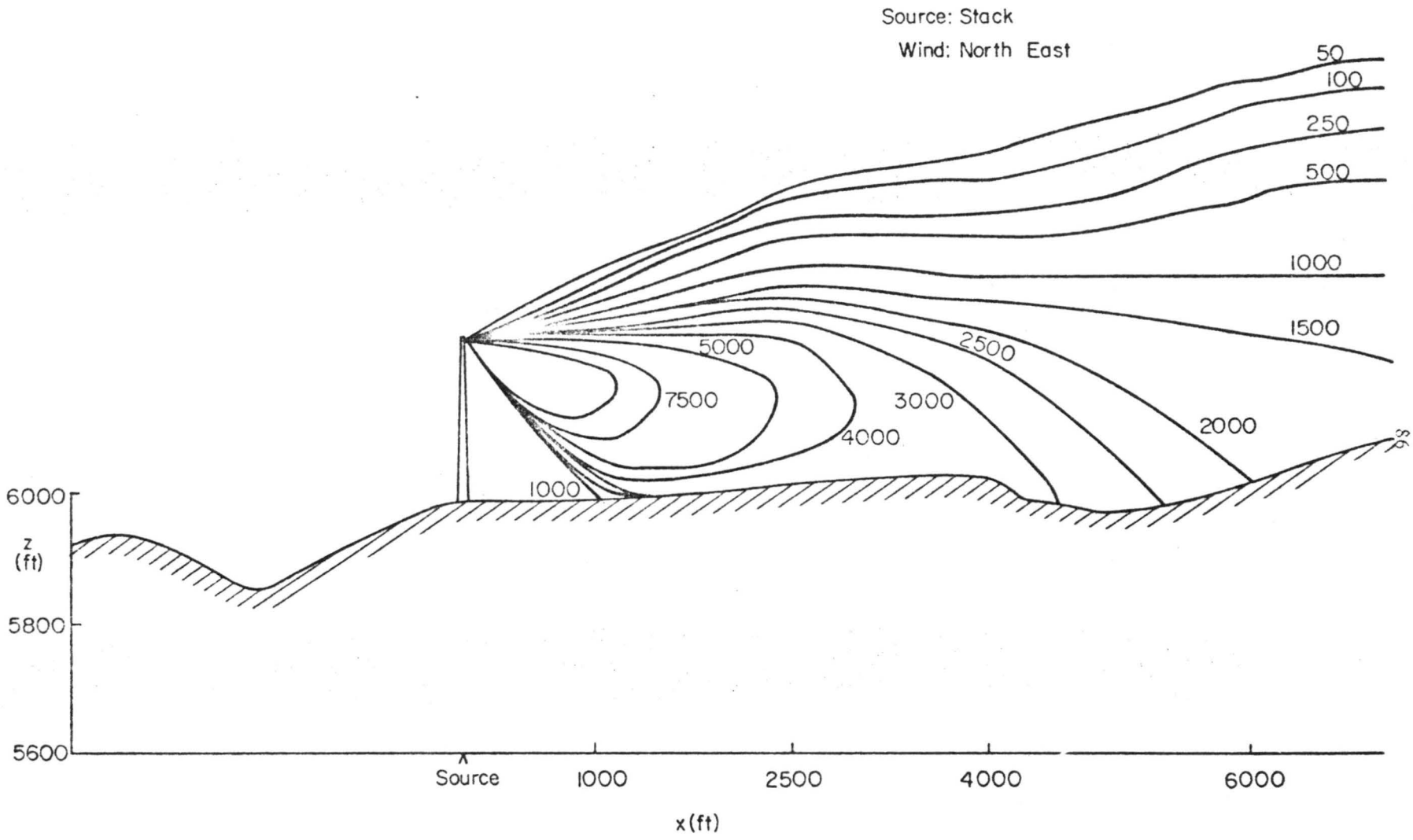

Fig. 36. Vertical concentration isopleth - source stack, wind orientation NE

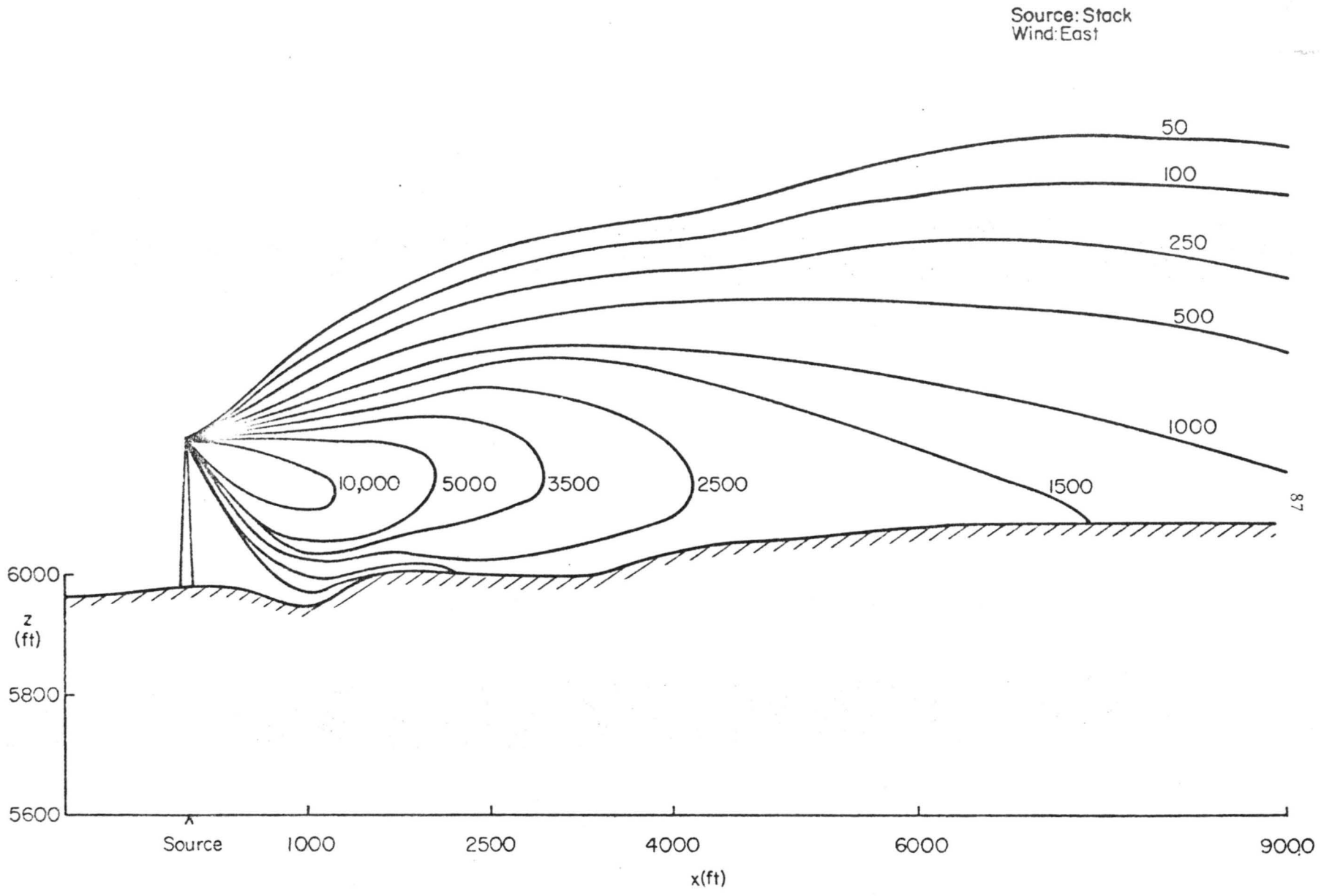

Fig. 37. Vertical concentration isopleth - source stack, wind orientation E

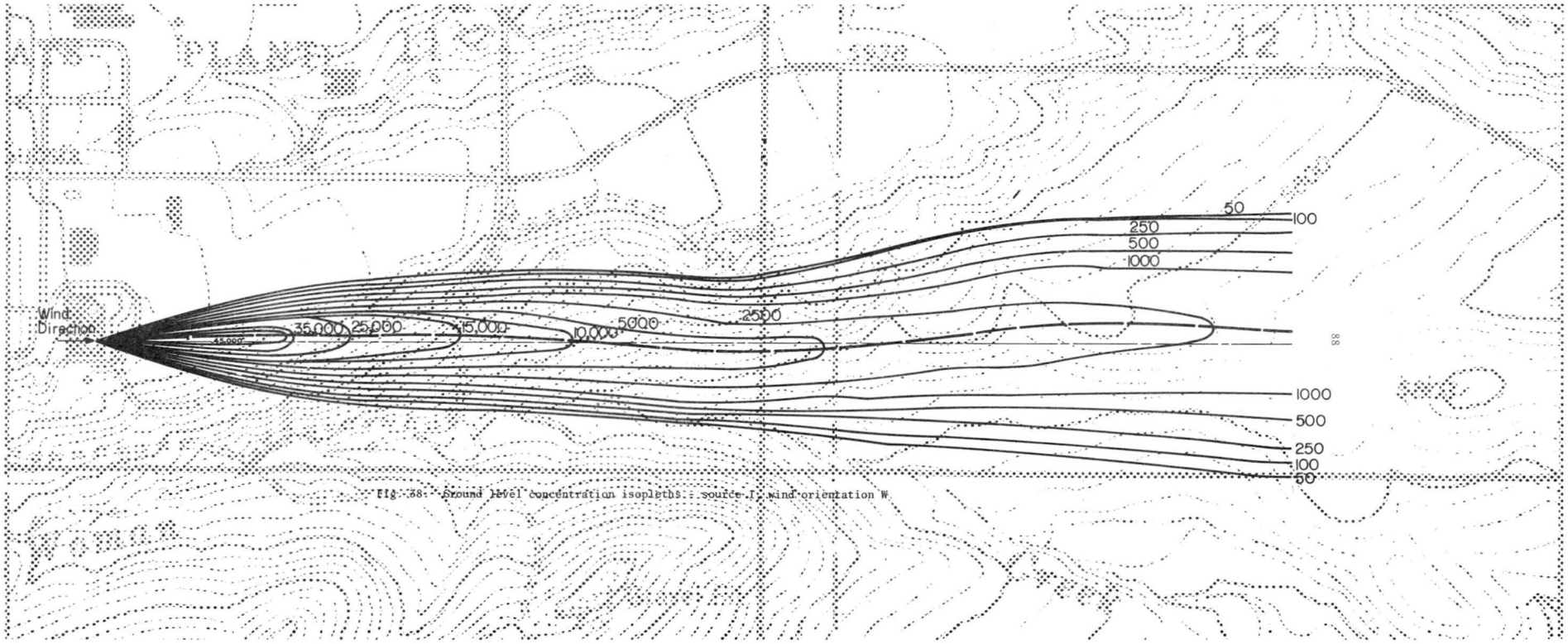

Fig. 38: Ground level concentration isopleths: source I, wind orientation W

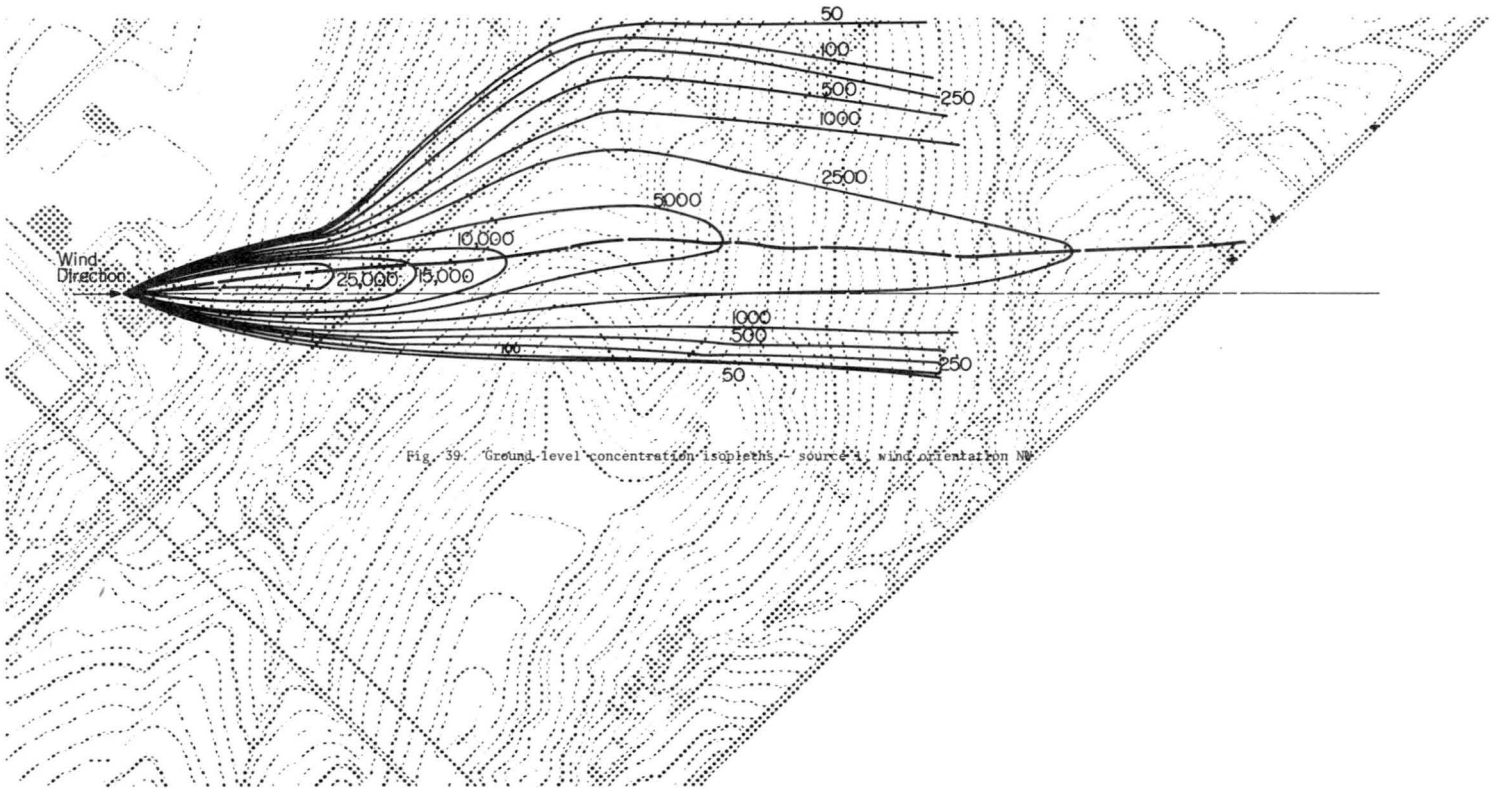

Fig. 39. Ground-level concentration isopleths - source 1, wind orientation NW

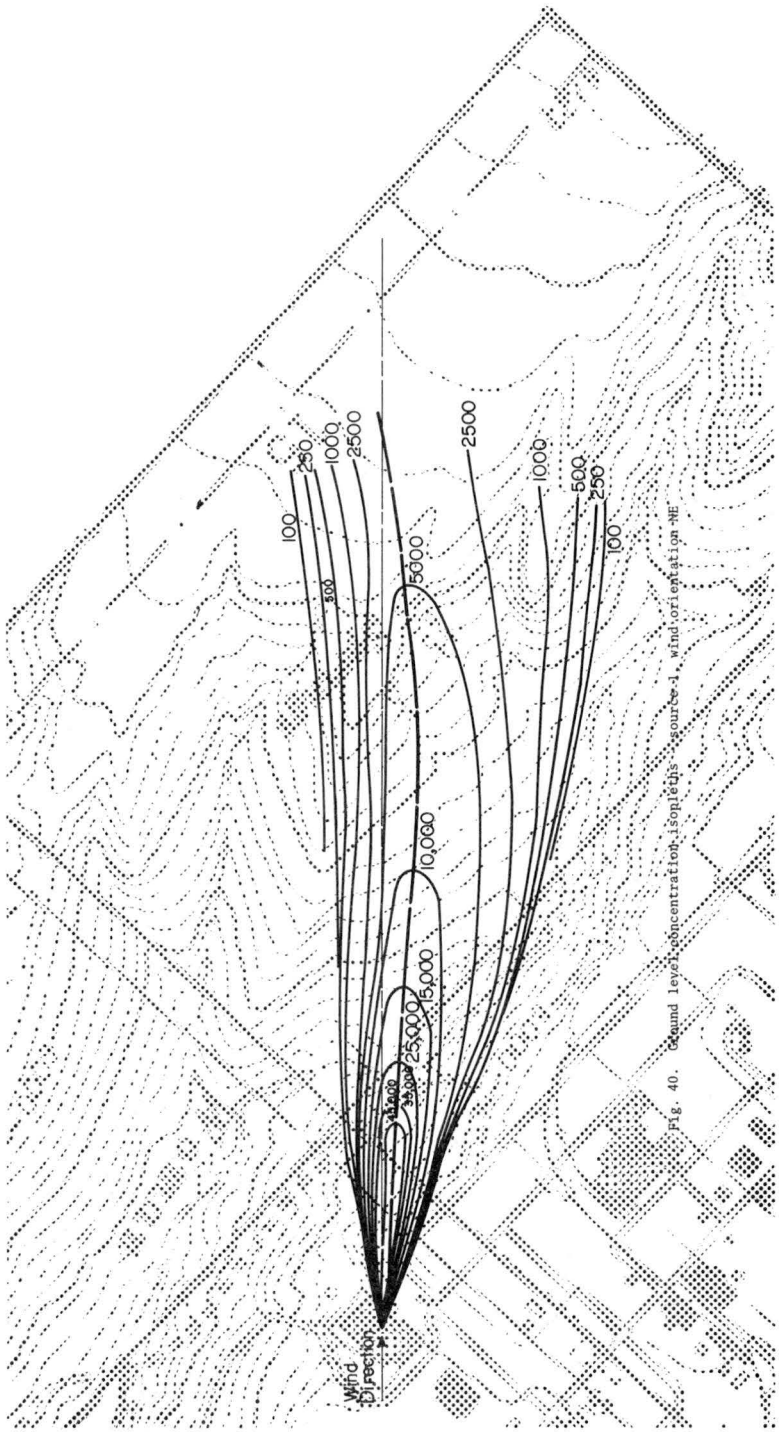

Fig. 40. Ground level concentration isopleths - source-1, wind orientation NE

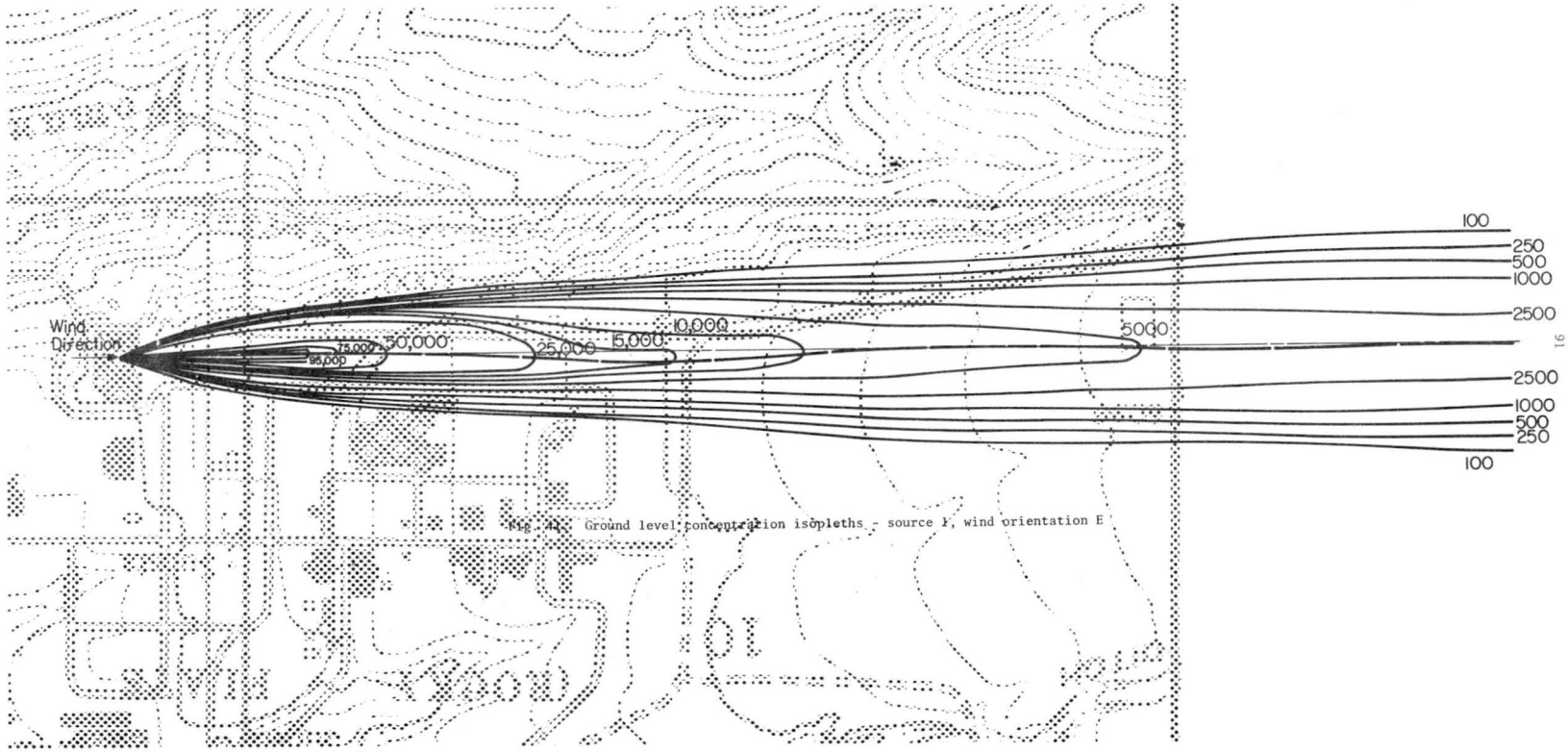

Fig. 41: Ground level concentration isopleths - source F, wind orientation E

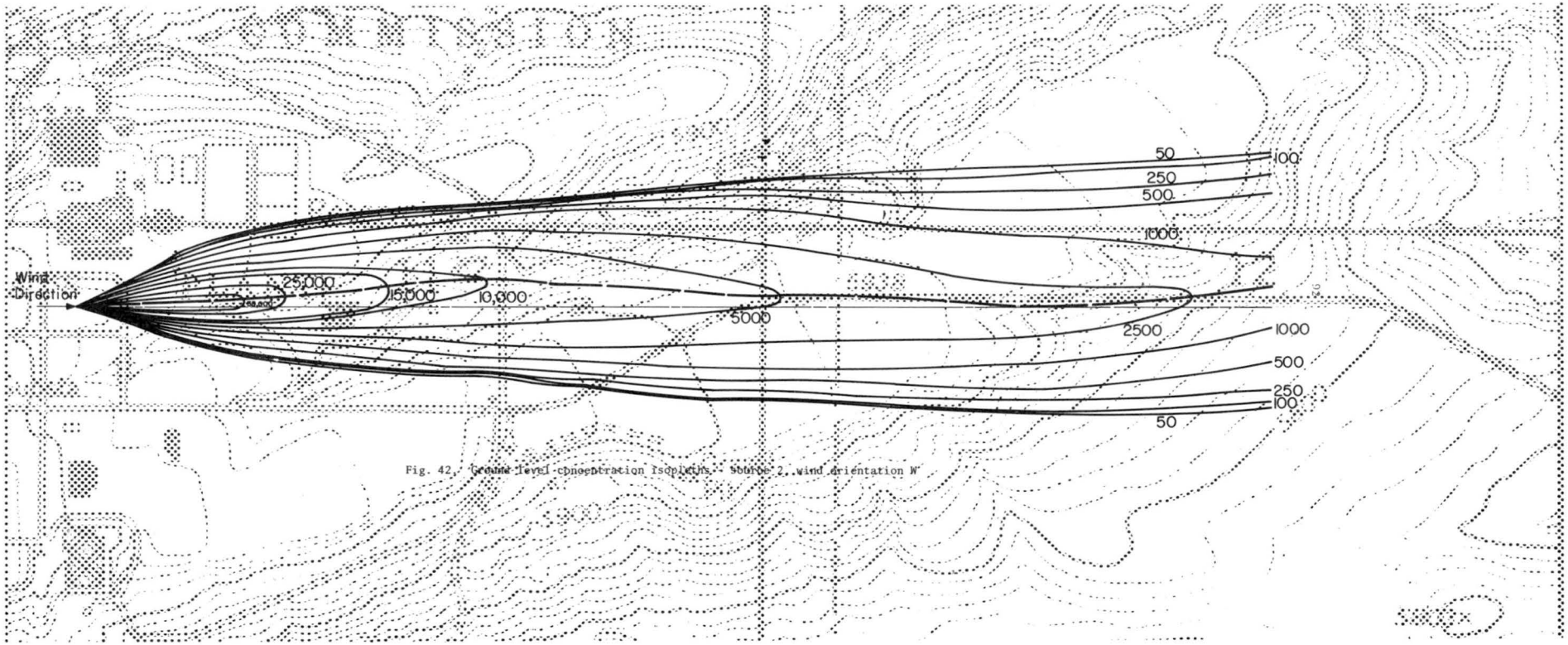

Fig. 42. Ground level concentration isopleths - source 2, wind orientation W

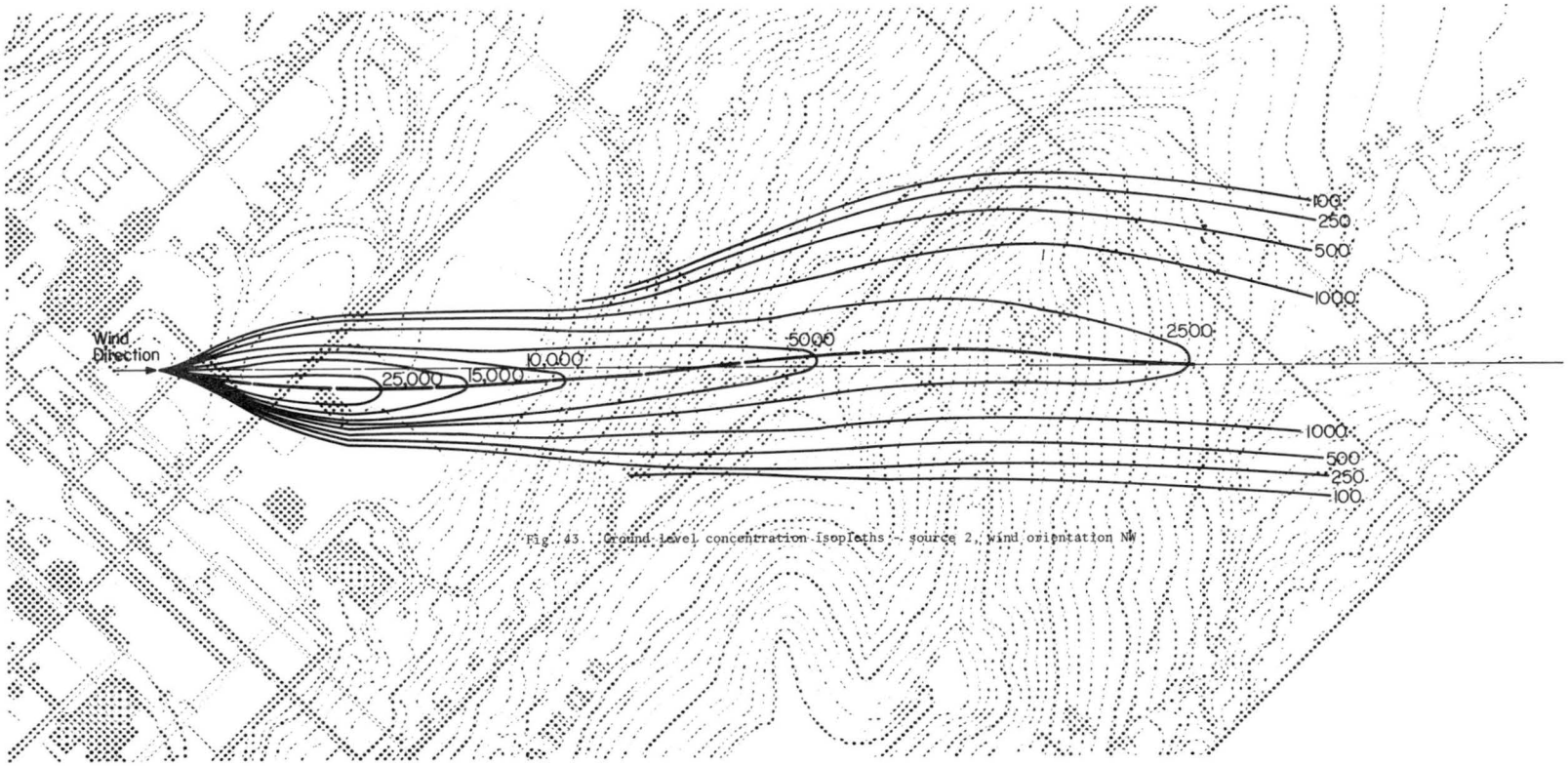

Fig. 43. Ground level concentration isopleths - source 2, wind orientation NW

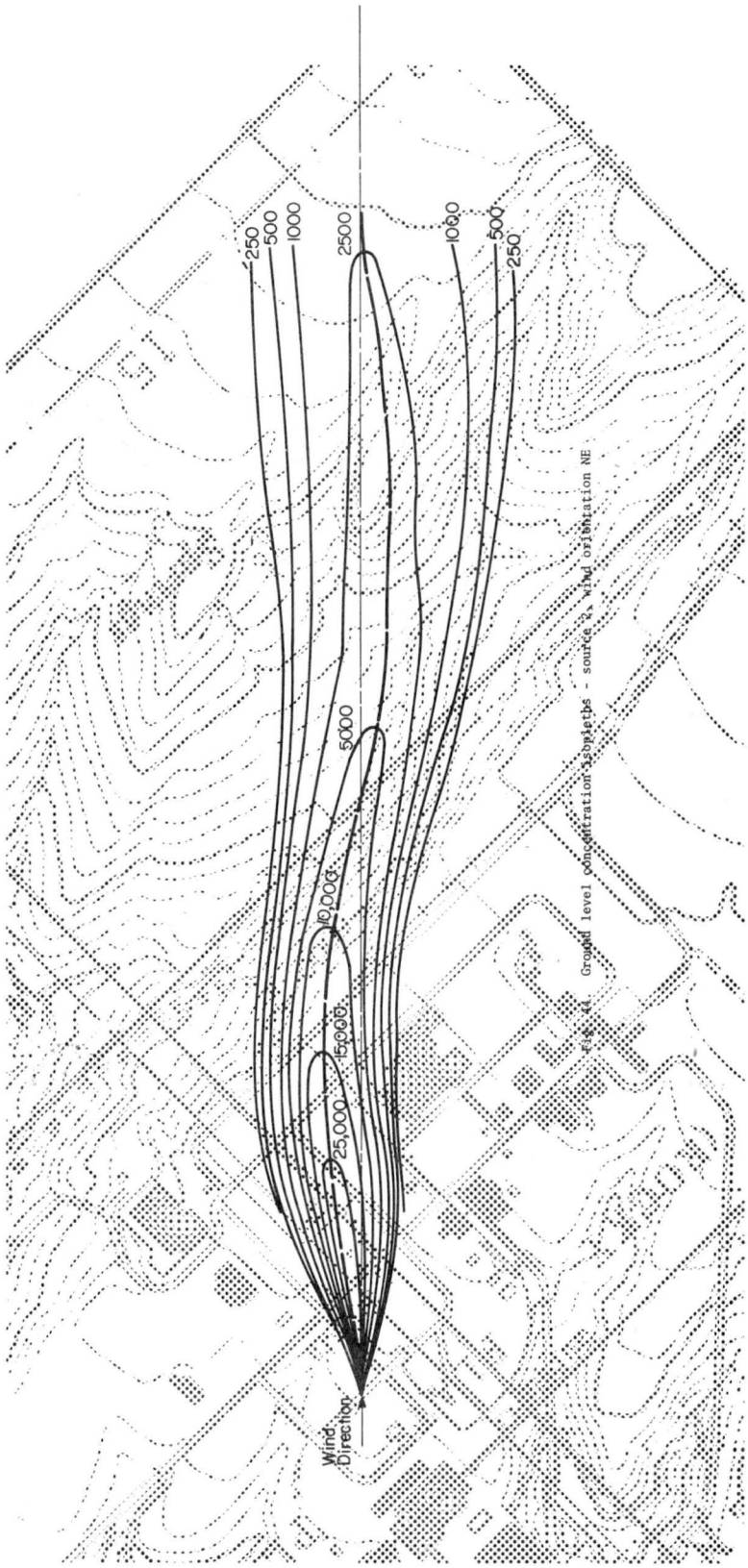

Fig. 44 Ground level concentration isopleths - source 2, wind orientation NE

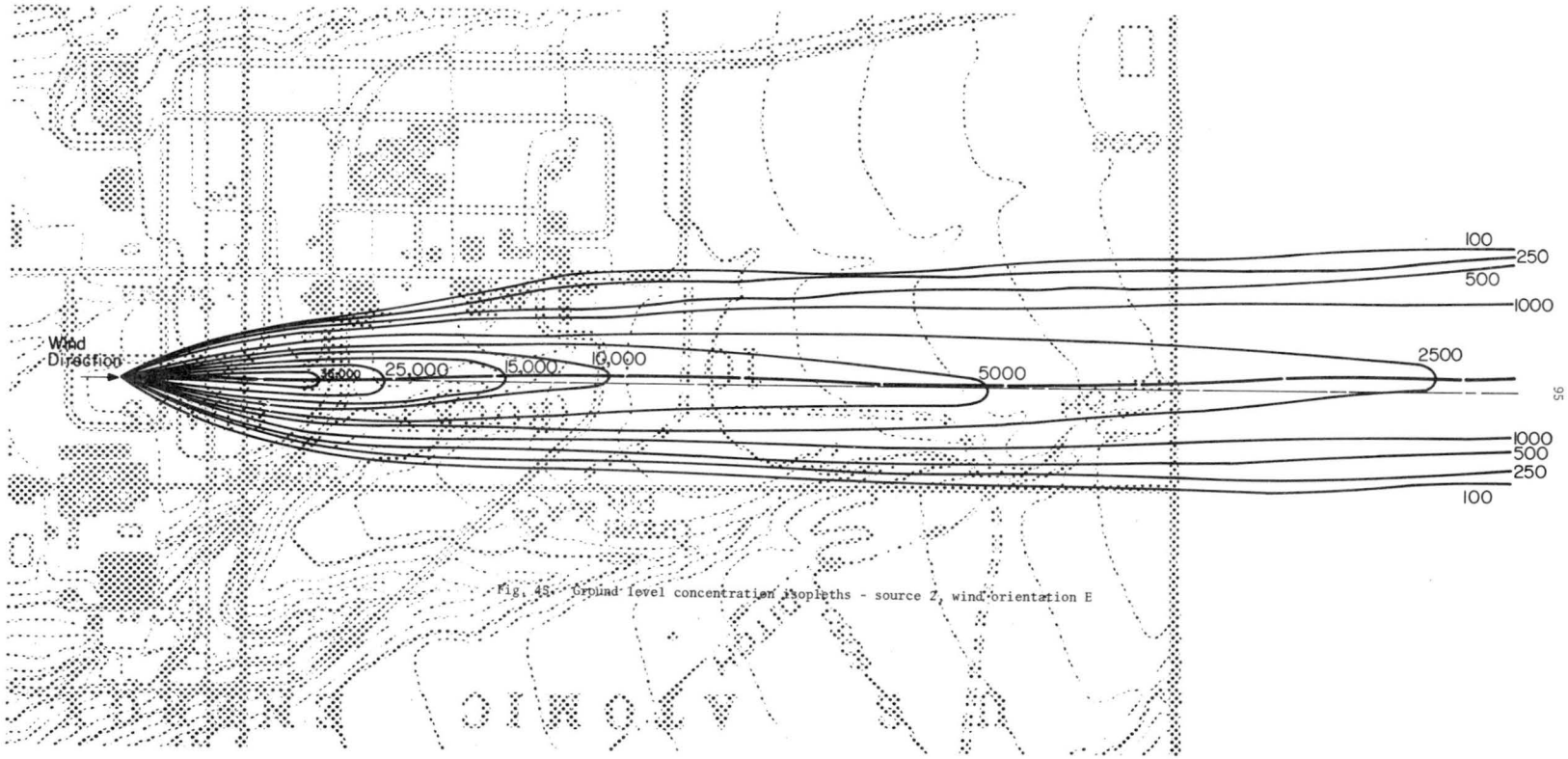

Fig. 45. Ground level concentration isopleths - source Z, wind orientation E

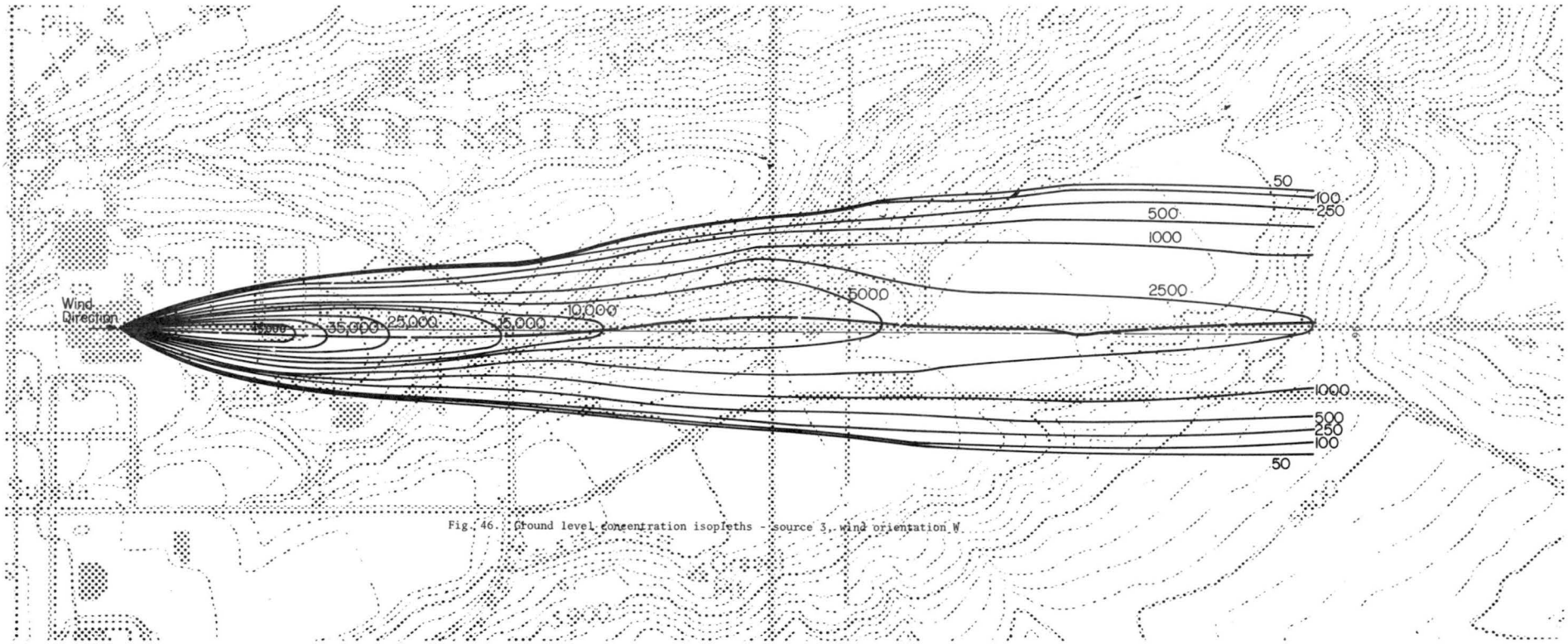

Fig. 46. Ground level concentration isopleths - source 3, wind orientation W

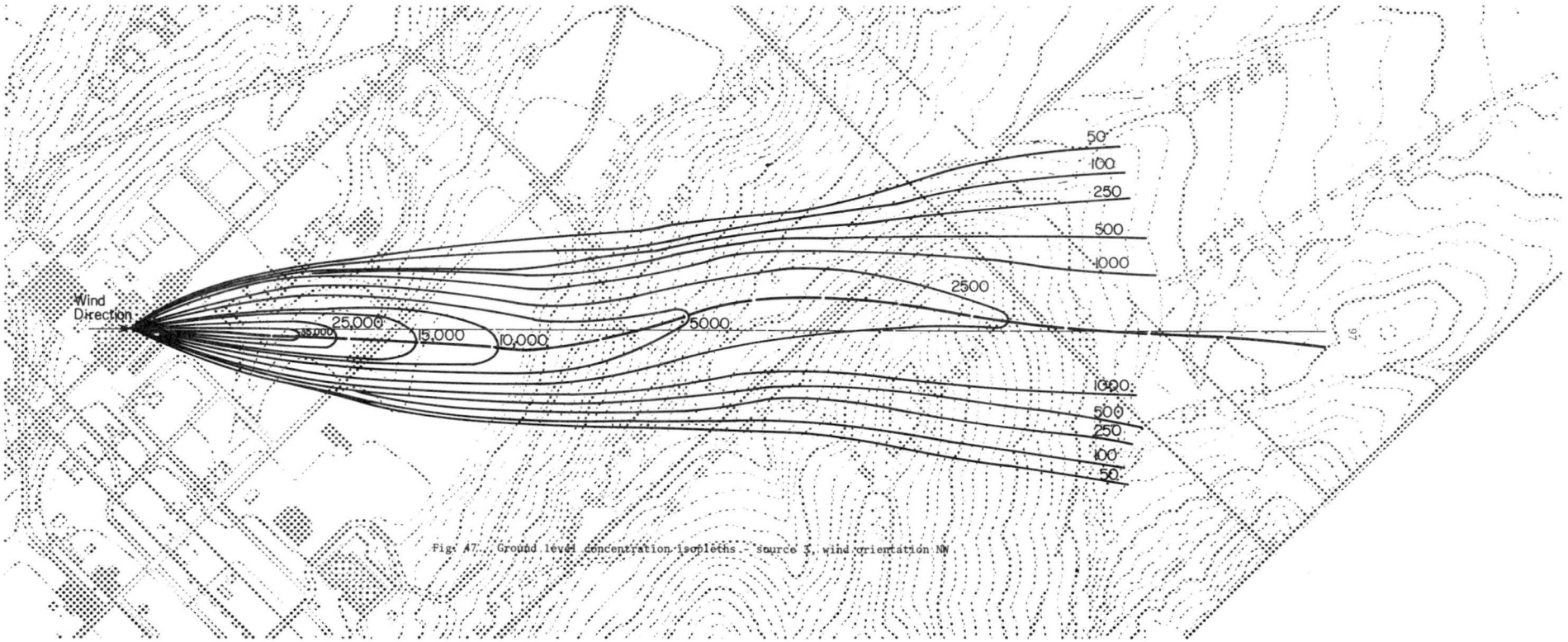

Fig. 47. Ground level concentration isopleths - source 5, wind orientation NW

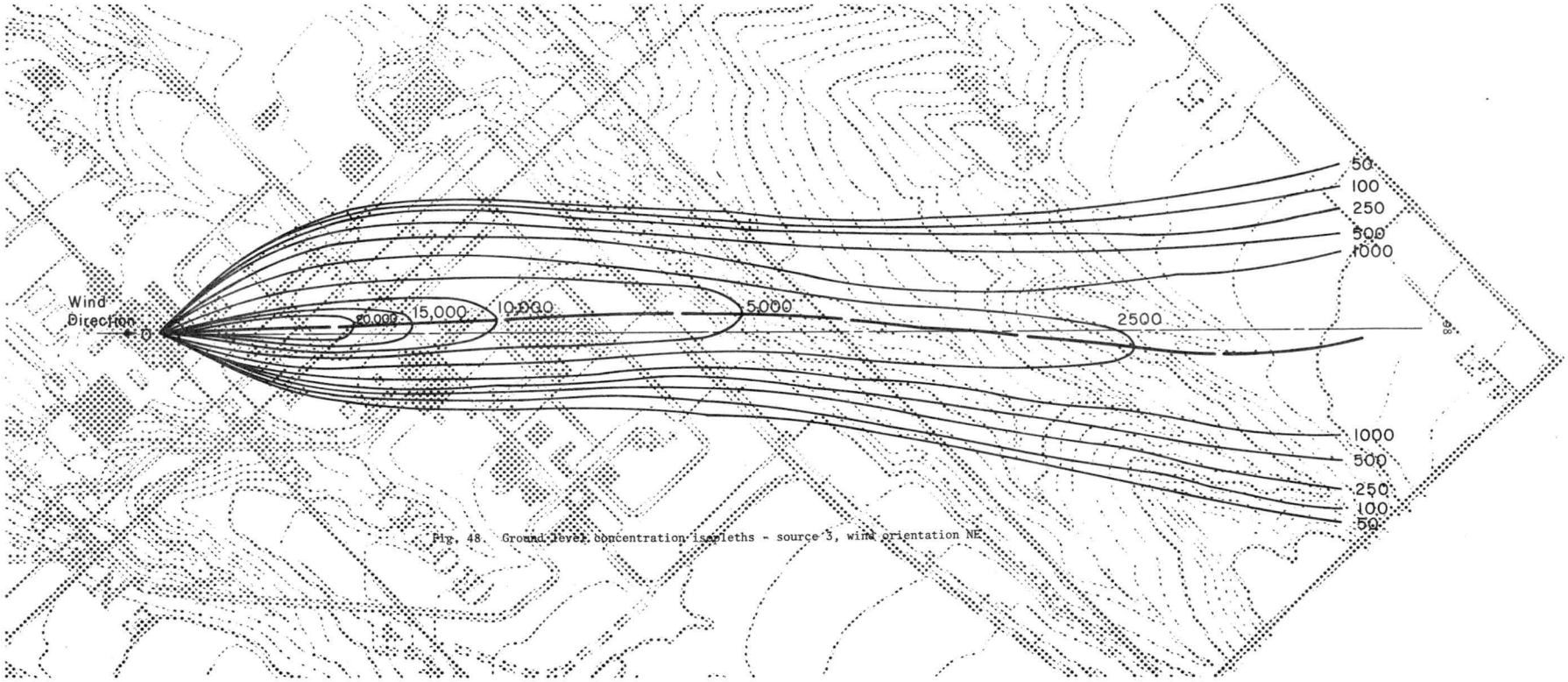

Fig. 48. Ground level concentration isopleths - source 3, wind orientation NE.

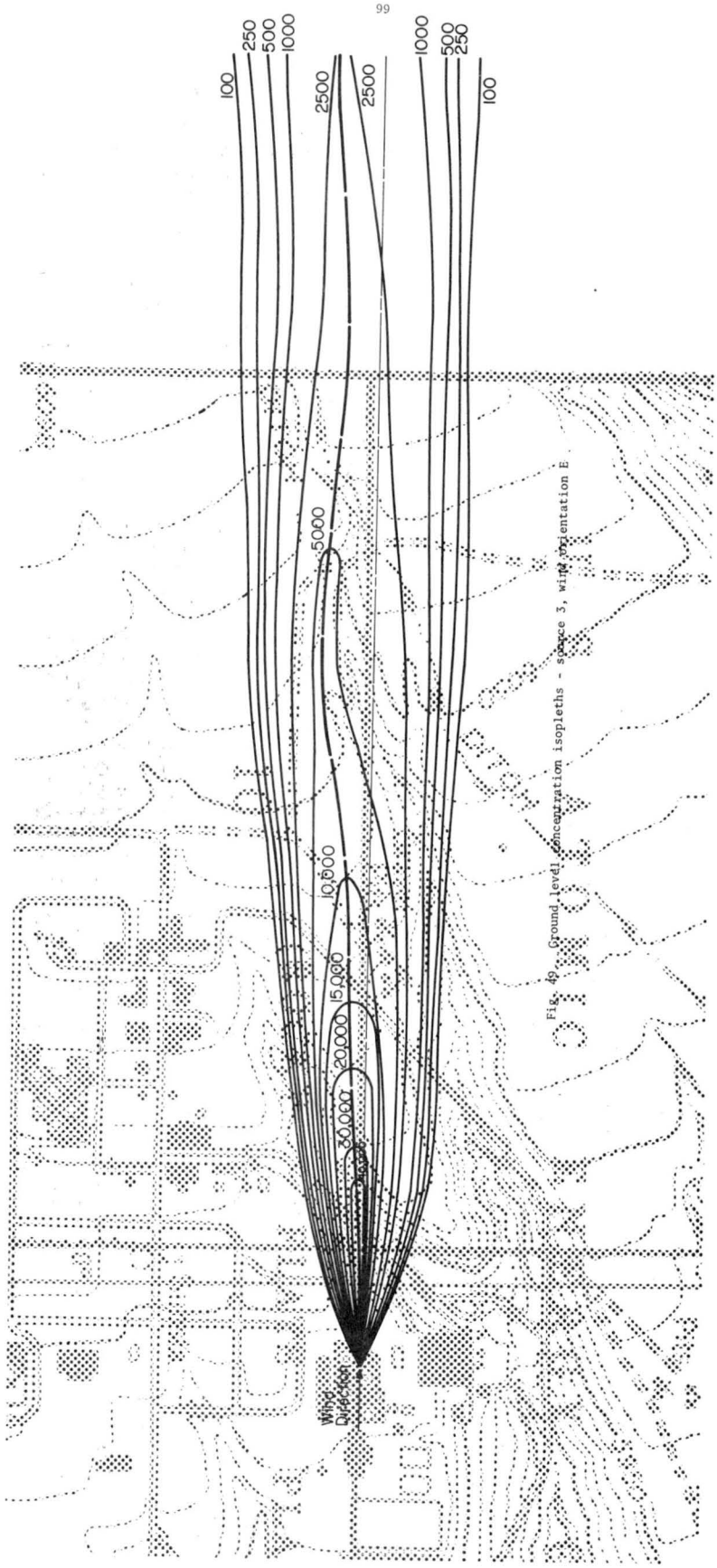

Fig. 49. Ground level concentration isopleths - source 3, wind orientation E

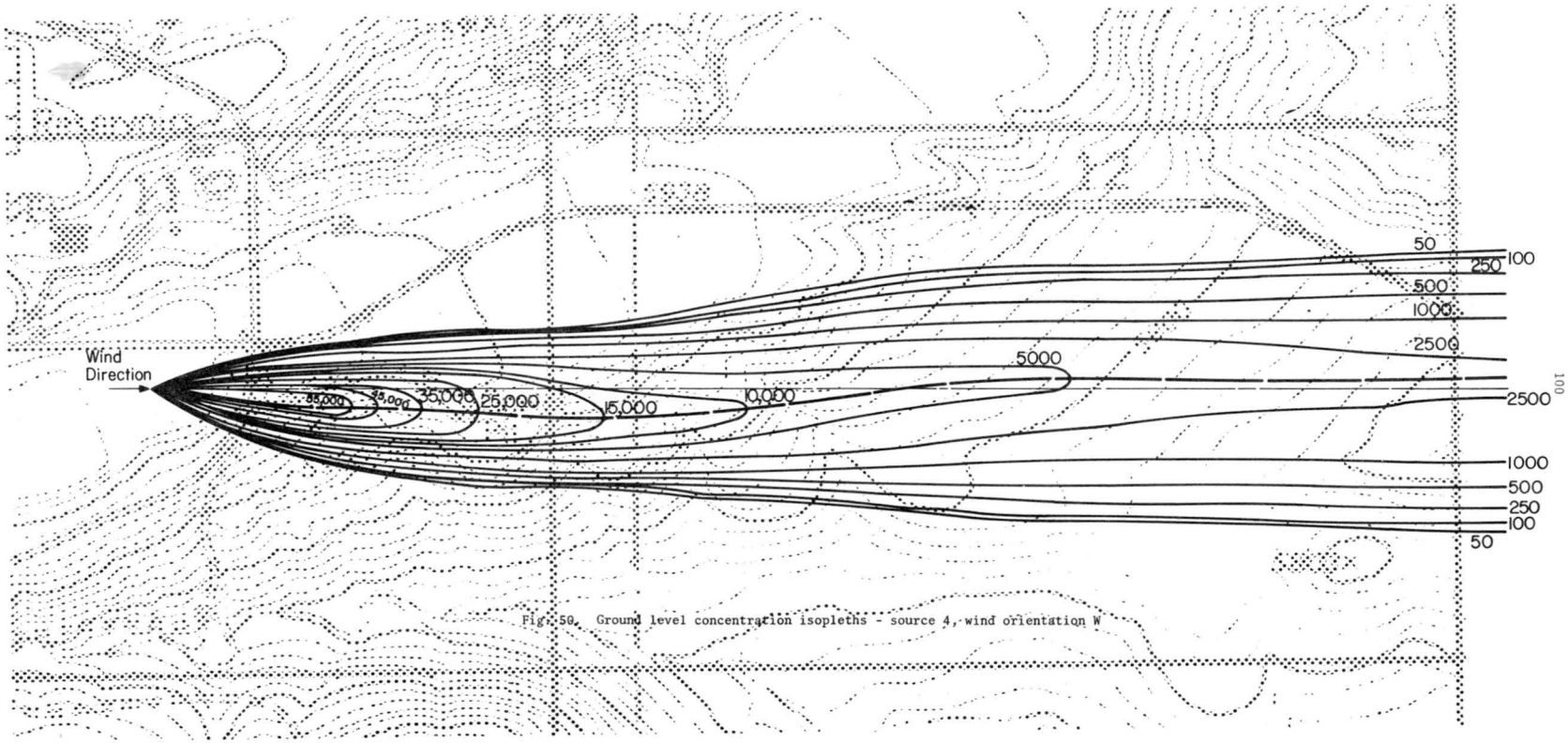

Fig. 50. Ground level concentration isopleths - source 4, wind orientation W

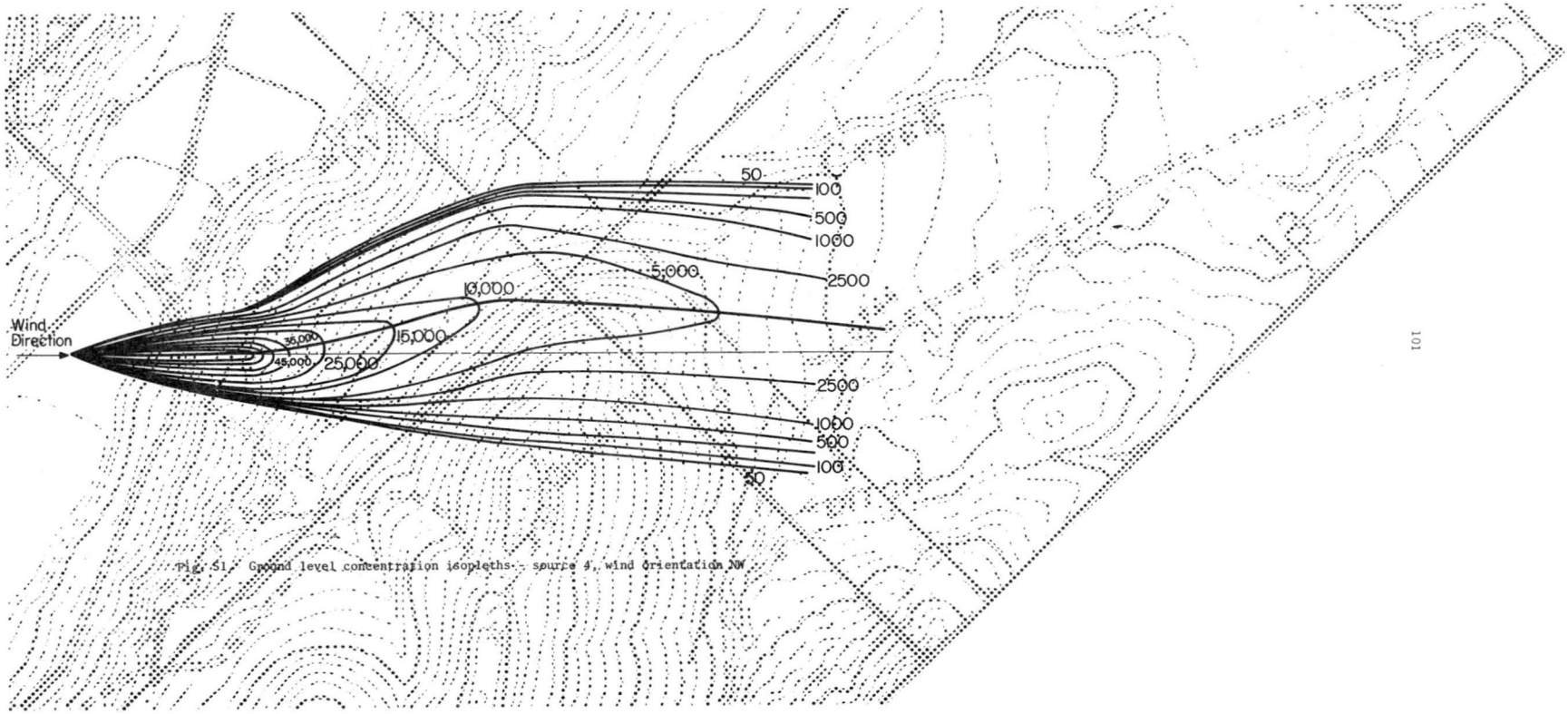

Fig. 51. Ground level concentration isopleths - source 4, wind orientation NW

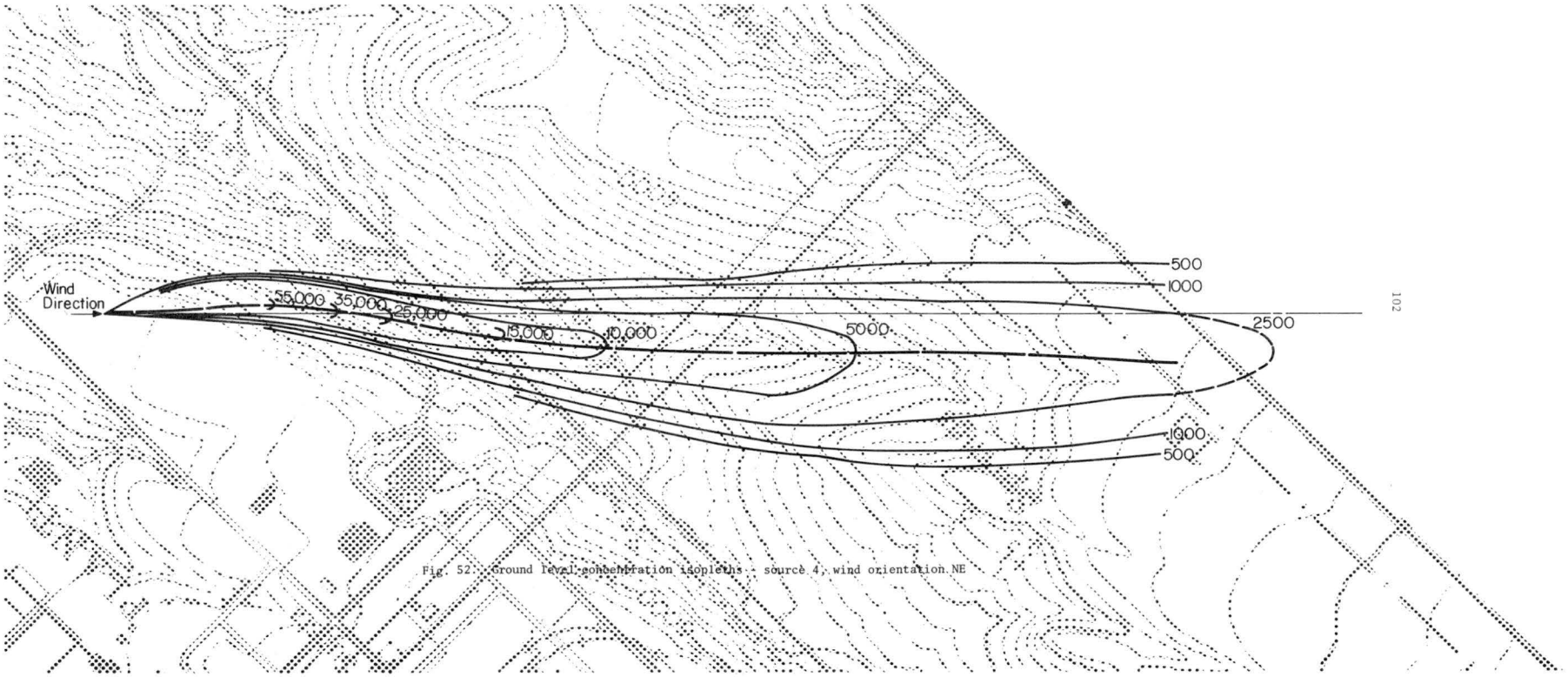

Fig. 52. Ground level concentration isopleths - source 4, wind orientation NE

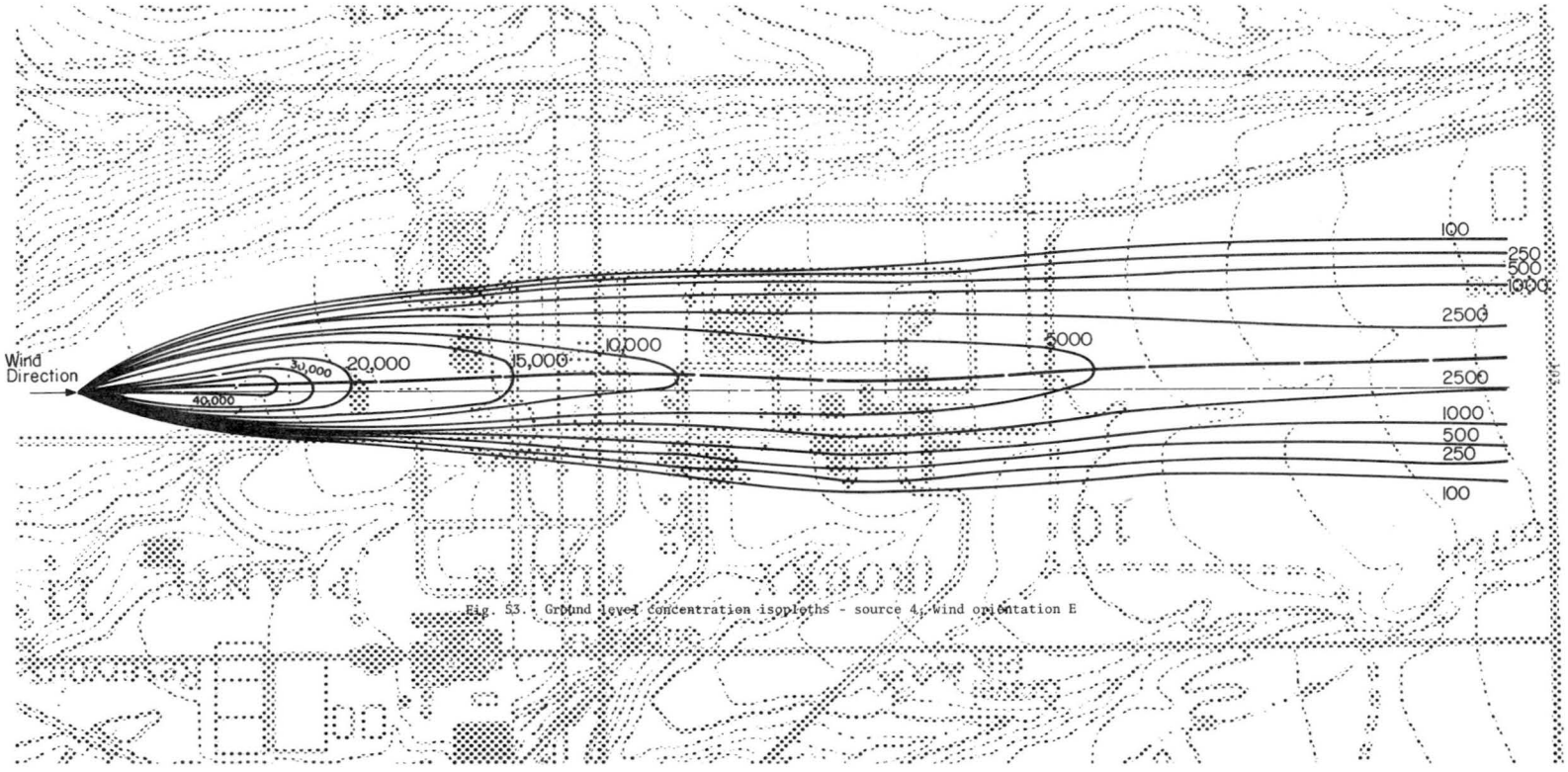

Fig. 53. Ground level concentration isopleths - source 4, wind orientation E

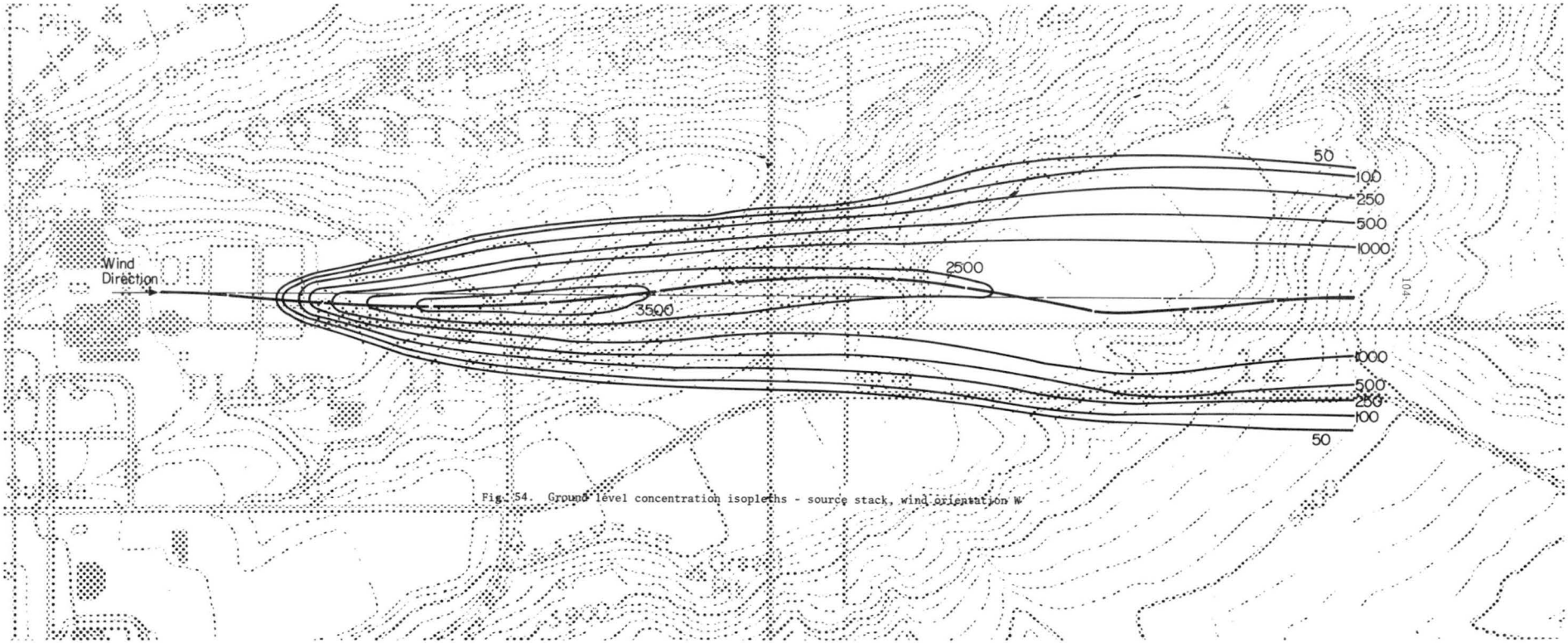

Fig. 54. Ground level concentration isopleths - source stack, wind orientation W

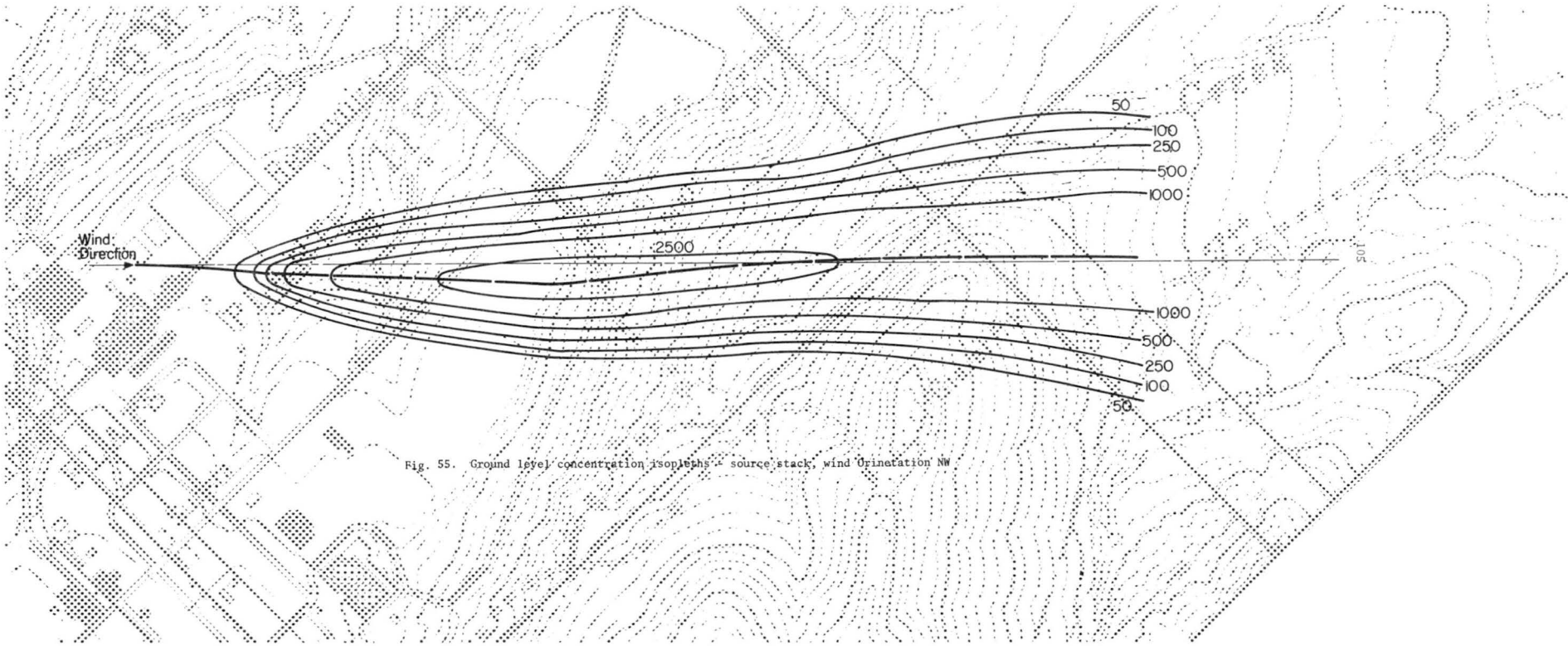

Fig. 55. Ground level concentration isopleths - source stack, wind orientation NW

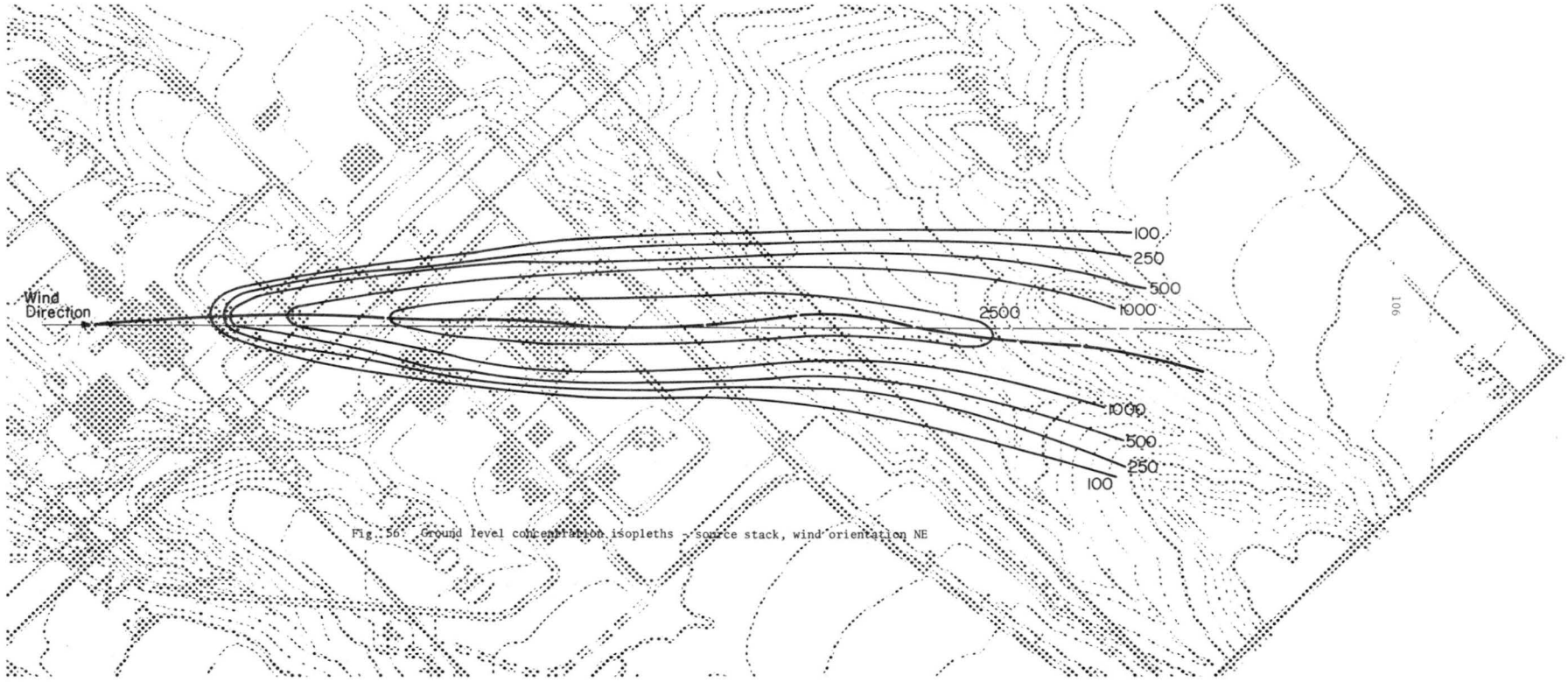

Fig. 56. Ground level concentration isopleths - source stack, wind orientation NE

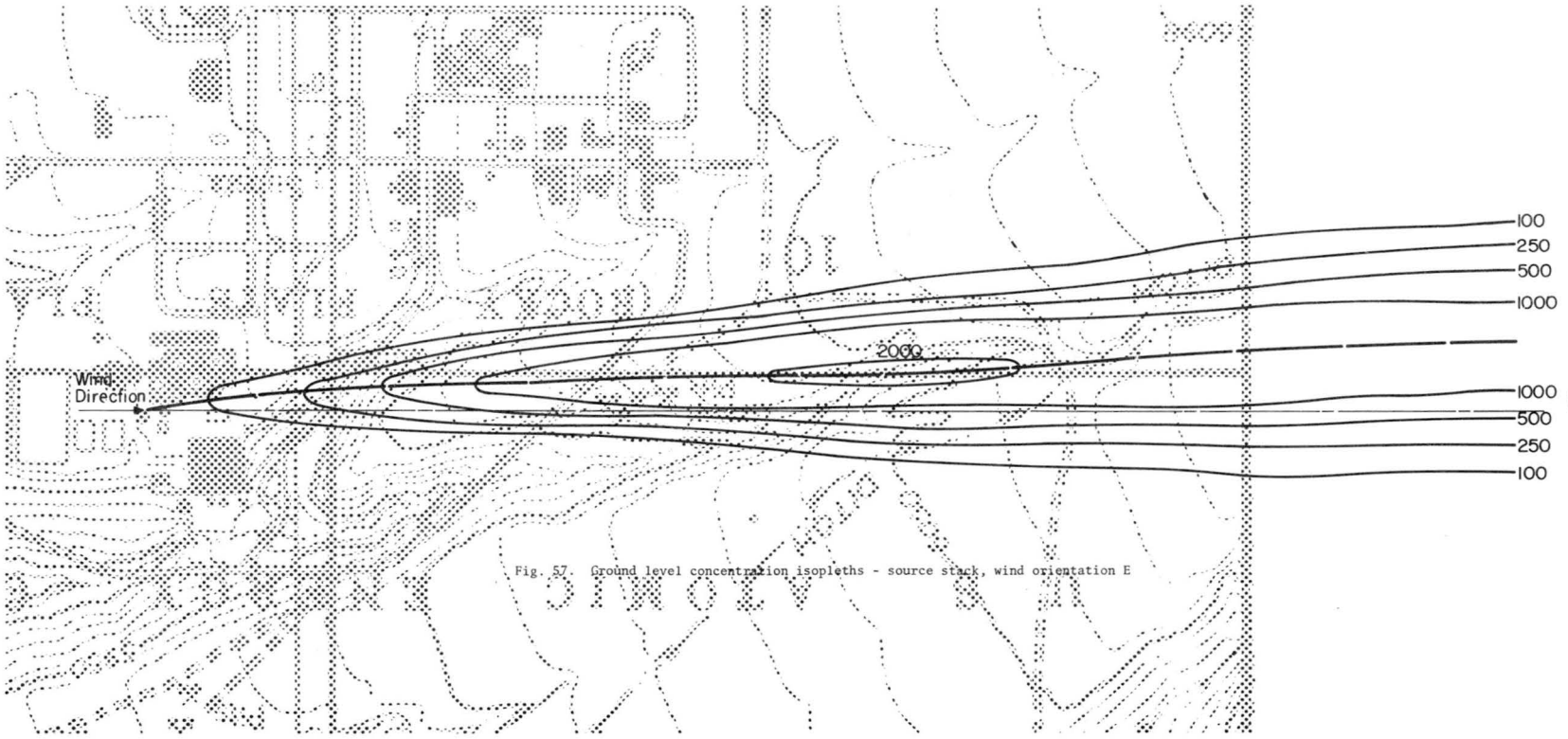

Fig. 57. Ground level concentration isopleths - source stack, wind orientation E

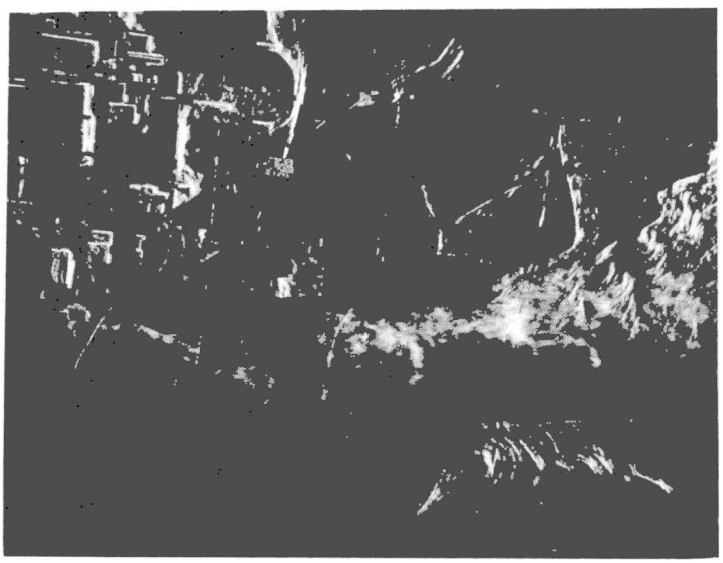

Fig. 58. Smoke visualization - top view - source 1, west wind

Fig. 59. Smoke visualization - top view - source 1, west wind

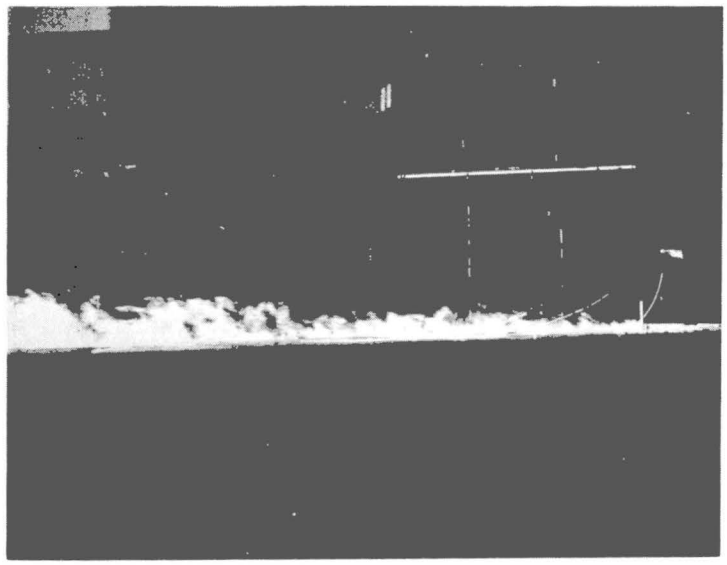

Fig. 60. Smoke visualization - side view - source 1, west wind

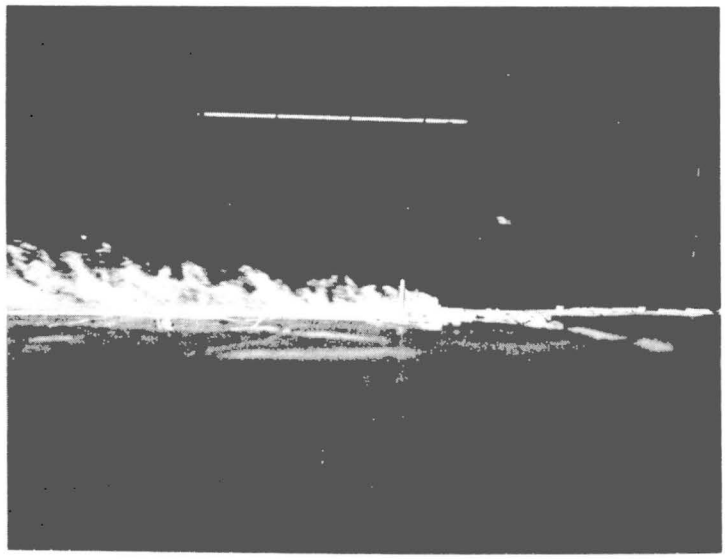

Fig. 61. Smoke visualization - side view - source 2, west wind

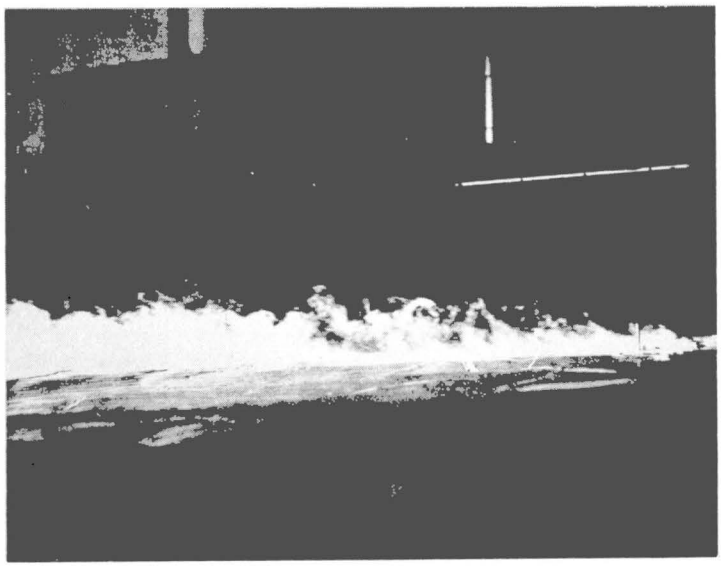

Fig. 62. Smoke visualization - side view - source 3, west wind

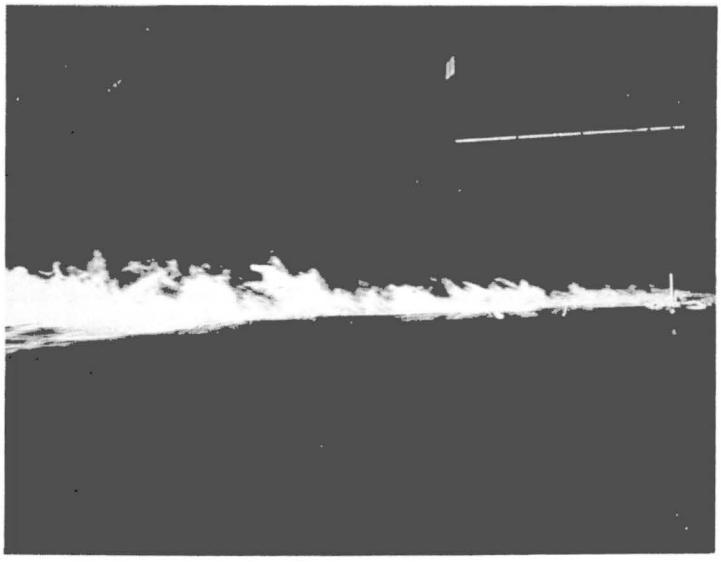

Fig. 63. Smoke visualization - side view - oil, west wind

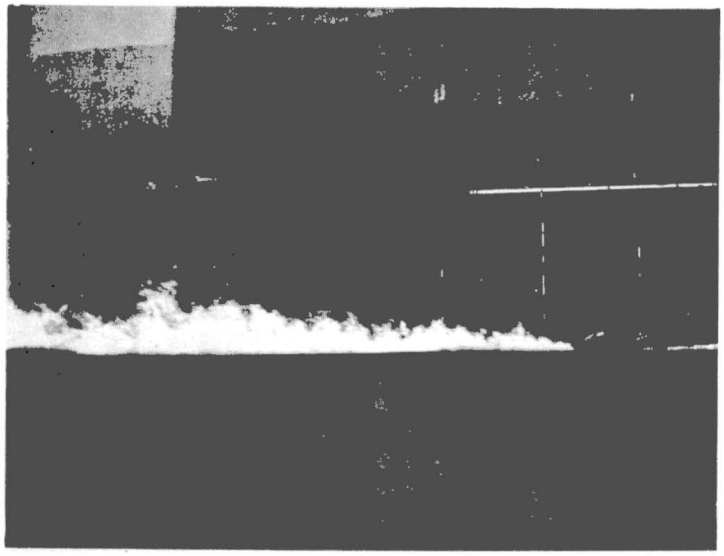

Fig. 64. Smoke visualization - side view - stack west wind

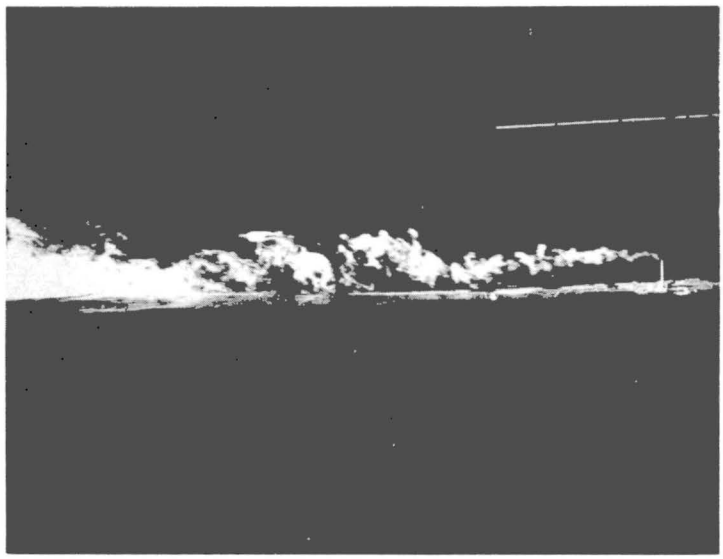

Fig. 65. Smoke visualization - side view - stack, west wind

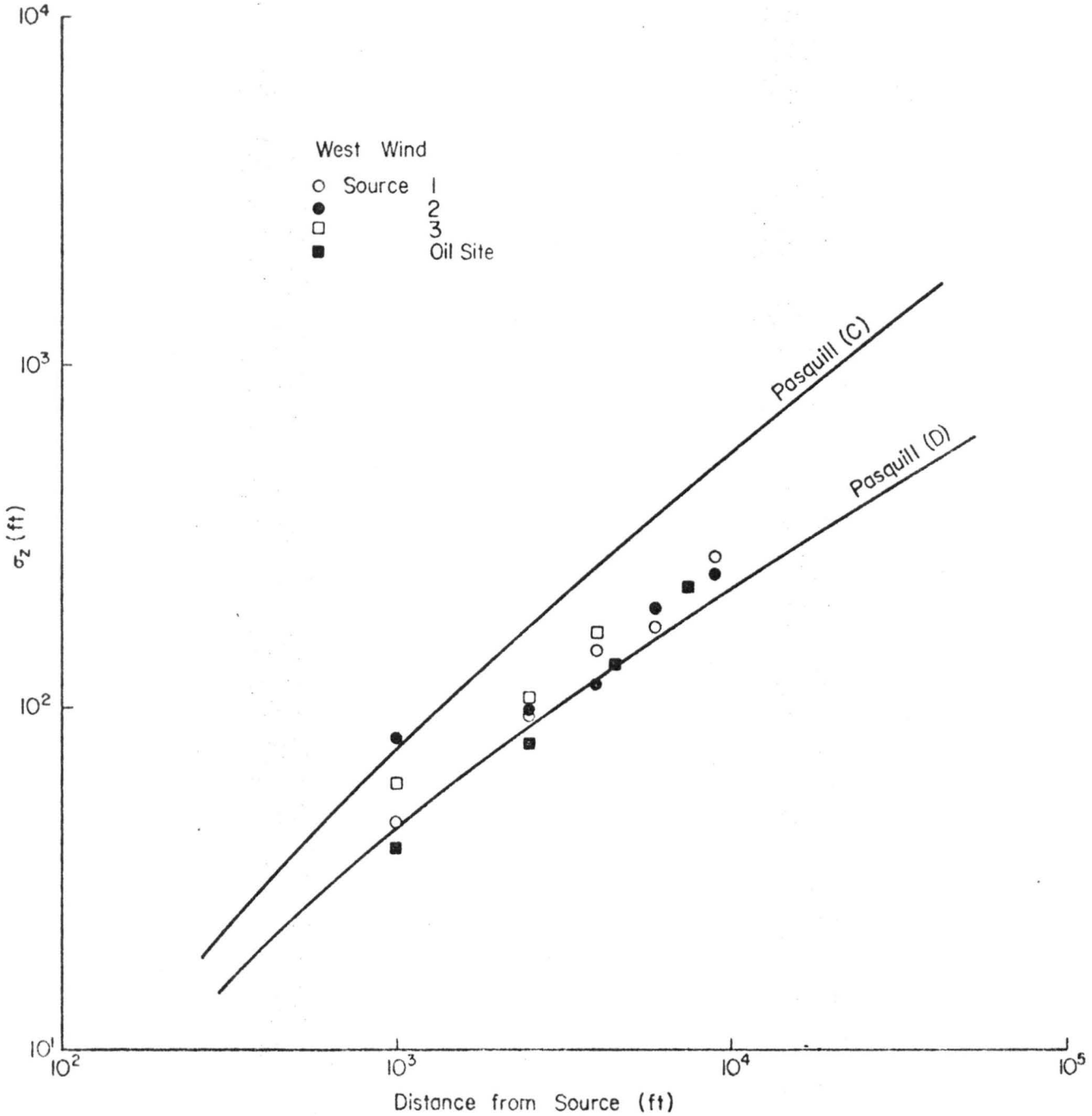

Fig. 66. Standard deviation of vertical concentration distribution - west wind

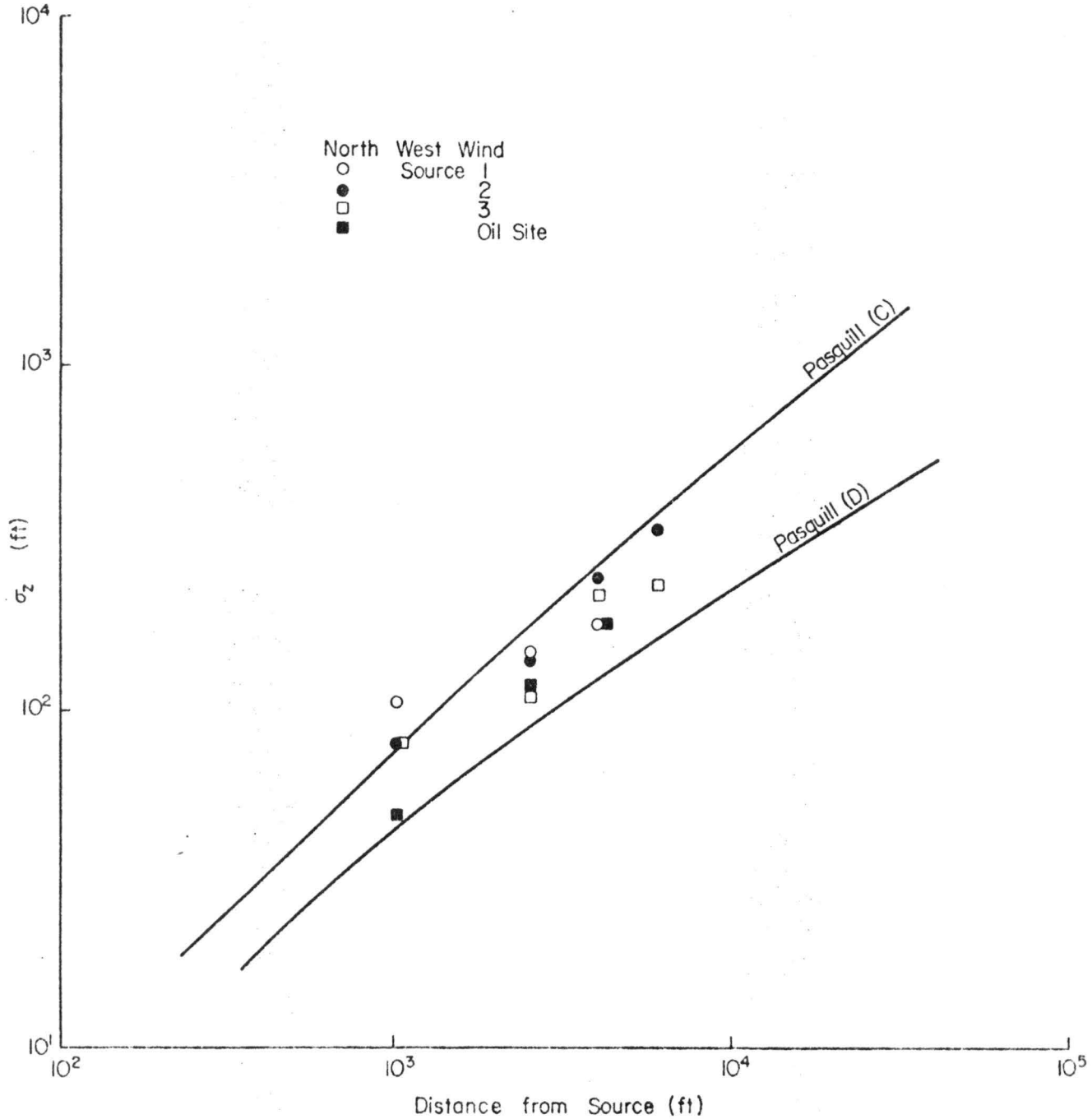

Fig. 67. Standard deviation of vertical concentration distribution - NW wind

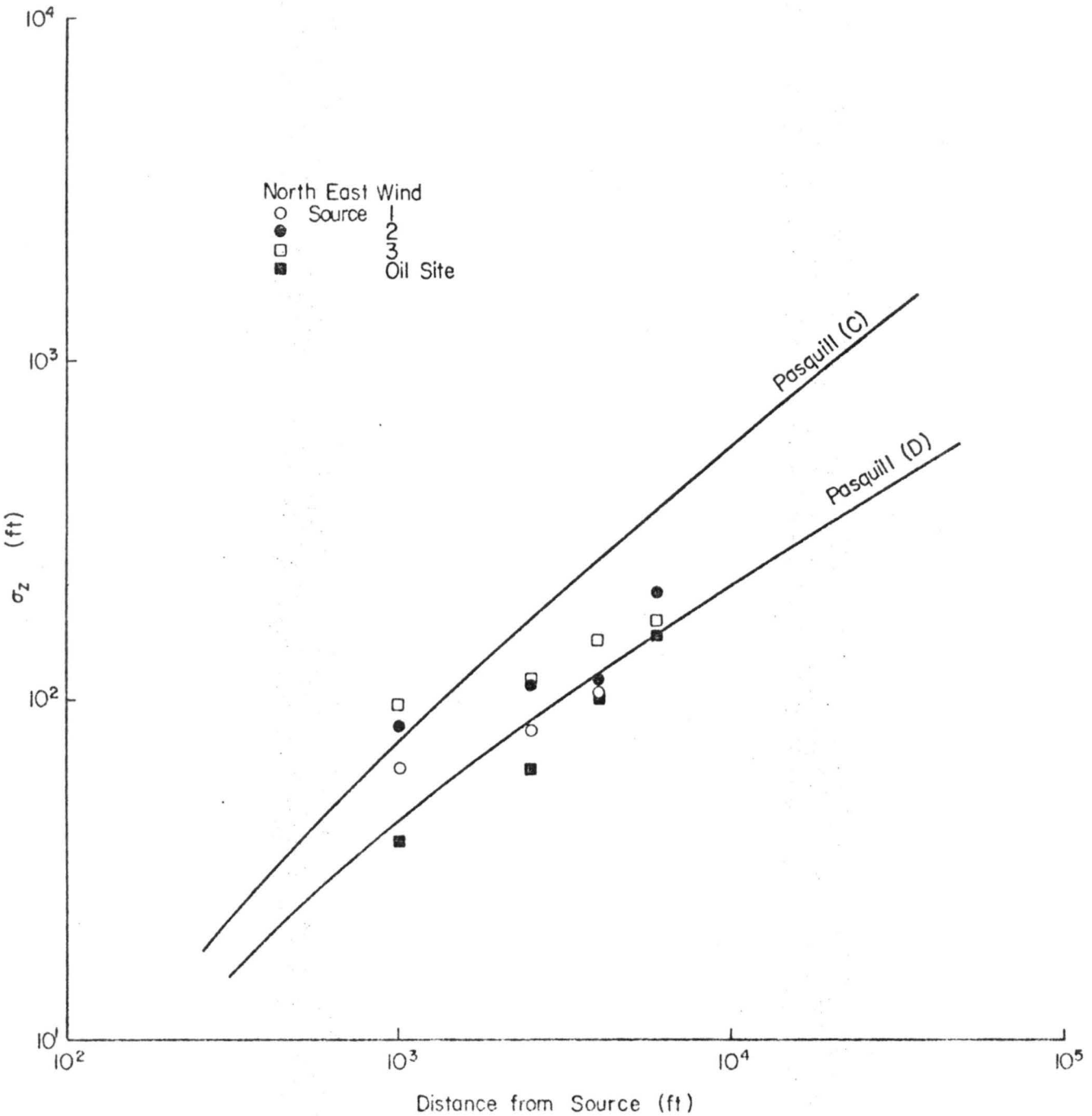

Fig. 68. Standard deviation of vertical concentration distribution - NE wind

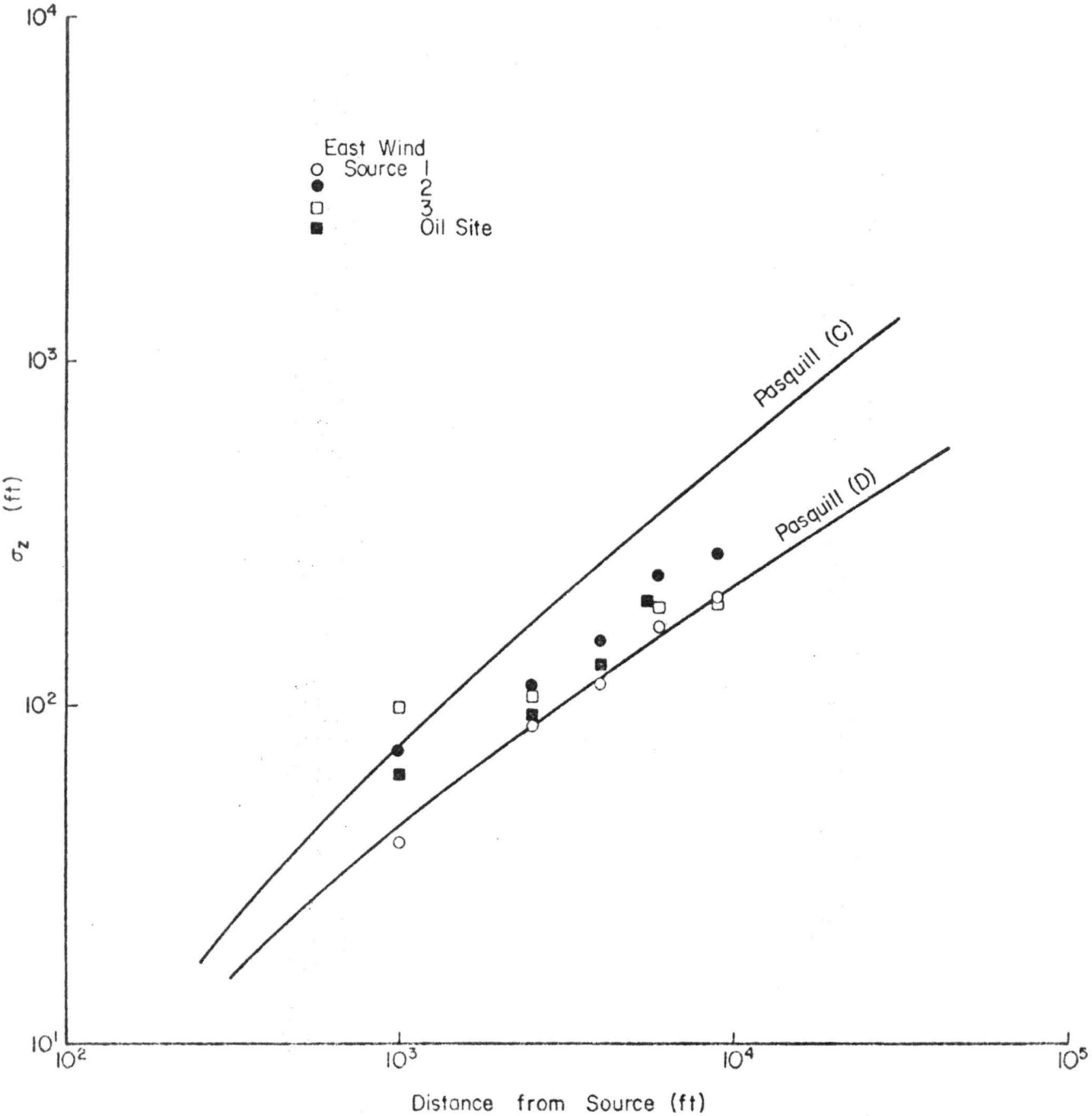

Fig. 69. Standard deviation of vertical concentration distribution - east wind

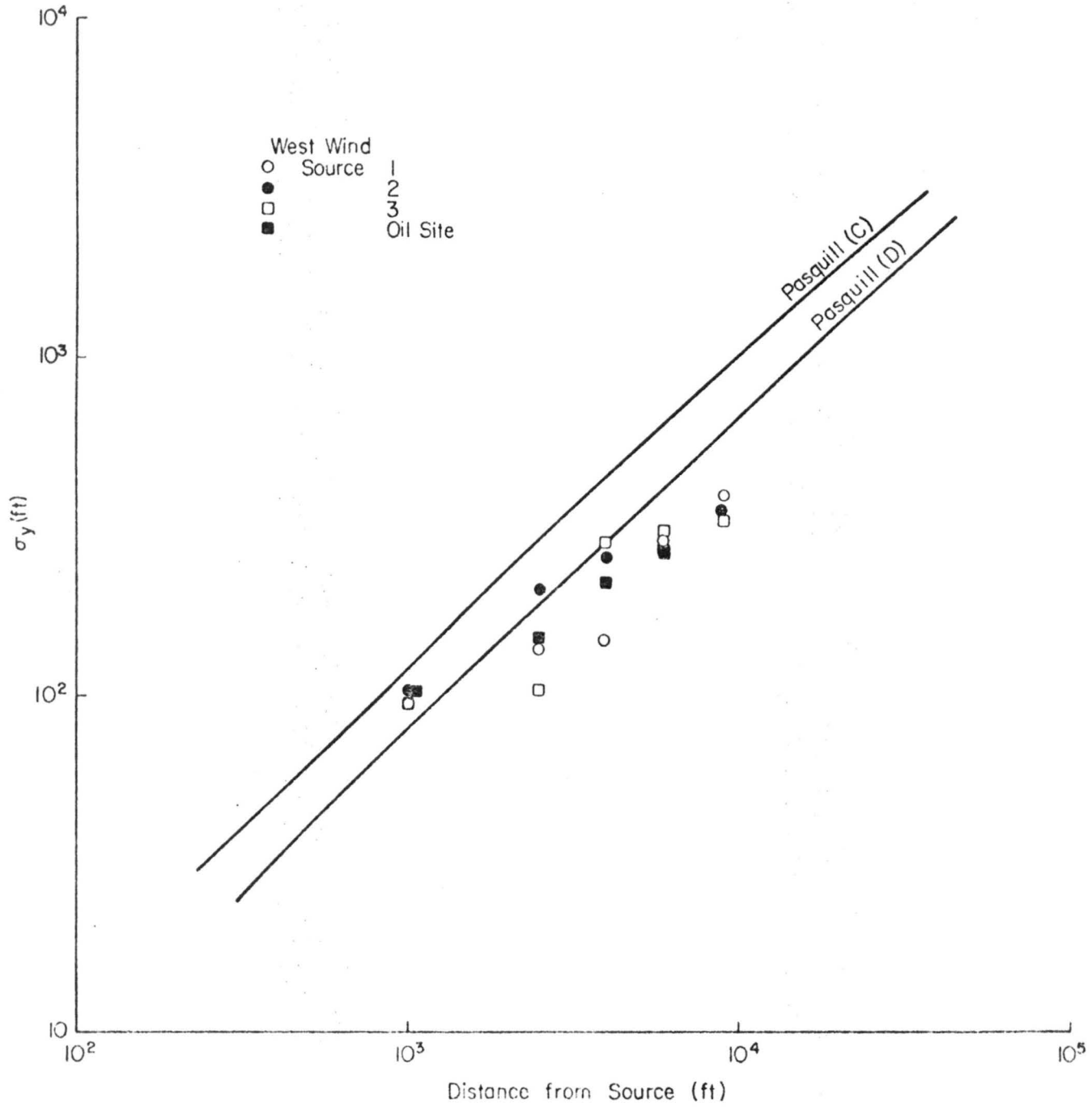

Fig. 70. Standard deviation of lateral concentration distribution - west wind

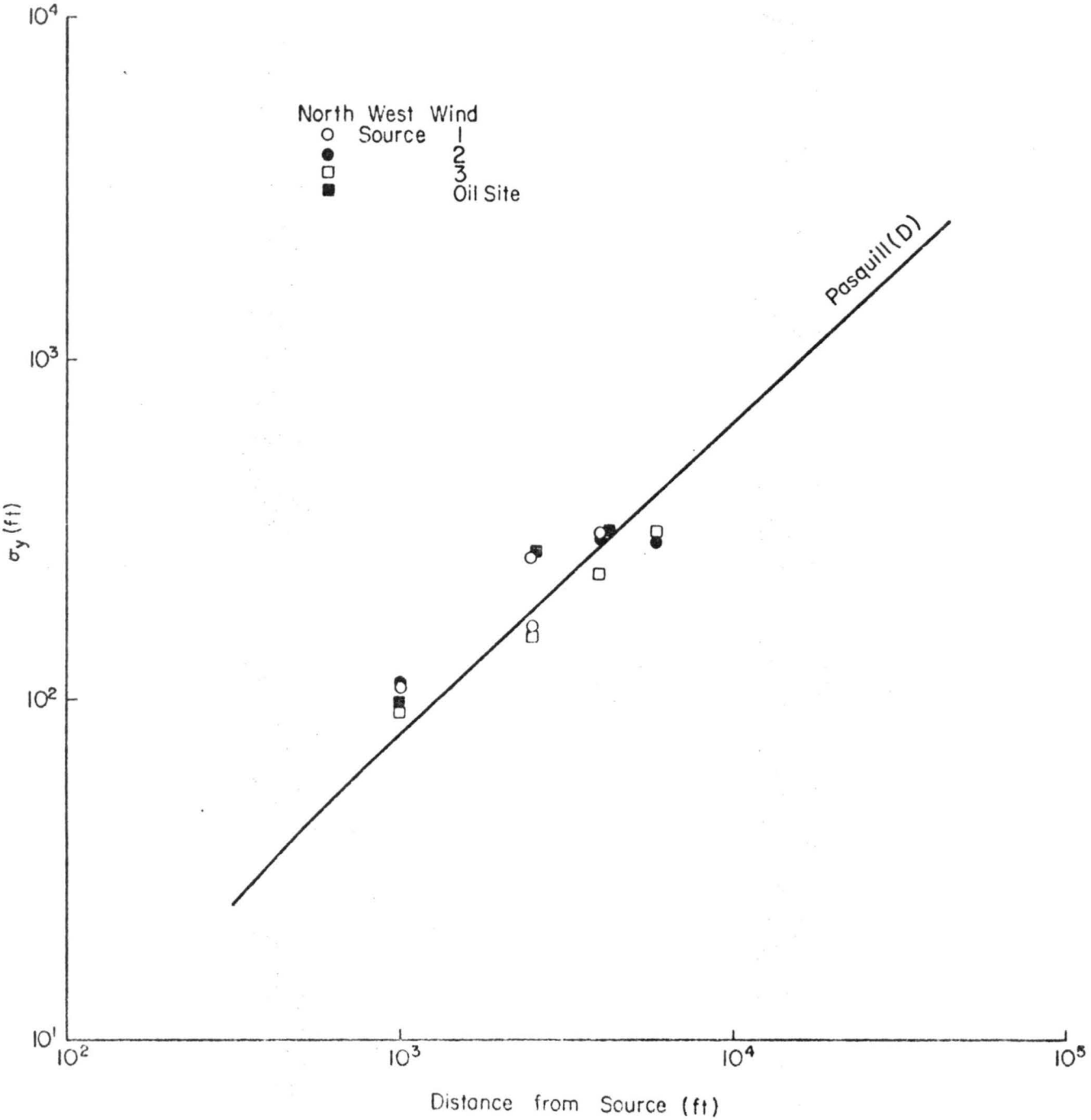

Fig. 71. Standard deviation of lateral concentration distribution - NW wind

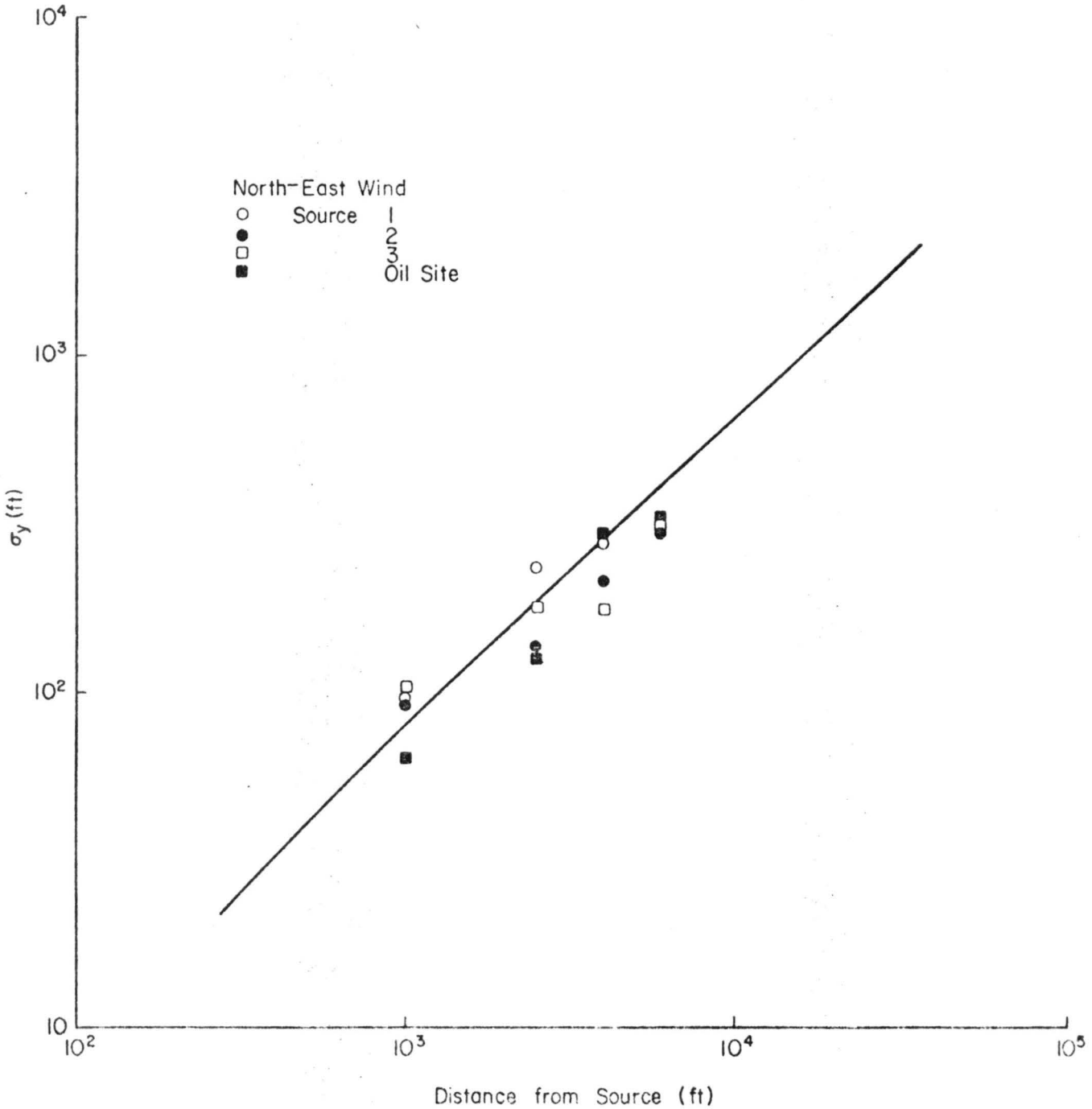

Fig. 72. Standard deviation of lateral concentration distribution - NE wind

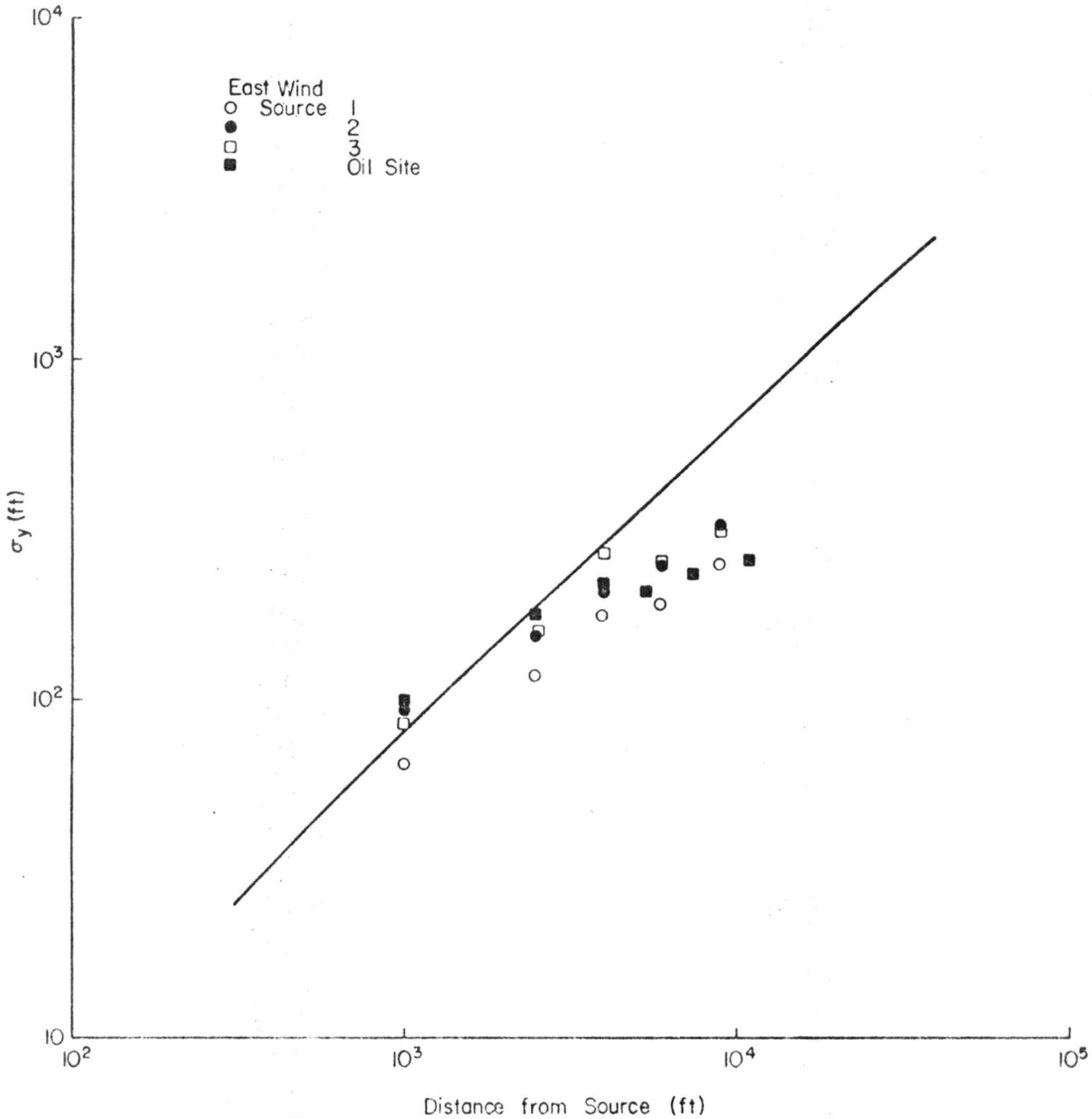

Fig. 73. Standard deviation of lateral concentration distribution - east wind

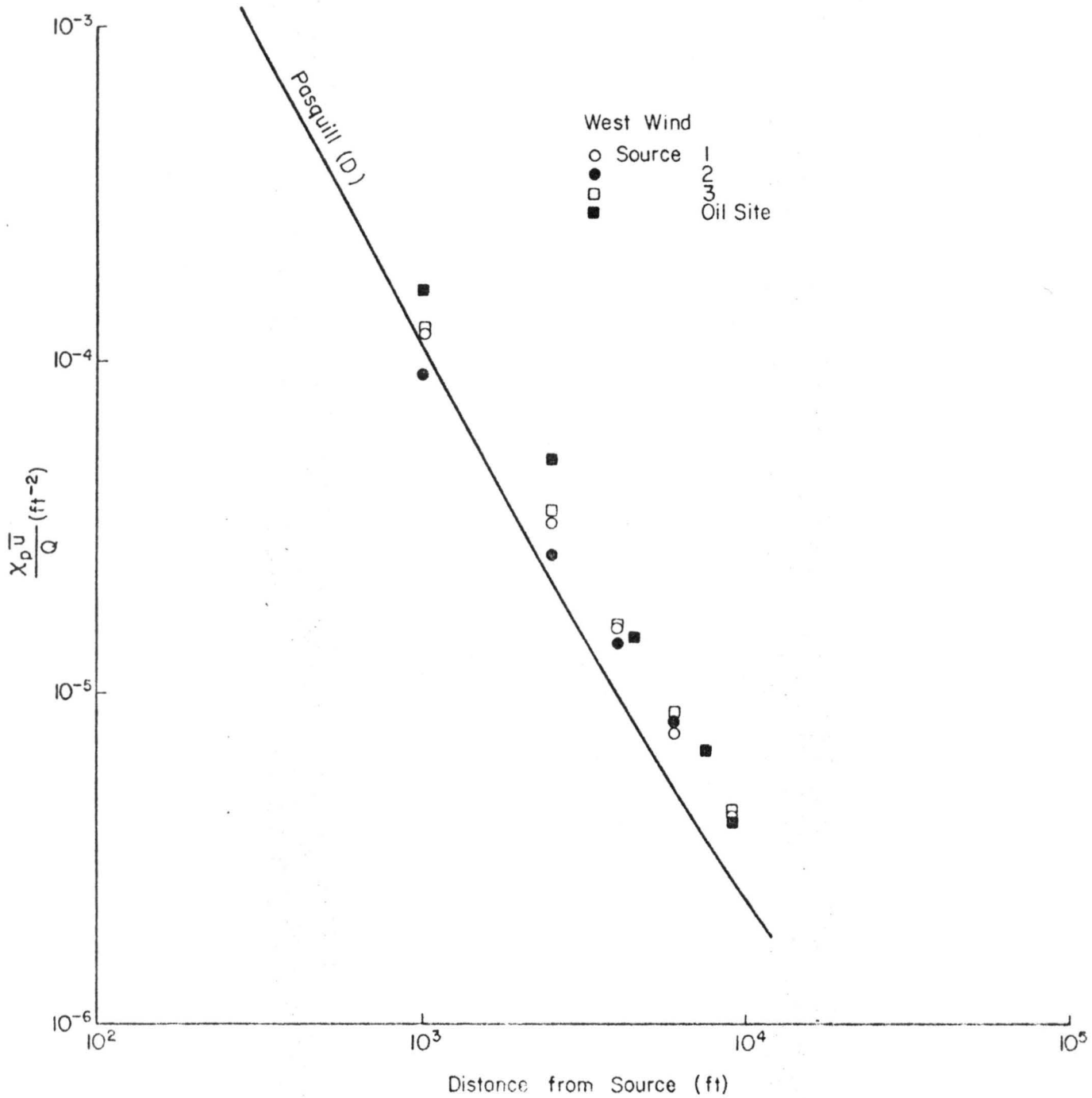

Fig. 74. Normalized ground level maximum average ground concentration - W wind

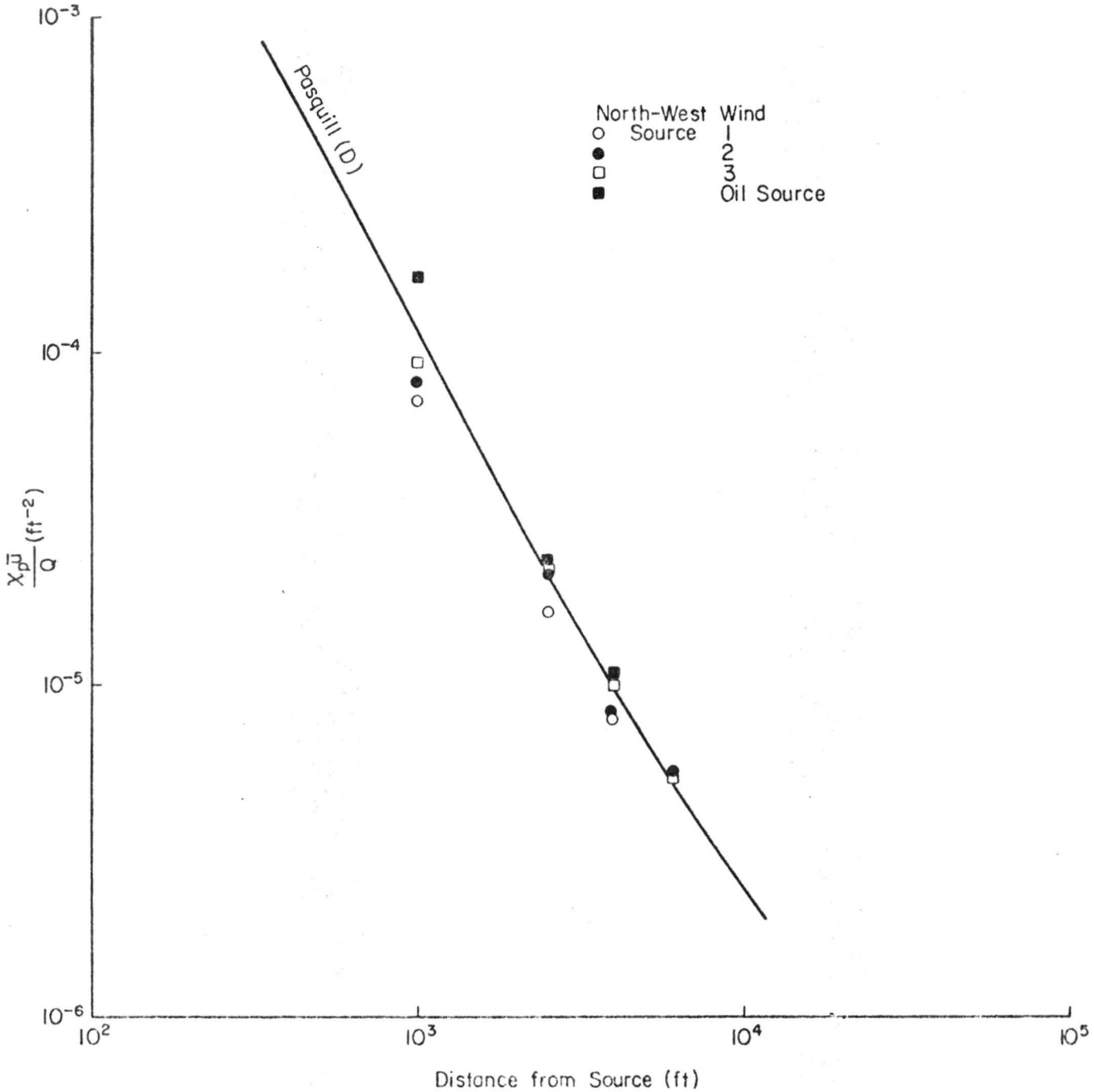

Fig. 75. Normalized ground level maximum average ground concentration - NW wind

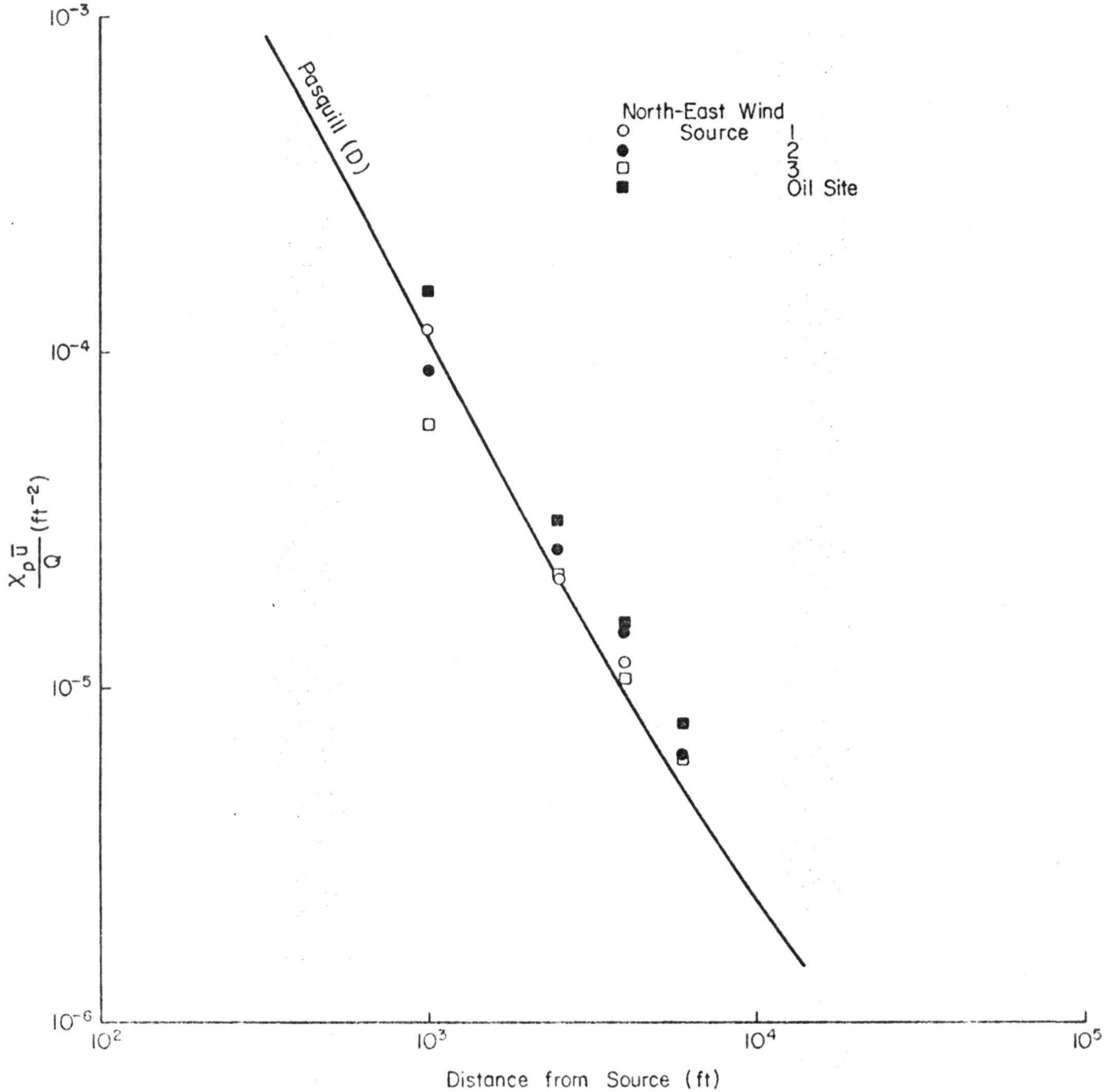

Fig. 76. Normalized ground level maximum average ground concentration - NE wind

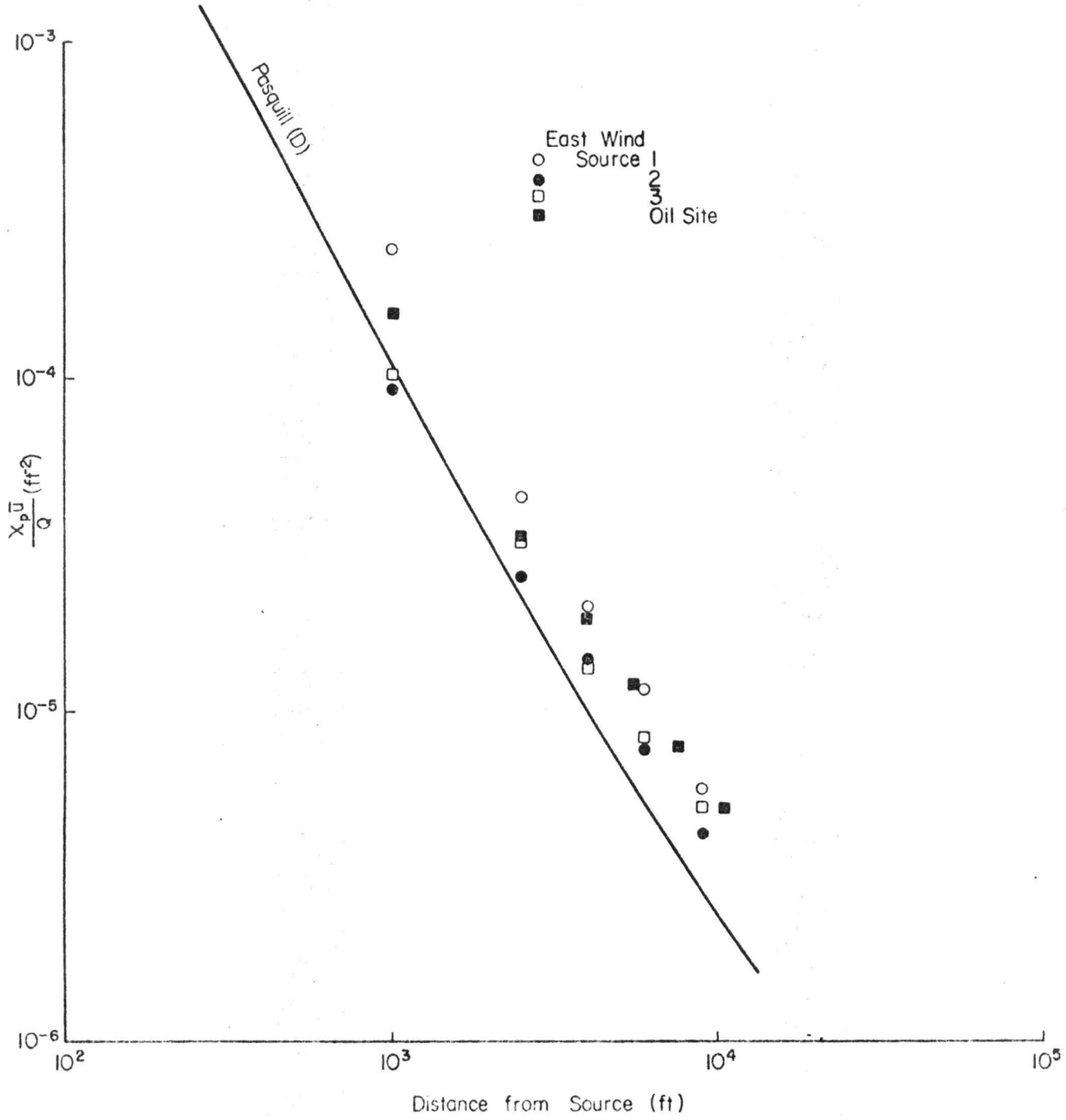

Fig. 77. Normalized ground level maximum average ground concentration - E wind

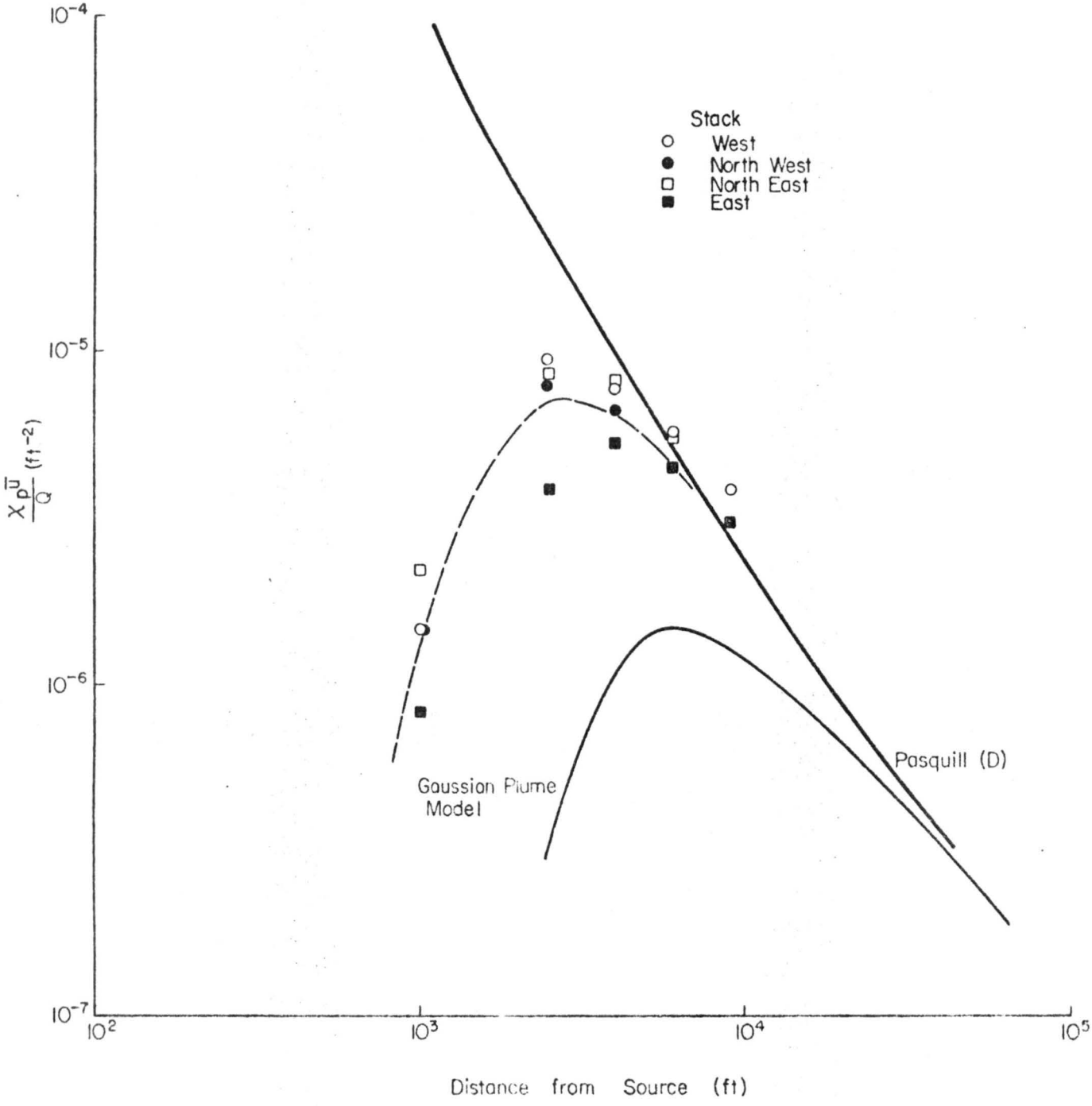

Fig. 78. Normalized ground level maximum average stack release

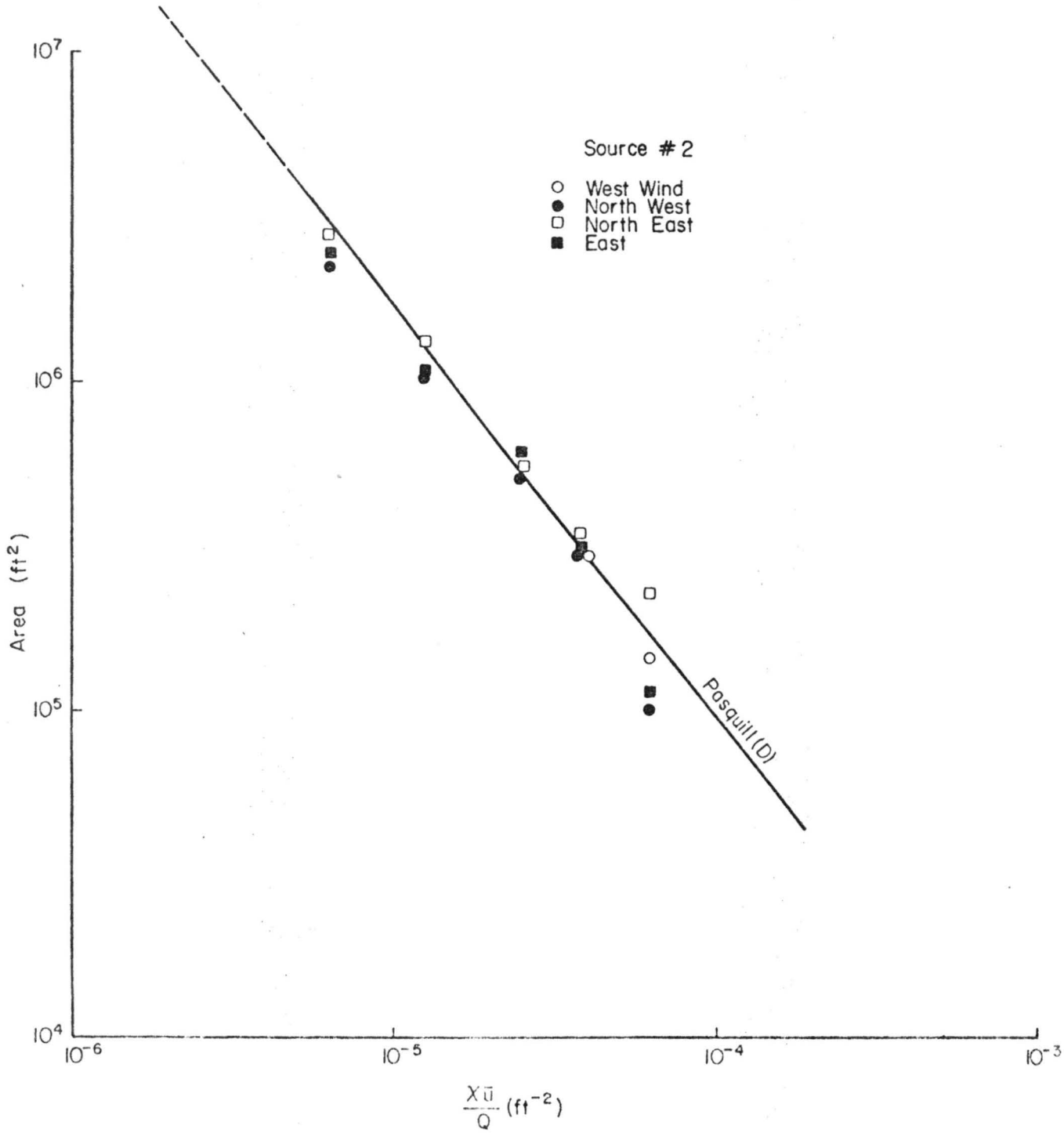

Fig. 79. Typical areas within ground level concentrations isopleths source 2